TECHNISCHE UNIVERSITÄT MÜNCHEN

Wissenschaftszentrum Weihenstephan für Ernährung, Landnutzung und Umwelt

Lehrstuhl für Lebensmittelchemie und molekulare Sensorik

Structure determination and quantitation of key antioxidant compounds in aged garlic extract

Toshiaki Matsutomo

Vollständiger Abdruck der von der Fakultät Wissenschaftszentrum Weihenstephan für Ernährung, Landnutzung und Umwelt der Technischen Universität München zur Erlangung des akademischen Grades eines

Doktors der Naturwissenschaften

genehmigten Dissertation.

Vorsitzender: Prof. Dr. Michael Rychlik

Prüfer der Dissertation:

1. Prof. Dr. Thomas F. Hofmann
2. Prof. Dr. Peter Schieberle

Die Dissertation wurde am 24.07.2015 bei der Technischen Universität München eingereicht und durch die Fakultät Wissenschaftszentrum Weihenstephan für Ernährung, Landnutzung und Umwelt am 25.01.2016 angenommen.

Danksagung

The experimental work of this Ph.D. thesis was carried out under the supervision of Professor Dr. Thomas Hofmann between 2009 and 2012 at the Lehrstuhl für Lebensmittelchemie und molekulare Sensorik, Germany.

First, I would like to express my deepest gratitude to my supervisor Professor Dr. Thomas Hofmann for setting up the research theme of my Ph.D. thesis. His great superintendence and his warm encouragement led me to the achievement in the research regarding this thesis.

I would like to extend my appreciation from the bottom of my heart to Dr. Timo Stark for his great advice and instruction. He was so kind that he was always ready to help me with anything. My research plans could not accomplished without his support.

I received generous support from all the colleagues of the laboratory at the Lehrstuhl für Lebensmittelchemie und molekulare Sensorik, Germany. In particular, I have had the constant support and encouragement of Andreas Dunkel, Christian Hegmanns, Karola Fastus, Lösch Sofie, and Maren Ilse.

I would like to express sincere appreciation to President Mr. Kanji Wakunaga of Wakunaga Pharmaceutical Co., Ltd, Japan for the research cooperation and support. I owe a very important debt to Vice President Mr. Hironobu Wakunaga for giving me the opportunity for this research. Dr. Takami Oka has been giving me constructive comments and warm encouragement.

I appreciate the valuable feedback offered by Dr. Yukihiro Kodera of Wakunaga Pharmaceutical Co., Ltd. I have greatly benefited from Dr. Hiroyuki Yamaguchi, Dr. Koichi Tamura, Dr. Makoto Ichikawa, Dr. Nagatoshi Ide, and Dr. Naoaki Morihara.

I am also indebted to former Professor Dr. Gisyou Honda and Associate Professor Dr. Michiho Ito for training me to do basic research during my undergraduate and graduate education at Kyoto University.

Finally, I want to thank my father Yuji and my mother Keiko for everything. I also want to offer my special thanks to my wife Keiko and my daughter Ia.

Publikation

Matsutomo, T.; Stark, TD.; Hofmann, T. In vitro activity-guided identification of antioxidants in aged garlic extract. *J. Agric. Food Chem.* **2013**, *61* (12), 3059-3067.

List of abbreviations and trivial names

AATS	2,2'-azobis(2-methylpropionamidine) dihydrochloride
ABTS	2,2'-azinobis(3-ethylbenzothiazoline-6-sulfonic acid)
acetone-d_6	deuterated acetone
AUC	area under the curve
BHA	butylated hydroxyanisole
brs	broad singlet
CD	Circular dichroism spectroscopy
$CDCl_3$	deuterated chloroform
cf	confer
COSY	correlated spectroscopy
d	doublet
dd	doublet of doublets
ddd	doublet of doublet of doublets
dt	doublet of triplets
DEPT	distorsionless enhancement by polarization transfer
DMSO-d_6	deuterated dimethyl sulfoxide
DPPH	2,2-diphenyl-1-picrylhydrazyl
ESI	electrospray ionization
ethanol-d_5	deuterated ethanol
HMBC	heteronuclear multiple bond correlation
HPLC	high performance liquid chromatography
HPS	hydrogen peroxide scavenging
HRMS	high resolution mass spectrometry
HSQC	heteronuclear single quantum coherence
Hz	hertz
IS	internal standard
J	coupling constant
LC	liquid chromatography
LOQ	limit of quantitation
m	multiplet
methanol-d_4	deuterated methanol
MPLC	medium pressure liquid chromatography
MRM	multiple reaction monitoring
MS	mass spectroscopy, mass spectrum

MS/MS	tandem mass spectroscopy
m/z	mass-to-charge ratio
NMR	nuclear magnetic resonance
ORAC	oxygen radical absorbance capacity
pt	pseudo triplet
q	quartet
qt	quartet of triplets
ROS	reactive oxygen species
RP	reversed phase
RSD	relative standard deviation
s	singlet
S.D.	standard deviation
SIDA	stable isotope dilution assay
t	triplet
TE	trolox equivalent
TMS	trimethylsilane
TMSP	3-trimethylsilyl-2,2,3,3-d_4-propionic acid sodium salt
TOF	time of flight
Trolox	(±)-6-hydroxy-2,5,7,8-tetramethylchromane-2-carboxylic acid
UV/VIS	ultraviolet visible spectroscopy
UPLC	ultra performance liquid chromatography
v	volume

1 Introduction

1.1 Reactive oxygen species and antioxidants

1.1.1 Reactive oxygen species and antioxidant defence systems

Reactive oxygen species (ROS) are broadly defined as chemically reactive molecules containing oxygen, such as superoxide anion ($O_2^{\bullet-}$), hydrogen peroxide (H_2O_2), and hydroxyl radical ($OH^{\bullet}$), which are generated intentionally or as byproducts in the living cells. The NOX family of NADPH oxidases, mitochondrial respiration, and the endoplasmic reticulum are reported as the major source of ROS generation (*Bedard et al., 2007*, *Kowaltowski et al., 2009*, and *Malhotra et al., 2007*). *Tahara et al.* (*2009*) reported that ROS formation is less than 0.2% of oxygen consumption in most tissues. There is increasing evidence that ROS play an important role in a variety of cellular processes by regulating several signaling pathways through interaction with critical signaling molecules (**Figure 1**, *Ray et al., 2012* and *Boonstra et al., 2004*).

When excessive amounts of ROS are generated by environmental stress (e.g., UV radiation), life style change, and so forth, undesirable oxidative stress occurs. Accumulating reports indicated oxidative stress results in direct or indirect ROS-mediated damage to lipids, proteins, and DNA (*Sharma et al., 2012*), leading to diabetes (*Bashan et al., 2009*, and *Maritim et al., 2003*), atherosclerosis (*Madamanchi et al., 2005*, *Park et al., 2011*, and *Stocker et al., 2004*), neurodegeneration (*Milatovic et al., 2009*, *Uttara et al., 2009*, and *Shukla et al., 2011*), cancer (*Pan et al., 2009*, and *Trachootham et al., 2009*) and ageing-related diseases (*Wei, 1992*, *Lee et al., 2007*, and *Haigis et al., 2010*).

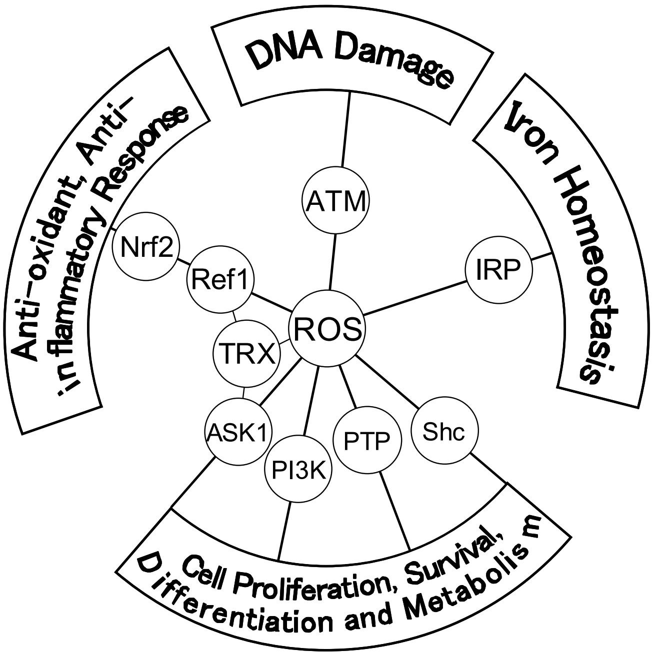

Figure 1: Cellular signaling pathways regulated by ROS. ASK1; apoptosis signal-regulated kinase 1. PI3K; PI3 kinase. PTP; protein tyrosine phosphatase. Shc; Src homology 2 domain-containing. TRX; thioredoxin. Ref-1; redox-factor 1. Nrf-2; NFE2-like 2. IRP; iron regulatory protein. ATM; ataxia–telangiectasia mutated (*Ray et al., 2012*).

All biological organisms have developed antioxidant defense systems against oxidative stress. The antioxidants may be classified into four categories based on function: preventive antioxidants, radical scavenging antioxidants, repair and de novo antioxidants, and adaptation (*Noguchi et al., 2000*).

The preventing antioxidants function as the first line of defense, which suppress the formation of ROS (**Figure 2**). Diverse enzymes, such as glutathione peroxidase, phospholipid hydroperoxide, glutathione peroxidase, selenoprotein, and catalase, prevent the ROS formation by reducing hydrogen peroxide and hydroperoxide molecules. On the other hand, proteins, such as transferrin, ferritin, and lactoferrin, sequester metal ions resulting in prevention of the formation of ROS. The second line of defense is executed by the radical scavenging antioxidants, removing active species rapidly before they attack biologically essential molecules. Lots of natural compounds including phenols, carotenoids, and aromatic amines, act as a free radical-scavenging antioxidant. Various enzymes, for example phospholipase A2, function in the third line of defense by repairing damages, clearing the wastes, and reconstituting the lost function. The fourth line of defense is an adaptation where the signal induces formation of the appropriate antioxidants and transportation of them to the appropriate site.

Physiological homeostasis is regulated under normal antioxidant defense system *in vivo*. When superabundant ROS, however, overwhelm the antioxidant defense system, oxidative stress induced by ROS causes pathogenesis and progression of disease.

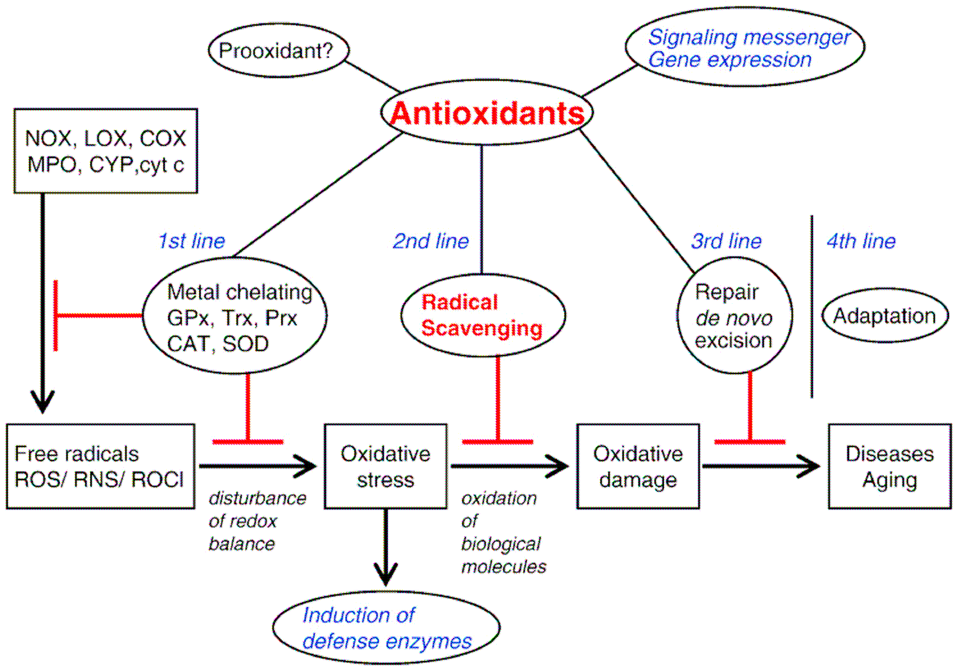

Figure 2: Defense network against oxidative stress *in vivo* (taken from *Niki, 2010*).

1.1.2 Natural antioxidants in food

Dietary antioxidants are important to decrease the adverse effects of ROS due to their antioxidant activity. A large number of natural antioxidants have been found in vegetables, fruits, and their products. For instance, vitamins C and E and antioxidant phytochemicals such as polyphenols, which are responsible for most of the antioxidant activity in foods, have been well investigated for their abilities to attenuate oxidative damage induced by ROS (*Jialal et al., 1990*, *Esterbauer et al., 1991*, and *Bellion et al., 2010*).

The hydrophilic vitamin C (ascorbate) and the hydrophobic vitamin E (α-tocopherol) are important both as nutrients and as antioxidants. It has been shown that no lipid peroxidation is observed in human plasma exposed to the water-soluble radical initiator or to the oxidants generated by polymorphonuclear leukocytes until the endogenous plasma ascorbate is completely consumed (*Frei et al., 1988*). In addition, the biochemical functions of vitamin C include enzymatic co-factor for physiological reactions such as hormone production, collagen synthesis, the production of Interferon, and regeneration of the damaged vitamine E to an active form (*Kim et al., 2013* and *Kadoma et al., 2006*). Vitamin E is well known as a major chain-breaking antioxidant in cell membrane, and its analogs have been proved to be selective inducers of apoptosis in cancer cells and efficient suppressors of tumors in experimental models (*Lawson et al., 2003* and *Weber et al., 2002*).

In general, phytochemicals are defined as natural compounds produced by plants that affect health although they are not essential nutrients. Thousands of phytochemicals have been identified to date, including polyphenols, flavonoids, carotenoids, terpenoids, sulfur-containing compounds, and so forth. Their antioxidant mechanism is prevention of ROS formation by chelating transition metals such as iron, inhibiting xanthine oxidase, and/or elevating endogenous antioxidants such as SOD, and direct radical scavenging. An increasing number of phytochemicals have been studied for their abilities to prevent and treat various diseases.

Among the phytochemicals, lignans have attracted increasing interest due to their potential bioactivities, such as anticarcinogenic, antioxidant, estrogenic and antiestrogenic activities (*Yatkin et al., 2014* and *Penttinen et al., 2007*).

Lignans are a class of secondary plant metabolites belonging to the group of diphenolic compounds derived from the oxidative coupling of two phenylpropanoid (C6-C3) units. Sesamin (**Figure 3**), a lipophilic lignan found in sesame seeds, is known for its antioxidant role. This compound has been revealed to play a distinct role as a potent neuroprotective antioxidant and anti-inflammatory agent (*Lahaie-Collins et al., 2008*). Furthermore, long-term treatment with sesamin indicated protective effect on kidney damage and renal endothelial dysfunction in hypertensive rats (*Wu et al., 2012b*). Besides sesamin, secoisolariciresinol diglucoside (**Figure 3**) is a potent lignan isolated from flaxseed. The results of *in vitro* and *in vivo* investigations of secoisolariciresinol diglucoside revealed that it changed hepatic enzyme activities and thereby plays a key role in the prevention of oxidative damage in immunologic (*Moree et al., 2013*). In addition, this compound suppressed the development of hypercholesterolemic atherosclerosis by reducing aortic oxidative stress (*Prasad, 2008*).

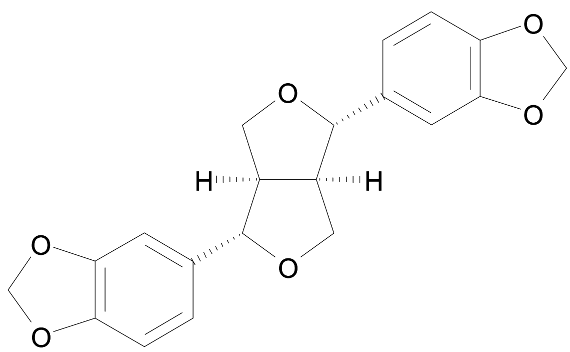

sesamin

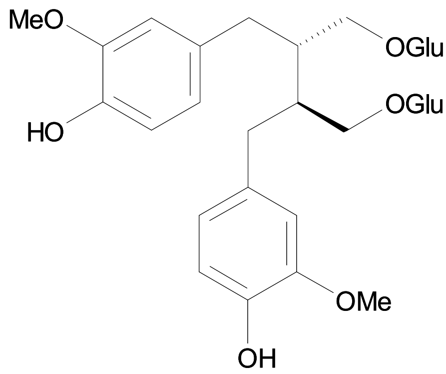

secoisolariciresinol diglucoside

Figure 3: Chemical structures of sesamin and secoisolariciresinol diglucoside.

Moreover, fruits and vegetables are rich in antioxidant phytochemicals, which may reduce cancer risk by operating multiple cancer-specific mechanisms, including scavenging of oxidative agents, modulation of detoxification enzymes, stimulation of the immune system, modulation of hormone level, and antiproliferative activities (*Pool-Zobel et al., 1998* and *Boffetta et al., 2010*). No single antioxidant can replace the natural combination of thousands of phytochemicals in fruits and vegetables because they may affect a diversity of mechanisms and cause synergistic effectiveness. Therefore, the WHO recommended a daily intake of at least 400 g (five portions a day) of fruit and vegetables in 1990, and seven or more portions intake have been proposed in many publications (*Oyebode et al., 2014*).

Beneficial fruits and vegetables can be classified into several groups based on their colors: red (tomatoes), red/purple (berries, grapes, and red wine), orange (carrots, mangoes, pumpkin), orange/yellow (cantaloupe, peaches, oranges, and papaya), yellow/green (spinach, avocado, and honeydew), green (broccoli, cabbage, and cauliflower), and white/green (garlic, onion, leeks, and chives) (*Heber, 2004*). They are closely related to the color of the containing phytochemicals and also to their unique functions including antioxidant effects. For example, red foods contain lycopene, the deep red pigment in tomatoes, which have powerful antioxidant activity and may be involved in maintaining prostate health, and which may decreased risk of cardiovascular disease. Garlic and other white/green foods contain allyl sulfides as phytochemicals, which may inhibit cancer cell growth. *Heber* (*2004*) insisted that intake of fruits and vegetables from each color group will be beneficial for health. A number of organizations, such as the American Institute for Cancer Research and the American Cancer Society, have held education campaigns that emphasized the value to eat a healthy diet in terms of a colorful plate of fruits and vegetables.

1.2 Garlic

1.2.1 Botany, cultivation, and use of garlic

Garlic (*Allium sativum* L.) belongs to the genus *Allium*, which includes 600-750 species, such as onion, shallot, chive, and leek. “*Sativum*” in the botanical name for garlic means cultivated. ”Garlic” is derived from “gar” meaning “spear” and “leac” meaning “leak”. Garlic can be distinguished from other *Allium* members by its flat leaves and bulbs (**Figure 4**). Each bulb of garlic contains several small cloves enclosed in a white or purplish sheath. As garlic is often a sterile plant and does not produce true seeds, it is propagated almost exclusively asexually from underground cloves. Garlic grows up in the range from 0.6 to 1.9 m in height.

There are two different types or sub-species of garlic, namely hardneck garlic and softneck garlic (*Volk et al., 2004*). Hardneck cultivars (*Allium sativum* var. *ophioscorodon*) produce scapes or flower stalks, and are often called “top-setting” or “bolting” cultivars. Bulbils are produced on the top of the scape. Typically, these cultivars have a single circle of 4 to 12 cloves around the woody stalk. Before flowering, hardneck garlic scapes are generally coiled as they grow, and are normally pinched off three weeks before the harvest time to enhance the growth of the bulbs. Softneck cultivars (*Allium sativum* var. *sativum*) produce just a short scape, and therefore they sometimes called short-necked garlic. These cultivars are more adaptable to cold climates, and are generally more productive than hardneck cultivars because all the energy is concentrated on producing a bulb. Bulbs of hardneck garlics have 10 to 40 cloves in several layers around a soft central stem with smaller cloves around and larger cloves further outside. Softneck garlics have much longer shelf life than hardneck garlic, and therefore typically can be stored for 6 to 8 months without any particular degradation

Figure 4: Garlic (*Allium sativum* L.).

Since ancient times, garlic has been grown and consumed. Garlic is a perennial plant, although it's often harvested as an annual plant. The global production of garlic was about 25 million tons in 2012 (*Food and Agricultural Organization, 2012*), which is the second most quantity among edible *Allium* plants. While garlic is grown almost all over the world, China produced by far the largest, accounting for more than 80% of the world production (**Table 1**). Although it remains unclear, the original habitat of garlic has been considered to be central Asia, and garlic spread to west, south and east from the center of origin (*Etoh et al., 2001*).

Table 1: Top 10 garlic producing countries (*Food and Agricultural Organization, 2012*).

Rank	Country	Production (t)
1	China	20,000,000[a]
2	India	1,150,000[a]
3	Republic of Korea	339,113
4	Egypt	309,155
5	Russian Federation	239,312
6	Bangladesh	233,609
7	Ethiopia	222,548
8	Myanmar	213,000[a]
9	United States of America	195,910
10	Ukraine	171,400

[a] The value was estimated by FAO (*Food and Agricultural Organization*).

Garlic is easy to cultivate since it can be grown in mild climates. The soil for cultivation of garlic is preferably prepared to be well-drained, fertile, and controlled between pH 6 and 7. Cloves are generally planted in fall (sometimes in early spring). Fall-planted garlic should be mulched with a straw to prevent injury in winter, and the straw should be moved to between the rows in early spring to allow the garlic foliage to emerge. Mulch helps control weeds and conserve soil moisture during the growing season. Garlic takes about 10 months to be mature enough for harvest. The bulbs should be dig when the foliage starts to turn yellow, and be dried in a warm, well-ventilated, and shaded place for 2 to 3 weeks. For storage, the best conditions of temperatures and moisture are about 15ºC and in the range from 40 to 60%, respectively.

Garlic has been used for both culinary and medicinal purposes. Garlic is one of the most popular materials in the field of culinary. The most commonly used part of garlic is the clove that is divided from the bulb. Garlic cloves are either consumed cooked or raw, and have considerable medicinal purposes. They have a characteristic pungent, spicy flavor, which gradually sweetens with cooking. The other parts of garlic are also edible, such as the leaves and flowers on the head. They have milder flavor than the bulbs, and are consumed while particularly immature and tender. The immature flower stalks of some types are sometimes used just like asparagus. Garlic is an important component of many dishes in the wide area of Asia, the Middle East, northern Africa, southern Europe, and parts of South and Central America.

Garlic has also been used as medicine in many cultures for thousands of years. An Egyptian holy book dating from about 1550 BCE details more than 875 therapeutic formulas, of which 22 contain garlic. Egyptians building the pyramids consumed garlic to build and keep strength, and garlic was placed along with the mummified bodies. In ancient Asia, garlic was used for high blood pressure and respiratory disease. Hippocrates, who is the ancient Greek physician and is considered to be one of the most outstanding persons in the history of medicine, prescribed garlic as a pain killer. Roman soldiers had a bulb of garlic around their necks to give them strength. In the Middle Ages, it was believed that garlic is useful to repel witchcrafts and vampires. In the 16th century, garlic was considered more as a medicine than a food.

1.2.2 Chemical composition of garlic

As shown in **Table 2**, the nutritional constituents of garlic are approximately 59% water, 33% carbohydrates, and 6% proteins (*USDA National Nutrient data base, 2014*). Fructan is a major polysaccharide component of carbohydrates, and garlic fructan is inulin-type that belongs to the neokestose family, which may contribute to the protection against gastrointestinal diseases by improving the microbial gastrointestinal environment (*Zhang et al., 2013*). Among free and protein-bound amino acids, the contents of L-arginine and L-glutamic acid are particularly high. Besides these constituents, the important chemical constituents of garlic bulbs are organosulfur compounds, and Generally garlic bulb contains approximately 2.3% organosulfur compounds (*Omar et al., 2010*).

Table 2: Nutrient value/100 g of garlic (*USDA National Nutrient data base, 2014*).

Constituents		Content (g) per 100 g of edible portion
water		58.58
proteins		6.36
lipids (fat)		0.50
carbohydrates		33.06
carbohydrates (fiber)		2.10
carbohydrates (sugars)		1.00
minerals	calcium	0.18
	phosphorus	0.15
	potassium	0.40
vitamins	vitamin C	0.03

A series of characteristic sulfur-containing compounds have been identified in garlic (**Table 3**).

Table 3: The composition of the major sulfur-containing constituents in garlic (*Koch et al., 1996*).

Constituents	Content in garlic (mg/g)
S-alk(en)yl-L-cysteine sulfoxides	
(+)-*S*-allyl-L-cysteine sulfoxide (alliin)	5.4-14.5
(+)-*S*-methyl-L-cysteine sulfoxide (methiin)	0.2-2.0
(+)-*S*-(*trans*-1-propenyl)-L-cysteine sulfoxide (isoalliin)	0.1-2.0
γ-glutamyl *S*-alk(en)yl-L-cysteines	
γ-glutamyl *S*-allyl-L-cysteine	1.9-8.2
γ-glutamyl *S*-methyl-L-cysteine	0.1-0.4
γ-glutamyl *S*-(*trans*-1-propenyl)-L-cysteine	3.0-9.0
thiosulfinates	
allicin	2.5-5.0

Organosulfur compounds in garlic are biosynthetically produced by enzymatic reactions. For example, *Lancaster et al.* (*1989*) reported that *S*-alk(en)yl-L-cysteine sulfoxides are biosynthesized from γ-glutamyl *S*-alk(en)yl-L-cysteines. Several *S*-alk(en)yl-L-cysteine sulfoxides, such as *S*-methyl-L-cysteine sulfoxide, *trans*-*S*-1-propenyl-L-cysteine sulfoxide, and *S*-allyl-L-cysteine sulfoxide, namely methiin, isoalliin, and alliin, respectively, and their precursors have been isolated and characterized (**Figure 5**).

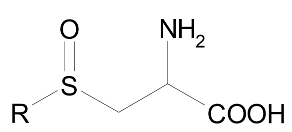

R= $-CH_3$ (methiin)
$-CH=CHCH_3$ (isoalliin)
$-CH_2CH=CH_2$ (alliin)

Figure 5: Chemical structures of *S*-alk(en)yl-L-cysteine sulfoxides.

The diversity and complexity of garlic chemistry is attributed to the relationship between enzymes and precursors in garlic. Alliinase, which accounts for about 10% of total protein and is localized to the bundle sheath cells surrounding the vascular bundles within the cloves, have the greatest influence on the production of organosulfur compounds in garlic preparations (*Ellmore et al., 1994*). At room temperature, when garlic is crushed, alliinase can react with alliin present in the clove mesophyll cells, resulting in formation of thiosulfinates such as allicin (**Figure 6**). As thiosulfinates, especially allicin, is extremely unstable and reactive, it undergoes self-decomposition to sulfides such as diallyl disulfide at room temperature and also can be converted to other derivatives depending on environmental and processing conditions. Crushing garlic cloves with ethanol at 0°C leads to inactivation of allicin and extraction of alliin, and steam distillation of crushed garlic gives garlic oil including sulfides, such as diallyl trisulfides, diallyl disulfides, and methylallyl trisulfides (*Block et al., 1993*).

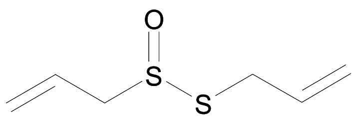

allicin

Figure 6: Chemical structure of allicin.

Sugii et al. and other researchers have identified several γ-glutamyl *S*-alk(en)yl-L-cysteines shown in **Figure 7** (*Sugii et al., 1964* and *Mütsch-Eckner et al., 1992*). These compounds were confirmed to be biosynthetic intermediates for corresponding *S*-alk(en)yl-L-cysteine sulfoxides. γ-Glutamyl peptides are considered to have function as reserve compounds, and their contents have been revealed to decrease during a long-term storage at 4°C or when germinating (*Lawson et al., 1991*). There are no report on remarkable physiological actibity of γ-glutamyl *S*-alk(en)yl-L-cysteines. On the other hand, *S*-allyl-L-cysteine, which is absent in raw garlic and is formed from γ-glutamyl *S*-allyl-L-cysteine during aging process of garlic, has been reported to be physiologically potent (*Sumiyoshiet al., 1990, Yeh et al., 2001* and *Nakagawa et al., 1989*).

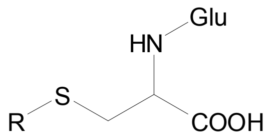

R= $–CH_3$ (γ-glutamyl *S*-methyl-L-cysteine)
$–CH{=}CHCH_3$ (γ-glutamyl *S*-(1-propenyl)-L-cysteine)
$–CH_2CH{=}CH_2$ (γ-glutamyl *S*-allyl-L-cysteine)

Figure 7: Chemical structures of γ-glutamyl *S*-alk(en)yl-L-cysteines.

Besides these organosulfur compounds, there are a few reports on phenolic compounds in garlic (**Figure 8**). *Mizuno et al.* (*1992*) quantified free quercetin in garlic and found out that the content of the compound was low (8 µg/g). In the recent literature, cyaniding 3-glucoside and its derivatives were identified in garlic cloves as pigment constituents (*Fossen et al., 1997*). Furthermore, several phenolic compounds have been confirmed in garlic, such as ferulic acid, *p*-coumaric acid, vanillic acid, and *p*-hydroxybenzoic acid (*Beato et al., 2011*).

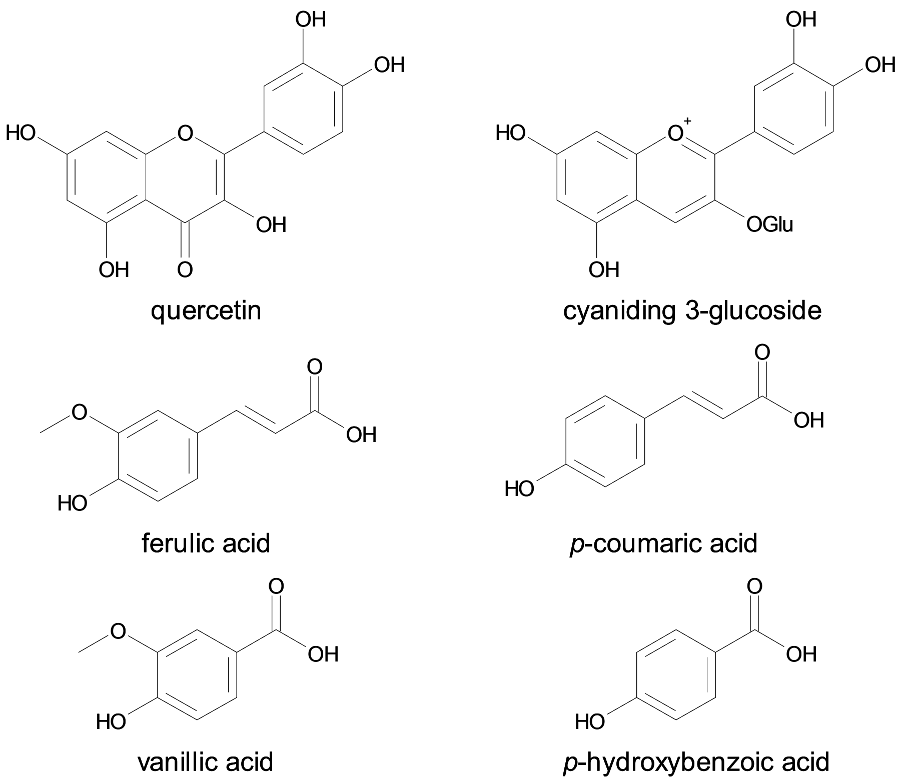

Figure 8: Chemical structures of phenolic compounds in garlic.

1.2.3 Pharmacological properties of garlic

Garlic has been widely examined for its pharmacological properties, particularly its antibacterial effect, cancer-preventive activity, effect on cardiovascular diseases, and anti-fatigue activity.

1.2.3.1 Antibacterial effect

Garlic has been used from time immemorial as an agent against infectious disease. In 1857, Pasteur reported antibacterial activity of garlic maybe for the first time (*Pasteur, 1857*). More recently, garlic has been proved to kill plenty types of bacteria including *Salmonella*, *Escherichia coli*, *Bacillus subtulis*, and so on. *You et al.* (*1998*) reported that garlic consumption is protective in the development and progression of gastric cancer by preventing *Helicobacter pylori* (*H. pylori*) infection, which is a risk factor of gastric cancer.

Allicin had been considered to be the key active ingredient because it indicates potent antibacterial activity *in vitro* (*Ankri et al., 1999*). However, allicin is quite unstable and reactive and, therefore, other sulfur-containing compounds such as diallyl disulfide and diallyl trisulfide were investigated for their effects and revealed to affect *H. pylori* growth (*O'Gara et al., 2000*).

1.2.3.2 Cancer-preventive activity

The National Cancer Institute described that garlic is one of the foods located at the top of the pyramid showing the importance on cancer-preventive property (**Figure 9**). A number of literatures have reported on the preventive activity of garlic and itsconstituents against chemical-induced cancers, such as skin cancer, gastric cancer, hepatoma, colorectal cancer, and lung cancer.

Sparnins et al. (*1988*) revealed that four sulfides, namely allylmethyl trisulfide, allylmethyl disulfide, diallyl trisulfide, and diallyl sulfide, inhibited benzo[a]pyrene -induced neoplasia of the forestomach. Interestingly, their saturated analogs showed no or little inhibitory activity, indicating the importance of the allyl groups for cancer-preventive effects.

Antioxidant activity of garlic constituents could contribute to prevention of cancer by scavenging ROS and radicals, which can be induced by a carcinogenic substance and cause DNA damage. In additon, the experimetn by *Arivazhagan et al.* (*2004*) suggested that garlic modulates oxidant-antioxidant status in liver and plasma, which may play a key role in preventing cancer.

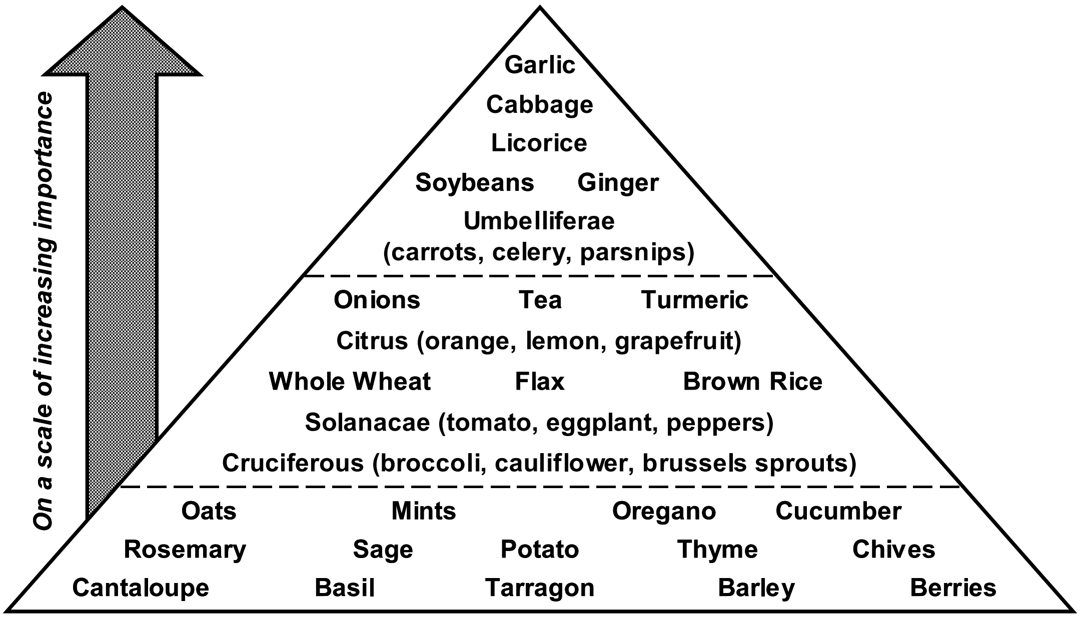

Figure 9: Possible cancer-preventive foods and ingredients (*Caragay, 1992*).

1.2.3.3 Effect on cardiovascular disease

Garlic has been recognized as preventive and therapeutic effects of cardiovascular disease based on lots of animal and clinical studies. The beneficial effects of garlic against cardiovascular disease have been reviewed in many literatures (*Rahman et al., 2006* and *Banerjee et al., 2002*). The effectiveness of garlic is associated with lowering blood pressure, antithrombotic and anti-platelet aggregation effects, prevention of atherosclerosis, increasing fibrinolytic activity, and reduction of serum cholesterol, triglyceride, and homocysteine.

The oxidation of LDL by ROS has been revealed to be an important mechanism in the initiation and progression of atherosclerosis, and therefore inhibition of the LDL oxidation is considered as one of the key points for prevention of cardiovascular disease. Garlic has been shown to protect vascular endothelial cells from injury caused by oxidized LDL by scavenging ROS, resulting in inhibiting the formation of lipid peroxides (*Ide et al., 1997*).

1.2.3.4 Anti-fatigue activity

Garlic has also been used as a nutrient and tonic medicine. In the ancient Egypt, the slaves that built the Pyramids were given garlic to resist disease as well as to restore their energy and reduce fatigue. In the review by *Morihara et al.* (*2007*), animal and clinical studies on anti-fatigue effects of garlic and its preparations were summarized.

Hi-intensity exercise, which can causes exhaustion, results in increase of ROS concentrations in muscle and liver, leading to mitochondrial damage and increased levels of lipid peroxidation products (*Davies et al., 1982*). Therefore, research on antioxidants as an agent against physical fatigue has been carried out. *Mizunuma et al.* (*1993*) reported dietary vitamin E prevents the increase of lipid peroxide in skeletal mascle of rat after acute exercise by inhibiting generation of lipid peroxide and also increasing superoxide dismutase activity. Anti-fatigue activity of garlic may be led mainly or partially by inhibition of the development of lipid peroxidation induced by ROS.

1.3 Garlic preparations

Although garlic is recognized as one of the most beneficial foods, freshly crushed garlic is chemically unstable and causes undesirable side effects, such as stomach injury (*Nakagawa et al., 1980*) and allergic reactions (*Papageorgiou et al., 1983*). Such side effects are considered to be attributable to allicin and diallyl disulfide.

Processing is the key for increasing the benefits of garlic and decreasing its detrimental effects. Processed garlic contains a variety of sulfur-containing compounds formed through chemical and biological reactions during the manufacturing processes. Garlic preparations can be classified into four categories: garlic powder, garlic oil, garlic oil macetate, and aged garlic extract (AGE). The composition of their major constituents is shown in **Table 4**.

Table 4: Garlic preparations and their composition. +++; >1.00 mg. ++; 0.20-1.00 mg. +; 0.05-0.20 mg. ±; 0.01-0.05 mg. N.D.; <0.01 mg. (values are amount in 1g equivalent of raw garlic.)

Constituents	Garlic powder	Garlic oil	Garlic oil macetate	AGE
alliin	+++	N.D.	N.D.	±
alliinase	detected	N.D.	N.D.	N.D.
allicin	N.D.	N.D.	N.D.	N.D.
allyl sulfides	N.D.	+++	+++	+
γ-glutamyl *S*-allyl-L-cysteine	+++	N.D.	++	++
S-allyl-L-cysteine	N.D.	N.D.	+++	+++
S-allylmercapto-L-cysteines	N.D.	N.D.	N.D.	+
fructan	+++	N.D.	+++	+++

Garlic powder is obtained simply by dehydration of pulverized garlic clove (*Amagase et al., 2001*). Some garlic powder products contain alliin and the enzyme, alliinase, which can produce allicin with the addition of water.

However, there is no scientific evidence the above reaction occurs in the stomach. Furthermore, garlic powder contains only a small amount of the alliin due to lost during the manufacturing process.

Garlic oil is generally prepared by steam-distillation process (*Amagase et al., 2001*). These products mainly contain several sulfides, which is the most potent source of garlic odor and causes body odor. In addition, garlic oils don't contain any of the potent water-soluble compounds.

Garlic oil macerate is manufactured by grounding raw garlic in vegetable oils (*Amagase et al., 2001*). It contains oil-soluble compounds derived from both of garlic and vegetable oils.

The most valuable garlic product is AGE. It is prepared by extracting sliced garlic in aqueous ethanol and maturing for more than 10 months (*Ide et al., 1999a*). This whole process converts the harsh and irritating compounds in raw garlic to mild, stable and beneficial water-soluble compounds. The safety of AGE has been confirmed by many scientific studies without any adverse effects (*Sumiyoshi et al., 1984* and *Steiner et al., 1996*).

1.3.1 Ingredients of aged garlic extract (AGE)

The unique aging process provides AGE with added value by decrease of the stimulative constituents in raw garlic and the odor, and by formation of physiologically useful compounds. An example of the former is conversion of thiosulfinates such as allicin to volatile sulfides. *Weinberg et al.* (*1993*) identified dimethyl disulfide, dimethyl trisulfide, diallyl sulfide, diallyl disulfide, diallyl trisulfide, allyl methyl sulfide, allyl methyl disulfide, and allyl methyl trisulfide in AGE by means of GC-MS. As an example of the latter formation, AGE contains *S*-allyl-L-cysteine, which is not or barely detectable in raw garlic. *S*-Allyl-L-cysteine is formed from γ-glutamyl-*S*-allyl-L-cysteine, and this reaction is catalyzed by γ-glutamyltranspeptidase (**Fig 10**, *Colín-González et al., 2012*). It has been proved to show inhibitory activity against carcinogenesis, hepato-protective effects, cholesterol lowering effect as well as antioxidant activity (*Sumiyoshiet al., 1990, Yeh et al., 2001* and *Nakagawa et al., 1989*).

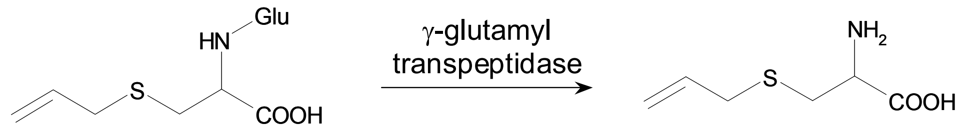

γ-glutamyl-S-allyl-L-cysteine   *S*-allyl-L-cysteine

Figure 10: Formation of *S*-allyl-L-cysteine during aging process of AGE.

Analogous sulfur-containing compounds, *S*-(*trans*-1-propenyl)-L-cysteine, *S*-methyl-L-cysteine, and *S*-allylmercapto-L-cysteine, are also present in AGE (**Fig 11**, *Allison et al., 2006*). *S*-Allylmercapto-L-cysteine has been widely investigated, showing its anticancer effect, liver protective effect, and antioxidant activity (*Xiao al. 2003* and *Nakagawa et al., 1989*).

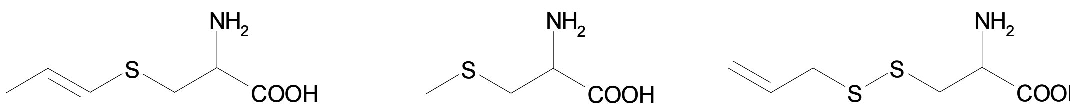

S-(*trans*-1-propenyl)-L-cysteine   *S*-methyl-L-cysteine   *S*-allylmercapto-L-cysteine

Figure 11: Chemical structures of sulfur-containing compounds in AGE.

Besides organosulfur compounds, Maillard reaction products were identified in AGE as potent antioxidants (**Figure 12**). *Ryu et al.* (*2001*) fractionated AGE using an antioxidant assay, resulting in identification of *N*α-(1-deoxy-D-fructos-1-yl)-L-arginine (**1’**). Interestingly, this compound is not existing in raw garlic, but is generated through the Maillard reaction between L-arginine and glucose derived from decomposition of fructan during aging of garlic. Its antioxidant activity was comparable to that of ascorbic acid (*Ryu et al., 2001*). The compound **1’** significantly inhibited the oxidizing effects of the copper ion on LDL and also reduced the release of peroxides by oxidized LDL (*Ide et al., 1999b*). In addition, *Ichikawa et al.* (*2002*) found four 1,2,3,4-tetrahydro-β-carboline derivatives: (*1R*,*3S*)-1-methyl-1,2,3,4-tetrahydro-β-carboline-3-carboxylic acid (**2’**), (*1S*,*3S*)-1-methyl-1,2,3,4-tetrahydro-β-carboline-3-carboxylic acid (**3’**), (*1R*,*3S*)-1-methyl-1,2,3,4-tetrahydro-β-carboline-1,3-dicarboxylic acid (**4’**), and (*1S*,*3S*)-1-methyl-1,2,3,4-tetrahydro-β-carboline-1,3-dicarboxylic acid (**5’**). These compounds were not detected in raw garlic, but their contents increased during the aging process. These compounds were reported as potent antioxidant as ascorbic acid, and inhibited AAPH-induced lipid peroxidation (*Ichikawa et al., 2002*).

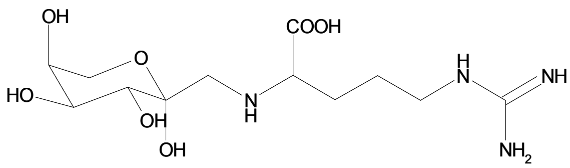

1’

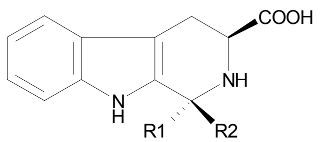

	R1	R2
2’	CH_3	H
3’	H	CH_3
4’	CH_3	COOH
5’	COOH	CH_3

Figure 12: Chemical structures of *N*α-(1-deoxy-D-fructos-1-yl)-L-arginine (**1’**), (*1R*,*3S*)-1-methyl-1,2,3,4-tetrahydro-β-carboline-3-carboxylic acid (**2’**), (*1S*,*3S*)-1-methyl-1,2,3,4-tetrahydro-β-carboline-3-carboxylic acid (**3’**), (*1R*,*3S*)-1-methyl-1,2,3,4-tetrahydro-β-carboline-1,3-dicarboxylic acid (**4’**), and (*1S*,*3S*)-1-methyl-1,2,3,4-tetrahydro-β-carboline-1,3-dicarboxylic acid (**5’**).

1.3.2 Pharmacological properties of aged garlic extract (AGE)

AGE and its constituents have been the subject in a large number of scientific studies around the world. They have been revealed to have a variety of pharmacological activity including anti-infection effect (immune enhancement), anticancer potential, cardioprotective effect, and anti-fatigue activity.

1.3.2.1 Anti-infection effect (immune enhancement)

AGE has been shown to have anti-infection effect through enhancement of the immune factors, such as the phagocytic activity of macrophages, T lymphocyte activity, natural killer cell activity, and antibody generation (*Kyo et al., 1998*). In a clinical study, the frequency of catching colds was significantly lower in the group taking AGE for more than one year than the control group (*Ushirotake et al., 2004*). People who caught a cold in the AGE group recovered quicker than the control group. In a randomized double-blind trial by *Ishikawa et al.* (*2006*), AGE was administered to patient group with inoperable colorectal, liver, or pancreatic cancer. As a result, both the number of NK cells and the NK cell activity increased significantly in the AGE group.

1.3.2.2 Anticancer potential

Inhibitory effect of cancer growth by AGE has observed in many cancer models such as bladder tumors, melanoma cells, neuroblastoma cells, skin cancer, breast cancer, colon cancer, prostate cancer, esophageal cancer, stomach cancer, lung cancer, and aflatoxin induced mutagenesis. In a double-blinded randomized study, 51 subjects who was diagnosed with colorectal adenomas were divided into two groups: high-AGE doses group and low-AGE dosed group (*Tanaka et al., 2004*). As a result, 50% of the subjects in the high-AGE group showed decrease of at least one adenoma after intake for 6 to 12 months, whereas there was no decrease observed in subjects in the low-AGE group. In terms of the size of adenomas, there was a significant difference between the two groups. The total size of adenomas in subiects who had adenomas on the base-line in the high-AGE group decreased (-0.86 mm), but that in the low-AGE group increased (2.56 mm). These results suggest the preventive and therapeutic effects of AGE on colorectal adenomas and also other cancers.

1.3.2.3 Cardioprotective effect

AGE has been shown to reduce multiple risk factors of cardiovascular disease including blood cholesterol, blood triglycerides, platelet aggregation, blood-thinning effects, and blood pressure as confirmed in a number of studies (*Rahman et al., 2001*). *Rahman et al.* (*2006*) reported that many chlinical trials revealed antioxidant activity of AGE, which may prevent oxidative stress mediated disorders such as cardiovascular diseases. In this literature, dietary supplementation with AGE for 14 days reduced concentrations of biomarkers for oxidative stress in plasma and urine in both non-smokers and smokers. After 14-days cessation, the reduced concentrations, however, returned to that before the intake. The plasma antioxidant capacity of smokers was significantly increased to the same level of non-smokers after supplementation with AGE for 14 days (**Figure 13**). However, after the 2-weeks washout period, the plasma antioxidant capacity of smokers decreased to that before AGE intake. Increased platelet activity has been found in smokers as well as in patients suffering from cardiovascular injury. Improvement of cardiovascular disease risk factors and increase in antioxidant status may play an important role in the prevention and development of cardiovascular diseases.

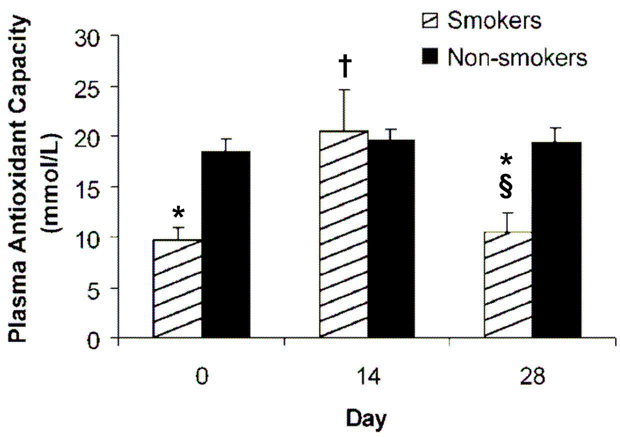

Figure 13: Antioxidant capacity of plasma in non-smokers and smokers before AGE consumption, after 14-days AGE consumption, and after 14-days AGE consumption and succeeding 14-days washout period. Antioxidant capacity is expressed as ascorbate equivalent antioxidant units (mmol/L). Values are means ± SEM (n = 10). *; P < 0.05 agains control (non-smokers). †; P < 0.05 against day 0. §; P < 0.05 agains day 14. (taken from *Rahman et al., 2006*)

1.3.2.4 Anti-fatigue activity

A number of pre-clinical and clinical studies of AGE have shown anti-fatigue activity and anti-stress effect. For example, AGE was shown to be effective in all of the stress tests in a pre-clinical study with four stress models in mice, whereas other garlic preparations didn't exhibit significant effects (*Ushijima et al., 1997*). Clinical trials of AGE combined with ginseng was performed by *Yaguchi et al.* (*2005*), indicating supplementation with AGE product reduced stress parameters, improved symptoms such as chill, stiff shoulder, fatigue lassitude, decline of physical strength, headache, abnormal bowel movement, and lumbago.

1.3.2.5 Antioxidant activity

Previous studies have provided strong evidence that AGE exhibits strong antioxidant activity. *Imai et al.* (*1994*) examined for the inhibitory effect of garlic preparations on low level chemiluminescence induced by *t*-butyl hydroperoxide in liver microsomal fraction (**Figure 14**). AGE decreased the light emission during the lipid peroxidation, whereas other garlic prepations enhanced it. Such antioxidant properties of AGE were created during long-term extraction of garlic through increase of stable and highly effective water-soluble organosulfur compounds, such as *S*-allyl-L-cysteine and *S*-allylmercapto-L-cysteine (*Imai et al., 1994*). AGE exerts antioxidant action by scavenging ROS, enhancing the cellular antioxidant enzymes such as superoxide dismutase, catalase and glutathione peroxidase, and increasing glutathione in the cells (*Wei et al., 1998, Ide et al., 1999a,* and *Morihara et al., 2011*).

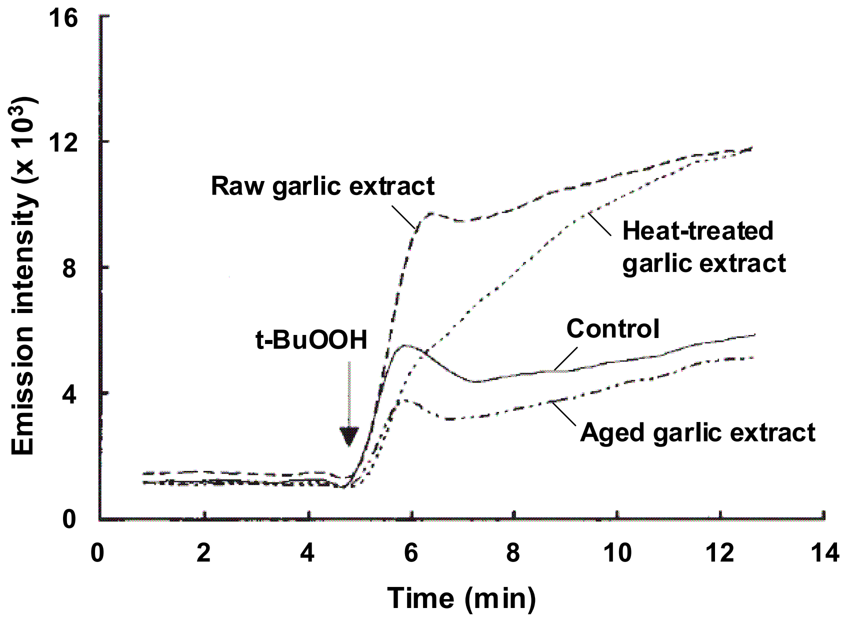

Figure 14: Effect of garlic preparations on low level chemiluminescence of microsomal fraction induced by *t*-butyl hydroperoxide (taken from *Imai et al., 1994*).

Among the constituents in AGE, some sulfur-containing compounds exhibits antioxidant activity. *S*-Allyl-L-cysteine, one of the evident antioxidants, was found to increase the glutathione level and the activities of catalase and glutahione peroxidase in kidney and liver (*Hsu et al., 2004*). It also decreased Fe^{2+}- and glucose-induced lipid oxidation in plasma, kidney, and liver. *S*-Allylmercapto-L-cysteine showed scavenging activity of hydroxyl radicals and singlet oxygen *in vitro* and also gentamicin-induced oxidative and nitrosative stress and nephrotoxicity were attenuated by *S*-allylmercapto-L-cysteine *in vivo* (*Pedraza-Chaverrí et al., 2004*). Other than sulfur-containing compounds, some Maillard reaction products, *N*α-(1-deoxy-D-fructos-1-yl)-L-arginine (**1'**) and four 1,2,3,4-tetrahydro-β-carboline derivatives (**2'**-**5'**) have been identified as potent antioxidants (*Ryu et al., 2001* and *Ide et al., 1999b*).

1.4 Objectives

AGE has demonstrated an array of antioxidant effect in a number of studies. This potent antioxidant activity may play a role mainly or partially in a variety of pharmacological effect against diseases associated with ROS. In the previous studies, some sulfur-containing constituents and Maillard reaction products have been proved to be strong antioxidants in AGE. Even though these studies gave a first insight into antioxidants in AGE, their antioxidant activities seem to be by far insufficient to show a major contribution to the overall antioxidant power of AGE. For example, ORAC activity of 1g dried AGE is more than 100 nmol TE, whereas a total of those of antioxidants identified in AGE is less than 20 nmol TE at the original concentration in 1g dried AGE. This fact suggests the occurrence of unknown antioxidants in AGE.

The objective of the present study was, therefore, to locate key antioxidants in AGE. In order to achieve this, two approaches were carried out: (i) activity-guided fractionation of AGE using *in vitro* antioxidant assays, and (ii) suitable model reactions based on educated guess to mimic chemical reactions leading to candidate antioxidants due to garlic extract aging. In the first approach, AGE was separated by HPLC to give some fractions, and then the fractions were examined for their antioxidant activity using the hydrogen peroxide scavenging (HPS) assay as well as the oxygen radical absorbance capacity (ORAC) assay. Fractionation and antioxidant assay were repeated until compounds were isolated, and their chemical structures were then elucidated by means of LC-MS and NMR experiments. In the second approach, model reactions were performed to obtain candidate antioxidants in AGE. The candidate compounds were screened to know whether they are present in AGE by means of LC-MS.

Thereafter, the compounds identified in AGE were quantified by means of LC-MS/MS analysis and were investigated for their antioxidant activity using two assays, thus giving first insight into their contribution to the overall antioxidant activity of AGE.

2 Results and discussion

2.1 Activity-guided fractionation of aged garlic extract (AGE) and identification of dilignol antioxidants

Since no single antioxidant assay alone is able to show comprehensive antioxidant capacity of a compound or a sample, *Prior et al.* (*2005*) recommended that more than two different antioxidant assays should be performed. Therefore, two different antioxidant assays, the HPS assay and the ORAC assay, were adopted in this study. The HPS assay, which is based on a single electron transfer mechanism, measures the radical reduction ability of an antioxidant by transferring one electron. On the other hand, the ORAC assay is based on a hydrogen atom transfer mechanism, and determines the radical-quenching ability of an antioxidant by hydrogen donation.

2.1.1 Activity-guided fractionation of aged garlic extract (AGE)

Aliquots of the aged garlic extract were separated by means of preparative RP18-HPLC to give four fractions (**Figure 15**), which were freed from solvent under vacuum. All fractions were redissolved in the same volume of assay solution to prepare them in their original concentration ratios, and were then analyzed in their antioxidant activity using the HPS and the ORAC assay, respectively. As a result of the assays, fraction 4 was found out to have by far the highest antioxidant activity accounting for 80 and 50% of the entire AGE in the HPS and the ORAC assay, respectively (**Figure 16**). In comparison, fraction 1 showed the second highest but only marginal activity in the HPS assay and did not exhibit any activity in the ORAC assay, whereas the contrary was observed for fraction 3. Fraction 2 did not show any activity in the assays used.

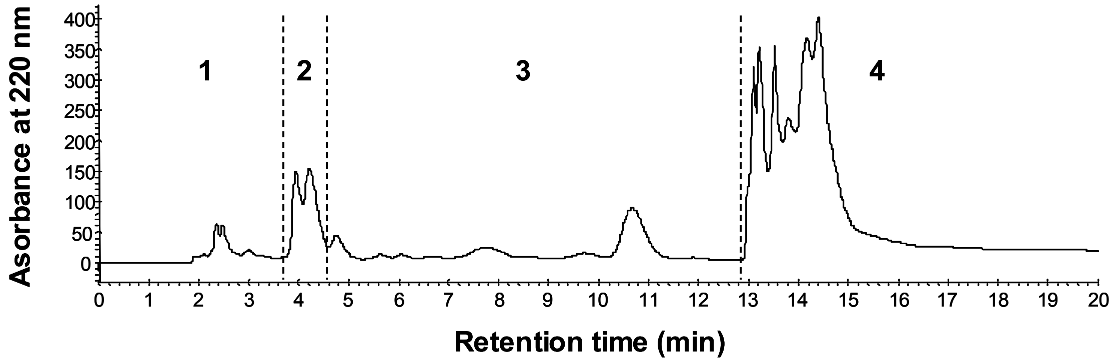

Figure 15: Flash RP-18 HPLC chromatogram of AGE separation.

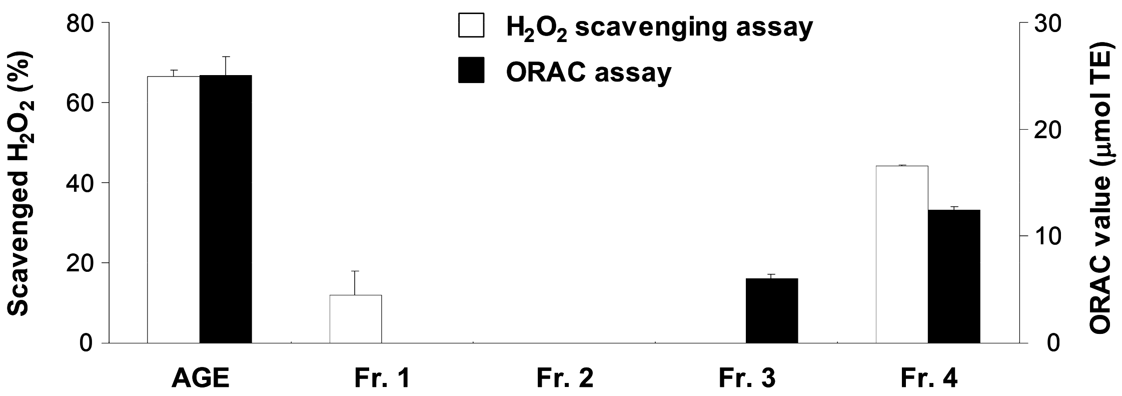

Figure 16: Antioxidant activity of total AGE and its fractions. Error bars represent S.D. of triplicate studies in the HPS assay and S.D. of quadruplicate studies in the ORAC assay.

UPLC-MS/MS screening of AGE for the known Amadori antioxidant *N*α-(1-deoxy-D-fructos-1-yl)-L-arginine (**1'**, **Figure 12**), followed by cochromatography with the synthetic reference substance, revealed this Amadori compound to be present in fraction 1 (**Figure 17**). As *N*α-(1-deoxy-D-fructos-1-yl)-L-arginine (**1'**) was absent in fraction 4, this most active fraction was analyzed for unknown antioxidants.

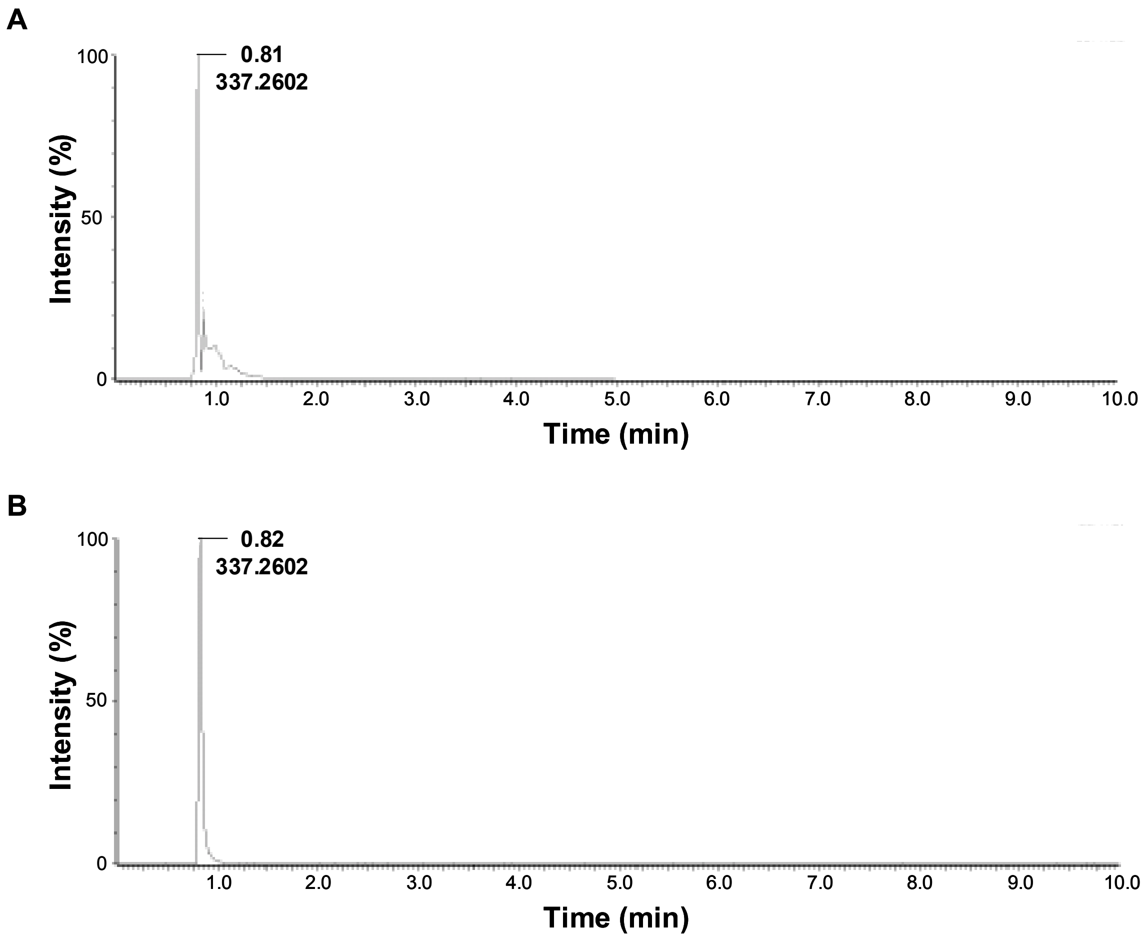

Figure 17: UPLC-MS/MS chromatogram for screening of *N*α-(1-deoxy-D-fructos-1-yl)-L-arginine (**1'**) using UPLC-MS/MS. **A**: Ffraction 1. **B**: Rreference compound of **1'**.

In order to identify the key antioxidants in AGE, fraction 4 was further separated by means of RP-HPLC to give a total of 16 subfractions, namely, fraction 4-1 to 4-16 (**Figure 18**). These subfractions were analyzed for their antioxidant activities using the HPS and the ORAC assay, respectively (**Figure 19**). The highest antioxidant activity in both assays was observed for subfractions 4-9 and 4-15, followed by subfractions 4-12 to 4-14, and 4-16. As a result, relatively hydrophobic subfractions showed high antioxidant activity, whereas relatively hydrophilic subfractions exhibited no or low activity.

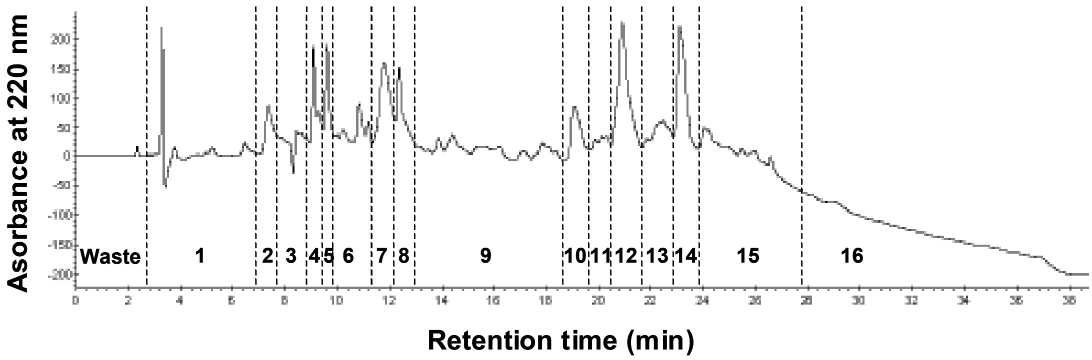

Figure 18: HPLC chromatogram and separation of fraction 4 obtained by preparative HPLC system.

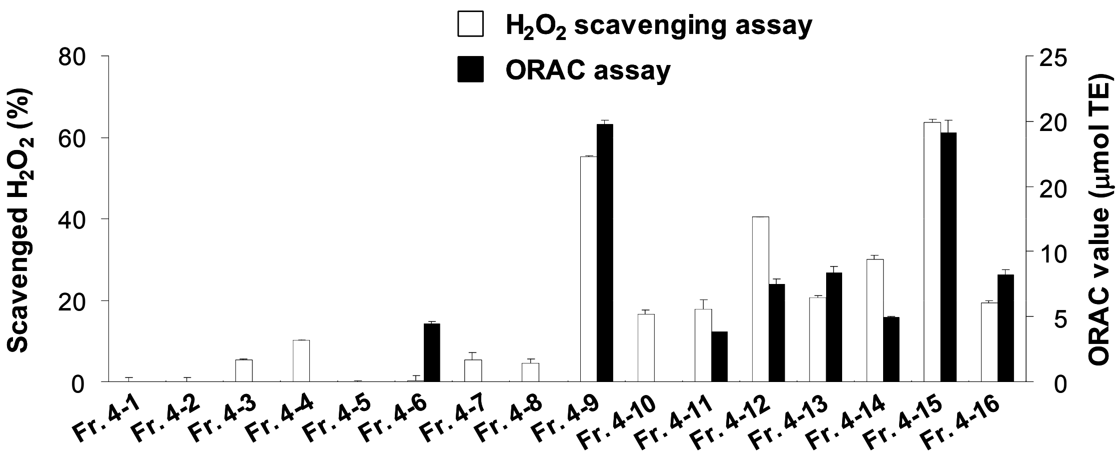

Figure 19: Antioxidant activity of fraction 4 and its subfractions. Error bars represent S.D. of triplicate studies in the HPS assay and S.D. of quadruplicate studies in the ORAC assay.

Rechromatography of subfractions derived from fraction 4, followed by HPLC-MS/MS analysis, revealed the presence of the tetrahydro-β-carboline derivatives (**2'**-**5'**, **Figure 12**), reported previously as antioxidants in AGE (*Ichikawa et al., 2002*). HPLC-MS/MS analysis, followed by cochromatography with the corresponding reference compound, led to the identification of (*1R*,*3S*)-1-methyl-1,2,3,4-tetrahydro-β-carboline-3-carboxylic acid (**2'**) and (*1S*,*3S*)-1-methyl-1,2,3,4-tetrahydro-β-carboline-3-carboxylic acid (**3'**) in fraction 4-11 and 4-13 (**Figure 20**), (*1R*,*3S*)-1-methyl-1,2,3,4-tetrahydro-β-carboline-1,3-dicarboxylic acid (**4'**) in fraction 4-9, and (*1S*,*3S*)-1-methyl-1,2,3,4-tetrahydro-β-carboline-1,3-dicarboxylic acid (**5'**) in fraction 4-11 (**Figure 21**). Further fractionation of these fractions and antioxidant assay of their subfractions revealed these tetrahydro-β-carbolines as one of the main antioxidants in each fraction. Although a series of investigation of other potent fractions 4-12, 4-15 and 4-16 were carried out, major constituents could not be isolated in the purity and amounts needed for an unequivocal structure determination by NMR spectroscopy.

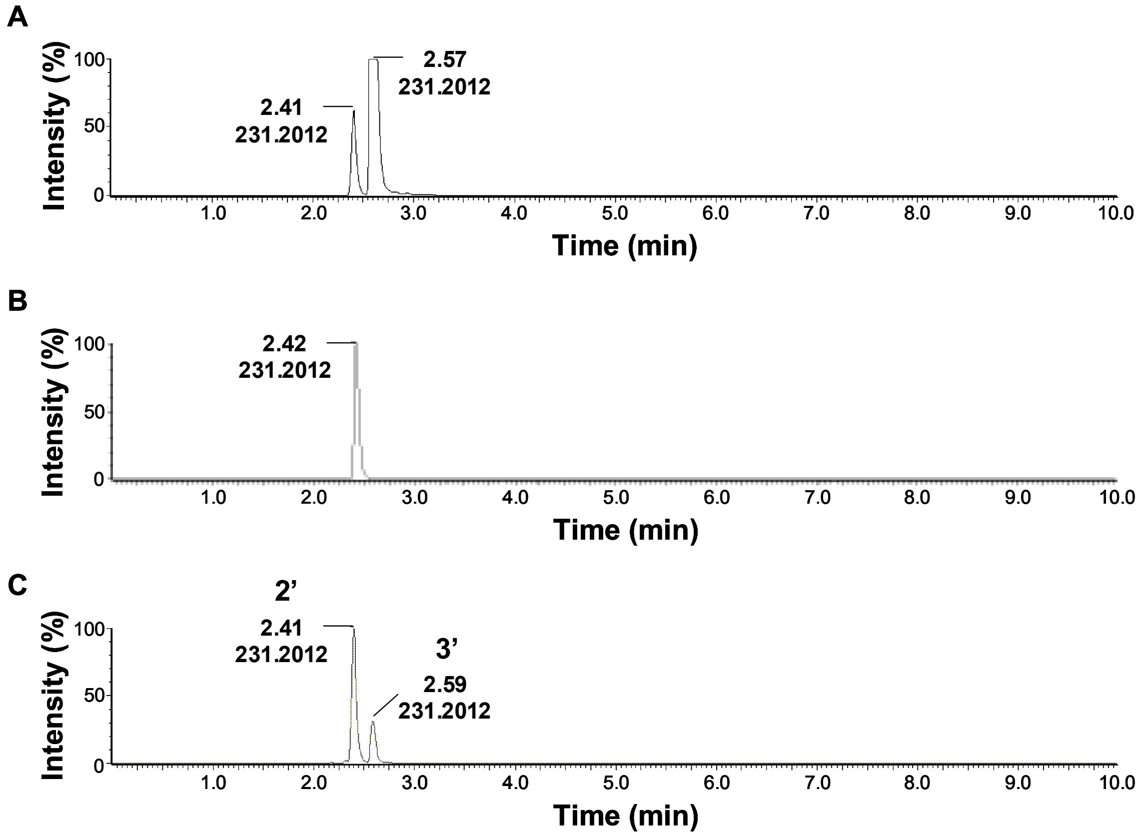

Figure 20: UPLC-MS/MS chromatogram for screening of tetrahydro-β-carboline-3-carboxylic acids using UPLC-MS/MS. **A**: Ffraction 4-13. **B**: Fraction 4-11. **C**: Reference mixture of (*1R*,*3S*)-1-methyl-1,2,3,4-tetrahydro-β-carboline-3-carboxylic acid (**2'**) and (*1S*,*3S*)-1-methyl-1,2,3,4-tetrahydro-β-carboline-3-carboxylic acid (**3'**).

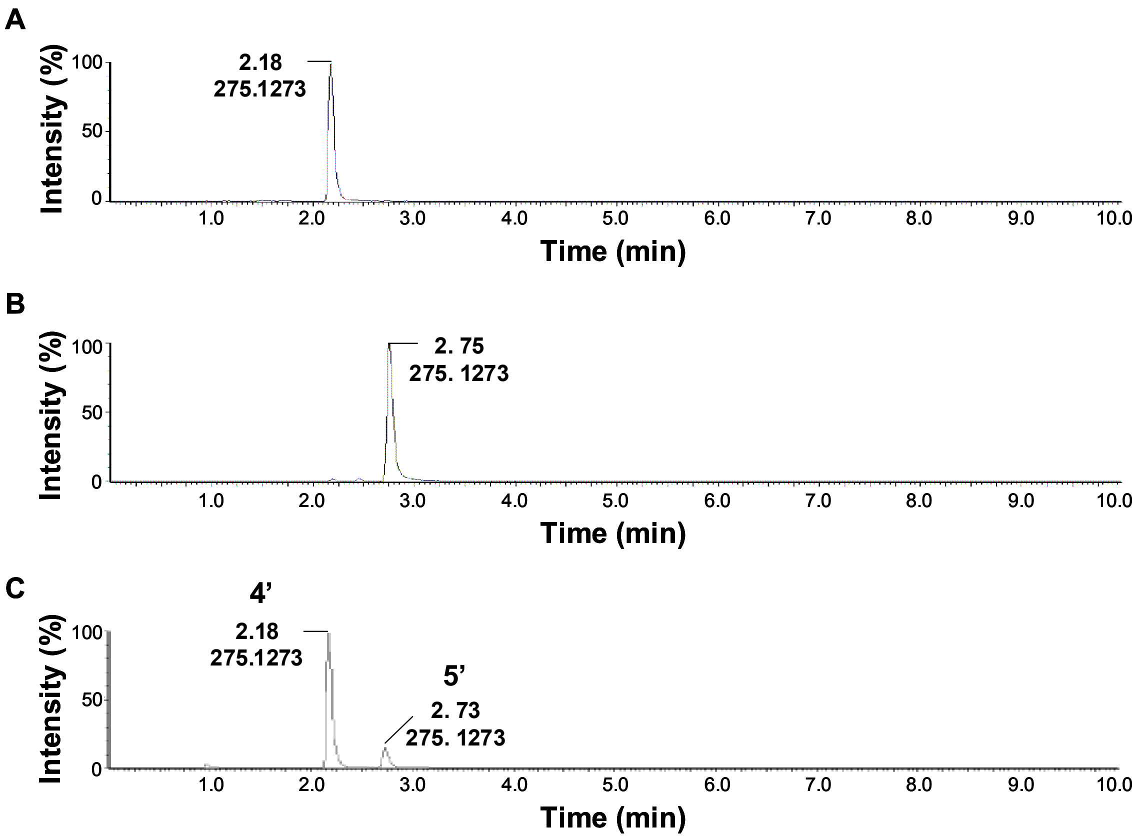

Figure 21: UPLC-MS/MS chromatogram for screening of tetrahydro-β-carboline-1,3-dicarboxylic acids using UPLC-MS/MS. **A**: Fraction 4-9. **B**: Fraction 4-11. **C**: Reference mixture of (*1R*,*3S*)-1-methyl-1,2,3,4-tetrahydro-β-carboline-1,3-dicarboxylic acid (**4'**) and (*1S*,*3S*)-1-methyl-1,2,3,4-tetrahydro-β-carboline-1,3-dicarboxylic acid (**5'**).

Since rechromatography of the active subfraction 4-14 showed one major peak and several minor peaks, 11 subfractions were isolated by means of RP-HPLC, namely, fraction 4-14.1 to 4-14.11 (**Figure 22**). Analysis of these fractions by means of the antioxidant assays revealed that the most potent fraction 4-14.6 contains active key compounds (**Figure 23**). Ffractions 4-14.2, 4-14.4, 4-14.7, and 4-14.9 also showed relatively high antioxidant activities, although these fractions contained a vast number of minor compounds. Since chromatography of the AGE ethyl acetate extract revealed the ethyl acetate solubles to contain the compounds of interest in clearly higher amounts than the water extract, the corresponding fraction 4-14.6 was separated from the ethyl acetate extract to obtain enough material for structure determination. Rechromatography of this fraction using acetonitrile as mobile phase indicated the presence of two major antioxidants (**1** and **2**) showing UV absorption maxima at 232 and 281 nm (**Figure 24**). In addition, fraction 4-14.2 and fraction 4-14.9, which exhibited strong activity as well, were further fractionated and assayed. No single compound, however, could be isolated in the purity and amounts required for NMR experiments.

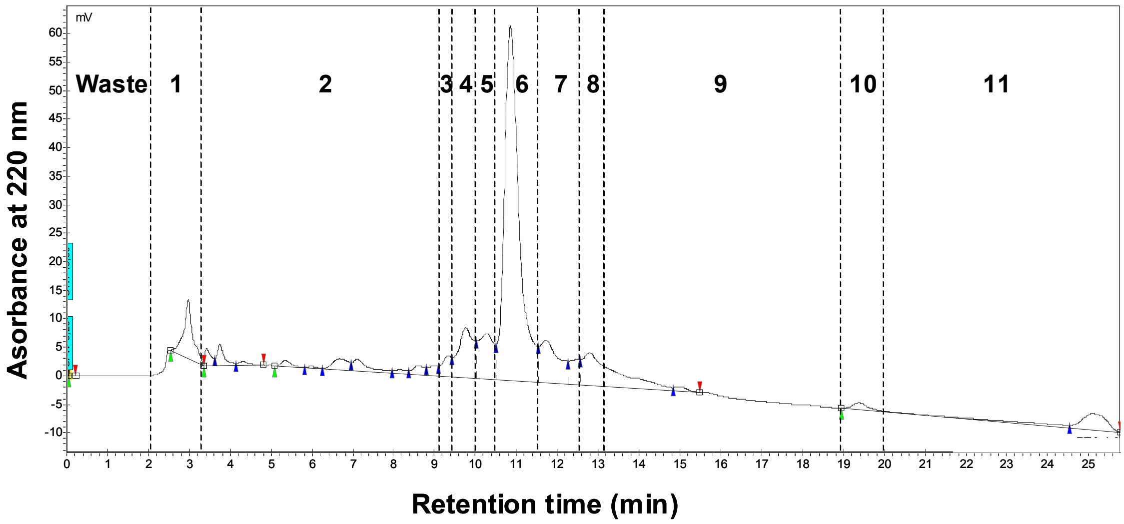

Figure 22: HPLC chromatogram and separation of fraction 4-14 obtained by preparative HPLC system.

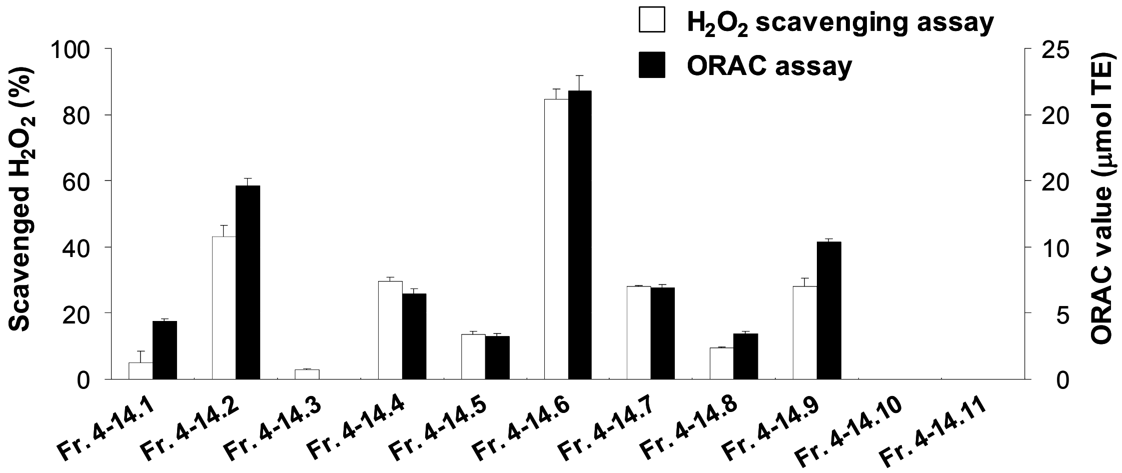

Figure 23: Hydrogen peroxide scavenging activities (error bars represent S.D. of triplicate studies) and ORAC values (error bars represent S.D. of quadruplicate studies) of fraction 4-14 and its subfractions.

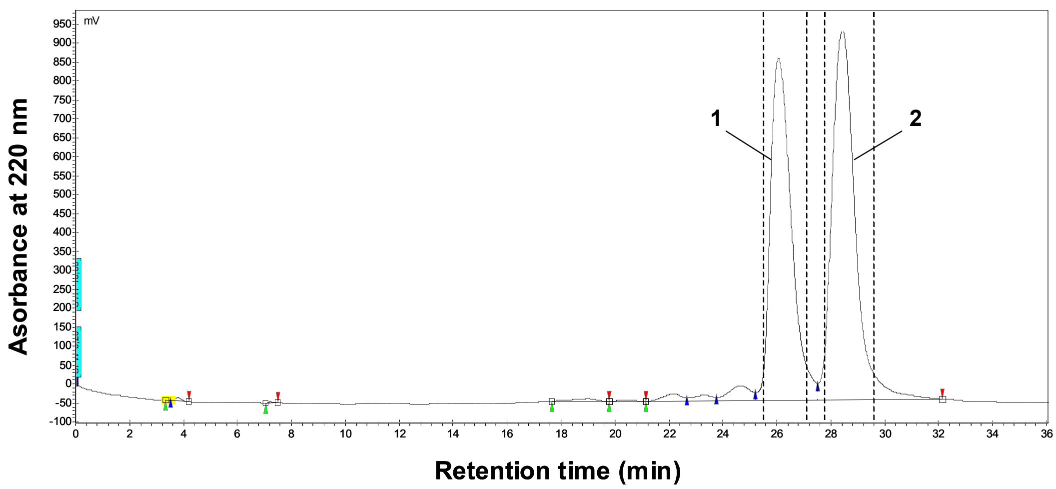

Figure 24: HPLC chromatogram of fraction 4-14.6 and separation of antioxidants **1** and **2**.

2.1.2 Structure determination of antioxidants 1 and 2 isolated from fraction 4-14.6

In order to determine the structures of antioxidants **1** and **2** isolated from AGE, UPLC-TOF-MS analysis and 1D- and 2D-NMR experiments were performed. UPLC-TOF-MS spectrum of compound **1** indicated a pseudo molecular ion of *m/z* 359.1497 for $[M{-}H]^-$, which is in accordance with the calculated exact mass of $[C_{20}H_{24}O_6{-}H]^-$ (*m/z* 359.1495) (**Figure 25**). MS analysis also gave two fragment ions (*m/z* 341.1391 and 329.1391), which matched the empirical formula of $[C_{20}H_{22}O_5{-}H]^-$ (calculated *m/z* 341.1389) and $[C_{19}H_{22}O_5{-}H]^-$ (calculated *m/z* 329.1389), most likely formed by elimination of water (−18 Da) and formaldehyde (−30 Da), respectively.

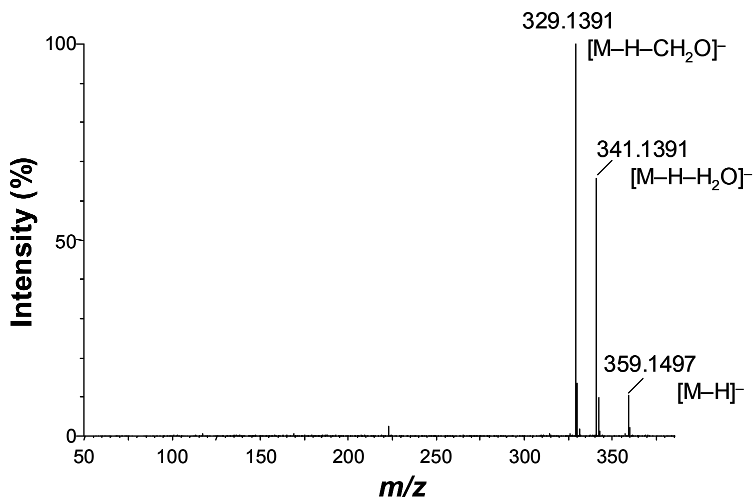

Figure 25: UPLC-HRMS spectrum of compound **1**.

A similar mass spectrum was observed of compound **2**, which resulted in a pseudo molecular ion *m/z* 357.1350 for $[C_{20}H_{22}O_6{-}H]^-$ (calculated *m/z* 357.1338) and the fragment ions *m/z* 339.1240 and 327.1240, being well in alignment with the cleavage of water and formaldehyde, respectively (**Figure 26**). *Morreel et al.* (*2010*) reported fragmentation of monolignol-derived dehydrodimers leads to water and formaldehyde cleavage as the major product ions (**Figure 27**). Therefore, compounds **1** and **2** were suggested to exhibit dilignol structures and give fragmentation ions due to the elimination of water and formaldehyde in MS spectrum.

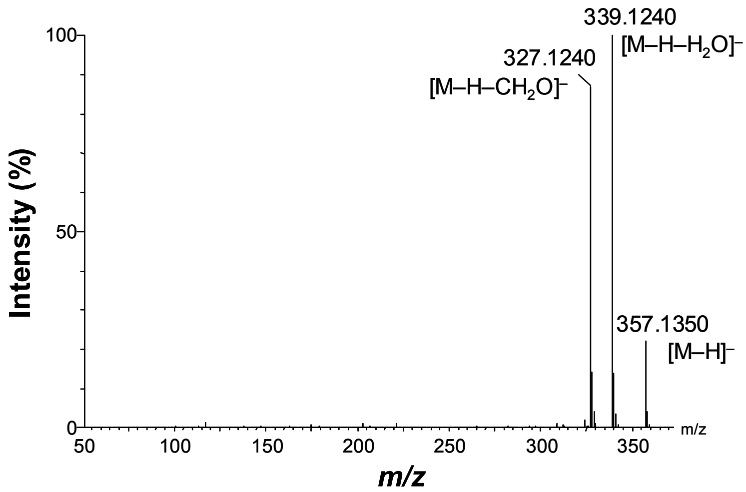

Figure 26: UPLC-HRMS spectrum of compound **2**.

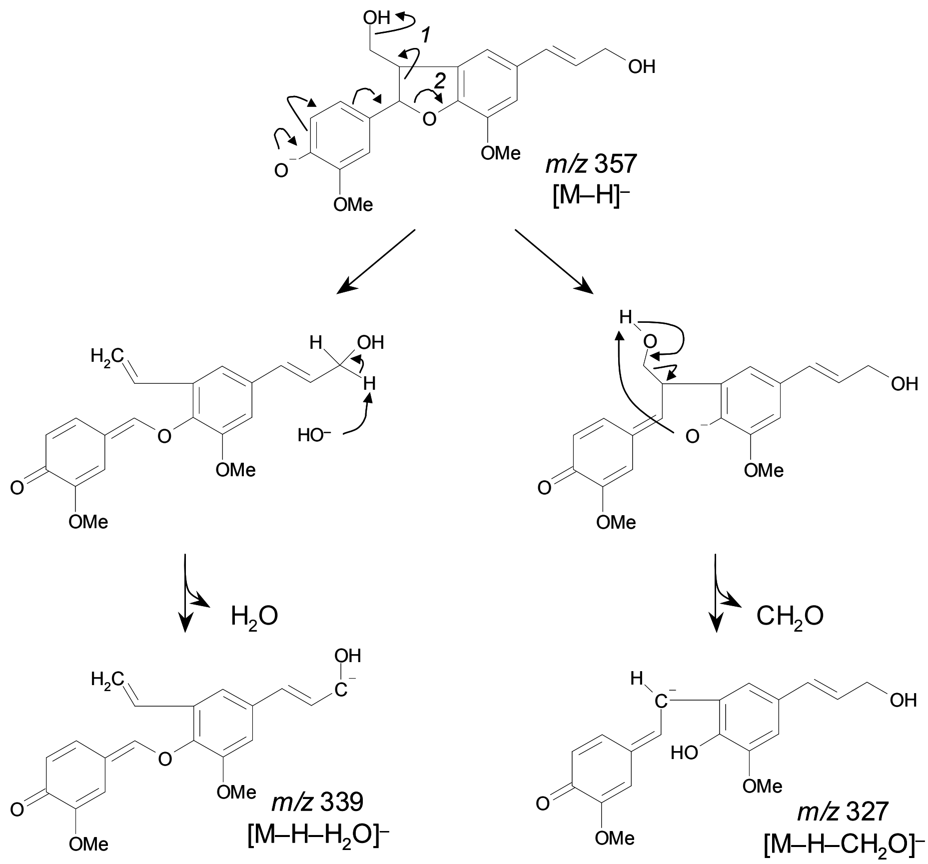

Figure 27: Putative fragmentation pathway of dehydrodiconiferyl alcohol (**2**) (*Morreel et al., 2010*).

The ^{1}H NMR and ^{13}C NMR data of compound **1** and **2** were summarized in **Table 5**. The protons on the two methoxy groups were observed between 3.72-3.73 ppm in the ^{1}H NMR experiment of compound **1**. In addition, the ^{1}H NMR spectrum of compound **1** showed aromatic proton signals for H−C(2'), H−C(6'), and H−C(5') with chemical shifts at 7.04, 6.89, and 6.81 ppm, respectively, which indicated the presence of a 1,3,4-trisubstituted benzene ring. Another correlating aromatic protons, H−C(4) and H−C(6), were observed at 6.75 and 6.73 ppm showing meta-coupling with a coupling constant of J = 1.6 Hz, which indicated the presence of a 1,2,3,5-tetrasubstituted benzene ring. Moreover, three aliphatic protons coupling with each other were observed at 5.52 ppm [d, 1H, J = 6.6 Hz, H−C(2)], 3.51 ppm [dd, 1H, J = 6.4, 6.6 Hz, H−C(3)] and 3.76−3.92 ppm [m, 2H, H−C(11)], and another three aliphatic protons were observed at 3.57 ppm [t, 2H, J = 6.4 Hz, H−C(10)], 2.62 ppm [t, 2H, J = 7.7 Hz, H−C(8)] and 1.79 ppm [m, 2H, J = 6.4, 7.7 Hz, H−C(9)], which coupled with each other. Well in accordance with the molecular formula proposed by TOF-MS experiment, 20 carbon signals were detected in the ^{13}C NMR spectrum of compound **1**. Comparison of data obtained by means of ^{13}C NMR and DEPT-135 experiment revealed nine primary or tertiary carbons, four secondary carbons, and seven quaternary carbon atoms. A heteronuclear multiple-bond correlation spectroscopy (HMBC) experiment revealed that compound **1** is composed of two phenylpropanoids (**Figure 28**). The HMBC experiment exhibits correlations of H−C(2) with C(3a) and C(7a), H−C(3) with C(4), C(3a) and C(7a), and H−C(11) with only C(3a), thus implying that C(2) and C(3) of a phyenylpropanoid are connected to an aromatic ring of another phenylpropanoid through an *O*-linkage and a *C*-linkage, respectively. Taking all spectroscopic data into consideration, compound **1** was unequivocally identified as dihydrodehydrodiconiferyl alcohol. Although this compound was earlier reported to be a novel constituent in *Cleistopholis glauca* (*Seidel et al., 2000*) and *Sarcandra glabra* (*Wu et al., 2012a*), this is the first report on the presence of **1** as an antioxidant in garlic.

Table 5: ^{1}H and ^{13}C NMR data of antioxidants **1** and **2**.

Position	(–)-(*2R*,*3S*)-Dihydrodehydrodiconiferyl alcohol (**1**)		(+)-(*2S*,*3R*)-Dehydrodiconiferyl alcohol (**2**)	
	^{1}H NMR	^{13}C NMR	^{1}H NMR	^{13}C NMR
2	5.52 (1H, d, *J* = 6.6 Hz)	88.18	5.57 (1H, d, *J* = 6.5 Hz)	88.55
3	3.51 (1H, m, *J* = 6.1, 6.4 Hz)	55.10	3.54 (1H, m, *J* = 6.1, 6.4 Hz)	54.81
3a	–	130.00	–	130.44
4	6.75 (1H, d, *J* = 1.6 Hz)	117.57	6.98 (1H, d, *J* = 1.6 Hz)	116.10
5	–	136.30	–	131.95
6	6.73 (1H, d, *J* = 1.6 Hz)	113.89	6.95 (1H, d, *J* = 1.6 Hz)	111.71
7	–	144.89	–	145.20
7a	–	147.35	–	148.98
7-OMe	3.83 (3H, s)	56.42	3.87 (3H, s)	56.39
8	2.62 (2H, t, *J* = 7.7 Hz)	36.00	6.53 (1H, d, *J* = 15.9 Hz)	130.54
9	1.79 (2H, tt, *J* = 6.4, 7.7 Hz)	36.00	6.25 (1H, dt, *J* = 5.3, 15.9 Hz)	128.41
10	3.57 (2H, t, *J* = 6.4 Hz)	61.84	4.20 (2H, d, *J* = 5.3 Hz)	63.43
11	3.76 - 3.92 (2H, m)	64.78	3.79 - 3.93 (2H, m)	64.64
1’	–	134.70	–	134.42
2’	7.04 (1H, d, *J* = 1.9 Hz)	110.45	7.04 (1H, d, *J* = 1.9 Hz)	110.49
3’	–	148.35	–	148.39
3’-OMe	3.82 (3H, s)	56.27	3.82 (3H, s)	56.28
4’	–	147.19	–	147.32
5’	6.81 (1H, d, *J* = 8.2 Hz)	115.64	6.81 (1H, d, *J* = 8.2 Hz)	115.69
6’	6.89 (1H, dd, *J* = 1.9, 8.2 Hz)	119.54	6.89 (1H, dd, *J* = 1.9, 8.1 Hz)	119.61

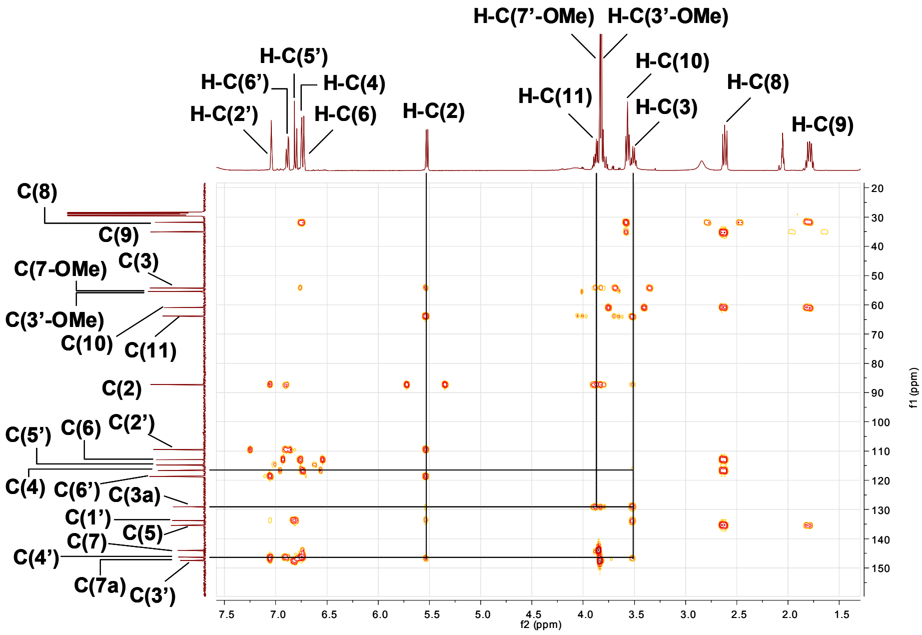

Figure 28: HMBC spectrum (400 MHz, acetone-d_6) of (–)-(2*R*,3*S*)-dihydrodehydrodiconiferyl alcohol (**1**).

The ^{1}H NMR signal pattern of compound **2** was similar to that of **1**. However, clear difference was observed in aliphatic proton signals H−C(8) and H−C(9) resonating at 6.53 ppm [d, 1H, *J* = 15.9 Hz] and 6.25 ppm [dt, 1H, *J* = 5.3, 15.9 Hz], respectively. A large coupling constant of *J* = 15.9 Hz indicated a *trans*-configured double bond between C(8) and C(9). With a detailed spectral assignment by means of heteronuclear correlation experiments (HSQC, HMBC), compound **2** was unequivocally identified as dehydrodiconiferyl alcohol (**Figure 29**). This is the first report of compound **2** in garlic, although this compound has been identified in *Rosa multiflora* (*Yeo et al., 2004*) and *Diplomorpha canescens* (*Devkota et al., 2012*).

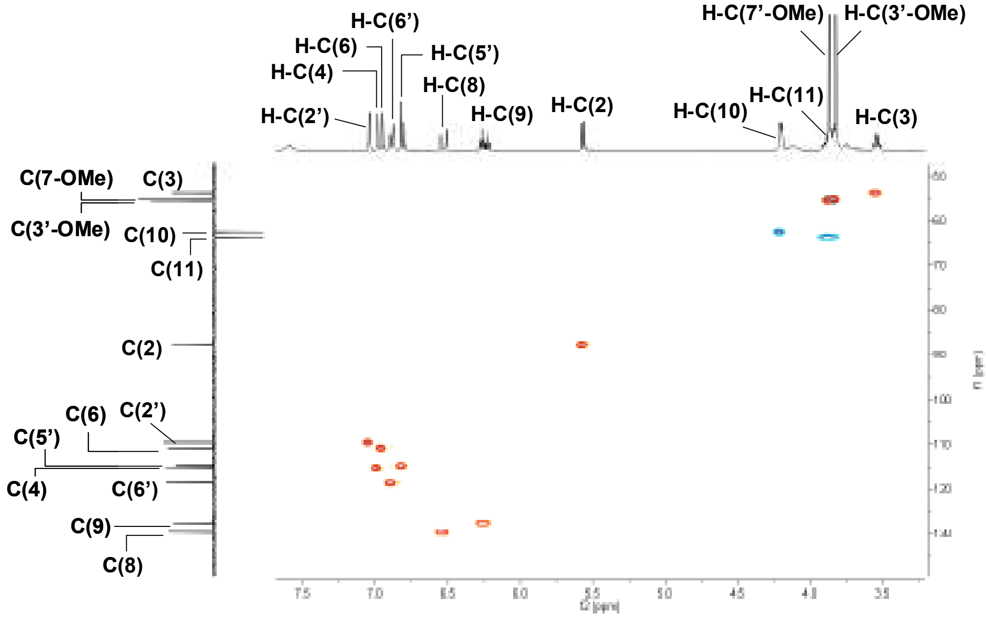

Figure 29: HSQC spectrum (400 MHz, acetone-d_6) of (+)-(2*S*,3*R*)-dehydrodiconiferyl alcohol (**2**).

The main spectroscopic differences between *cis*- and *trans*-stereoisomers of dilignols are due to H−C(2). The ^{1}H NMR signal of H−C(2), which appeared as a doublet at 5.52 ppm (J = 6.6 Hz) of compound **1** and at 5.57 ppm (J = 6.5 Hz) of compound **2**, clearly indicated the relative stereochemistry as *trans*-configured in both compounds (*García-Muñoz et al., 2005*). To confirm the absolute configuration of carbon atoms C(2) and C(3) in **1** and **2**, both compounds were analyzed by means of circular dichroism (CD) spectroscopy and the obtained data were compared with those reported in literature. As depicted in **Figure 30**, the CD spectrum of **1** showed a positive Cotton effect at 224 nm and negative Cotton effects at 242 and 294 nm. Since this data is well in line with the data published for the (–)-(2*R*,3*S*)-configumer (*Fukuyama et al., 1996; Matsuda et al., 1996*), the structure of compound **1** could be determined as (–)-(2*R*,3*S*)-dihydrodehydrodiconiferyl alcohol (**Figure 31**). On the other hand, the CD spectrum of **2,** exhibiting a negative Cotton effect at 231 nm and a positive Cotton effect at 286 nm (**Figure 30**), was in agreement with literature data for (+)-(2*S*,3*R*)-configumer (*Hirai et al., 1994*). Thus, the structure of compound **2** could be deduced as (+)-(2*S*,3*R*)-dehydrodiconiferyl alcohol (**Figure 31**).

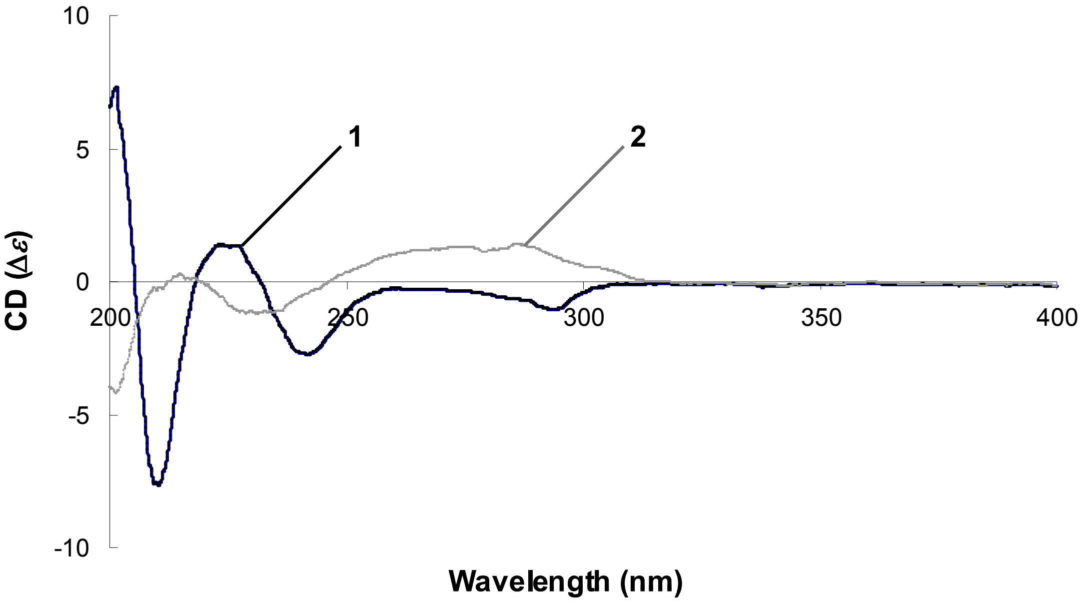

Figure 30: CD spectra of (–)-(*2R*,*3S*)-dihydrodehydrodiconiferyl alcohol (**1**) and (+)-(*2S*,*3R*)-dehydrodiconiferyl alcohol (**2**).

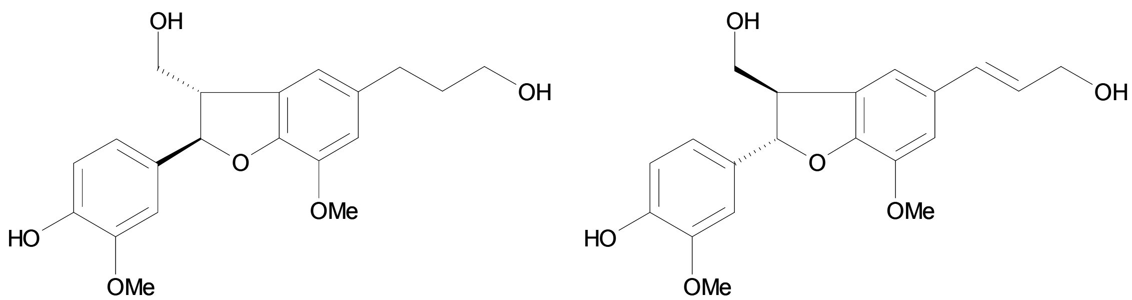

1 **2**

Figure 31: Chemical structures of (–)-(*2R*,*3S*)-dihydrodehydrodiconiferyl alcohol (**1**) and (+)-(*2S*,*3R*)-dehydrodiconiferyl alcohol (**2**).

2.1.3 Synthesis and identification of dilignols in aged garlic extract (AGE)

Dehydrodiconiferyl alcohol (**2**) was reported to be produced by dimeric dehydrogenation of coniferyl alcohol (**6'**) through an enzymatic radical coupling of a β-radical of one coniferyl alcohol unit with a 5-radical of another coniferyl alcohol unit (*Reale et al., 2010*), while dihydrodehydrodiconiferyl alcohol (**1**) is proposed to be produced by allylic bond-reduction of **2** (*Gang et al., 1999*). As coniferyl alcohol (**6'**, **Figure 32**) is reported to dimerize frequently to form β-O-4 intermolecular linkages (*Adler, 1977*), the dilignols with a β-O-4 linkage was expected to be present in AGE as well.

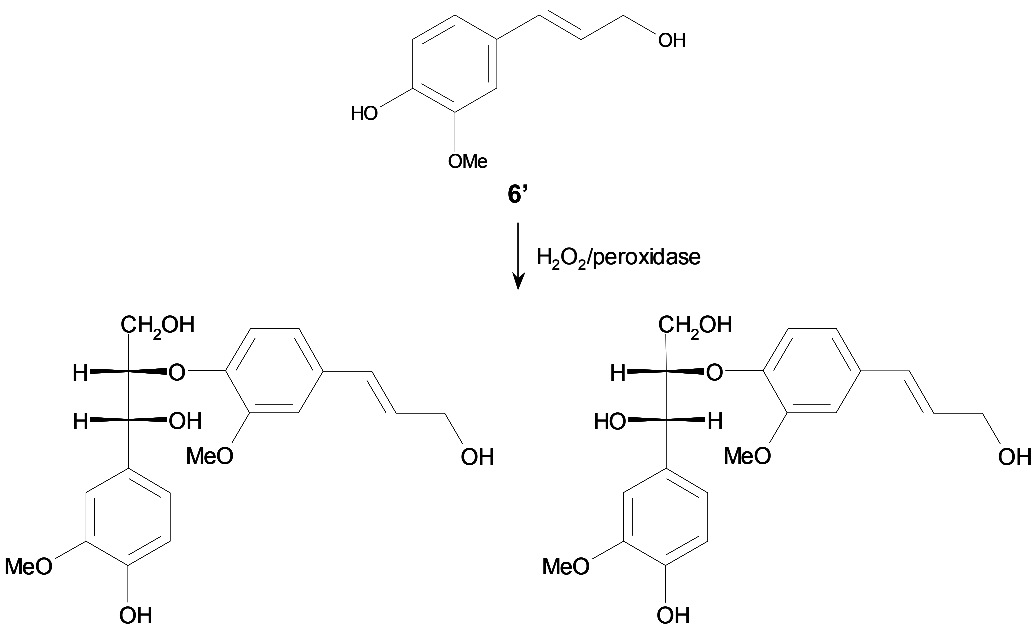

3 4

Figure 32: Preparation of *erythro*-guaiacylglycerol-β-O-4'-coniferyl ether (**3**) and *threo*-guaiacylglycerol-β-O-4'-coniferyl ether (**4**) by oxidative coupling of coniferylal cohol (**6'**) by H_2O_2 and horseradish peroxidase.

Therefore, reference compounds of the β-O-4 linked dilignols **3** and **4** (**Figure 32**) were synthesized by dehydrogenative polymerization of coniferyl alcohol (**6'**) as reported before (*Ito et al., 2002*). Oxidative coupling of coniferyl alcohol (**6'**) by hydrogen peroxide in the presence of horseradish peroxidase led to the reaction products **3** and **4** as well as dehydrodiconiferyl alcohol shown in **Figure 33**.

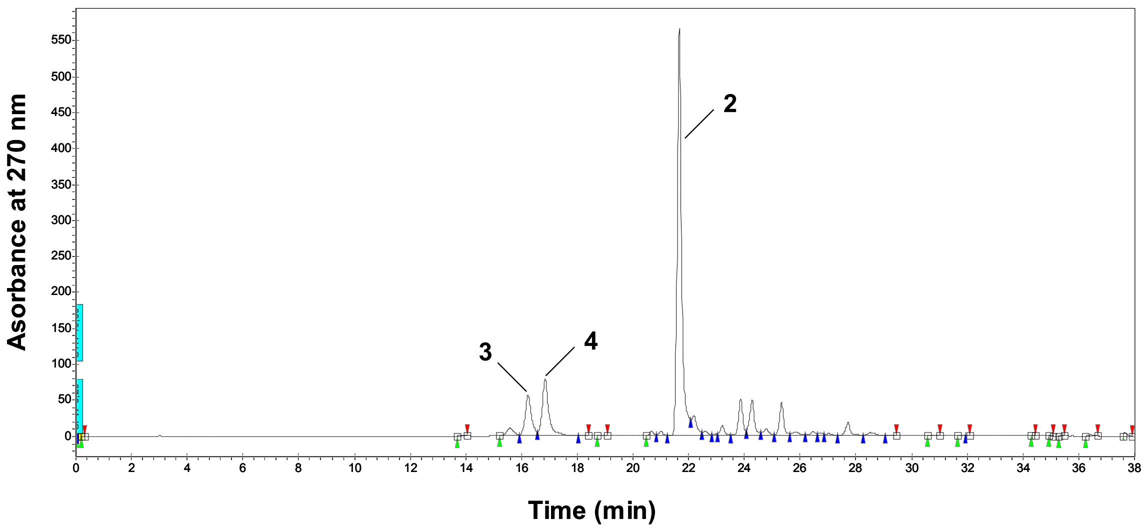

Figure 33: Preparative HPLC chromatogram of reaction products formed from coniferyl alcohol (**6'**) in the presence of H_2O_2 and horseradish peroxidase.

After isolation and purification of the products by means of RP-HPLC, LC-ESI-TOF-MS analysis was carried out with the purified products **3** and **4**, indicating pseudo molecular ions of *m/z* 375.1446 and 375.1447, respectively, which are both well in agreement with the calculated exact mass of $[C_{20}H_{24}O_7{-}H]^-$ (*m/z* 375.1444) (**Figure 34**).

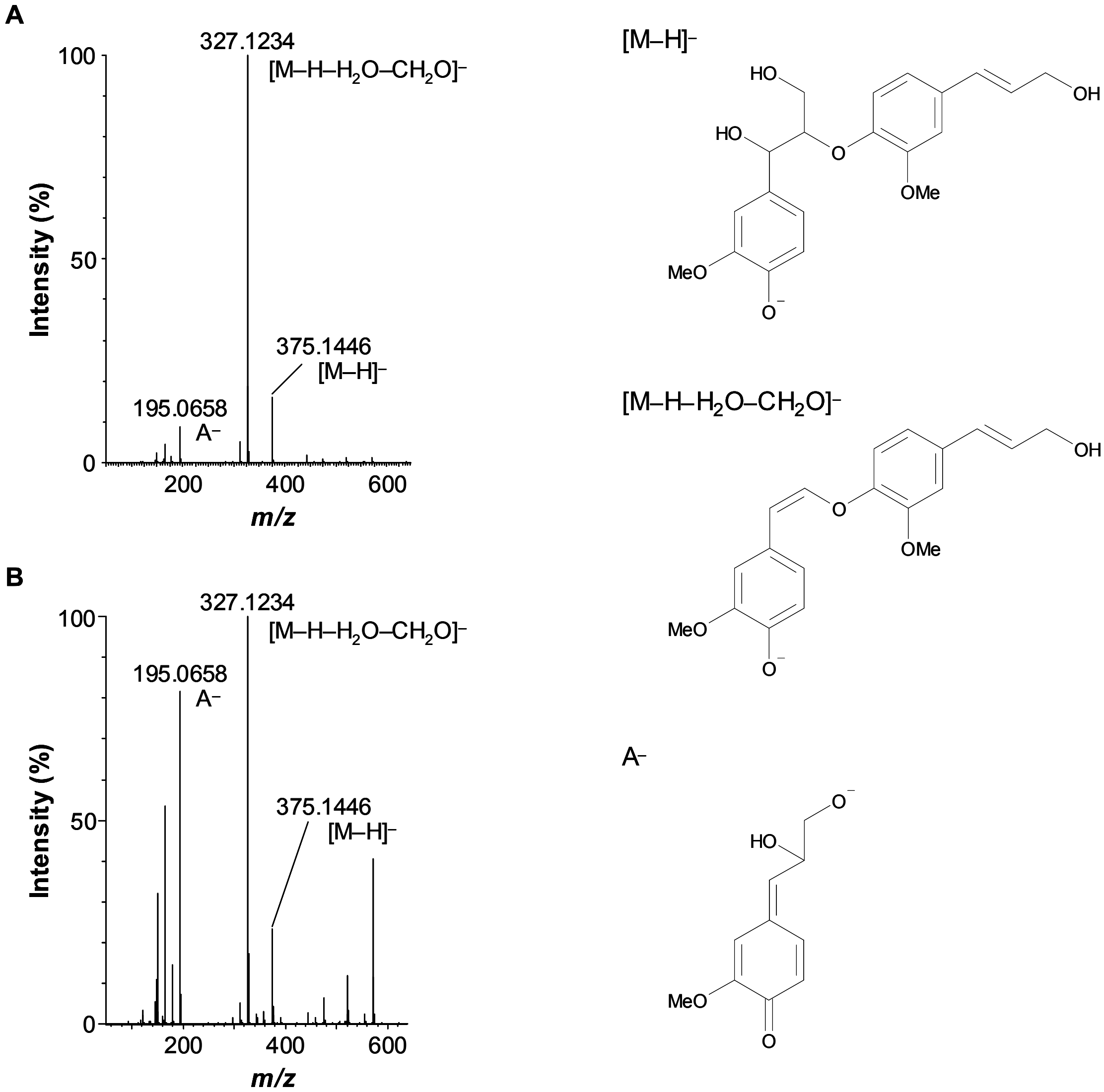

Figure 34: UPLC-HRMS spectra of synthesized compounds and putative structures for the pseudo molecular ions and their fragment ions. A: *erythro*-Guaiacylglycerol-β-O-4'-coniferyl ether (**3**). B: *threo*-Guaiacylglycerol-β-O-4'-coniferyl ether (**4**).

Morreel et al. (*2010*) reported these β-O-4 linked dilignols to show a loss of 48 Da and C-C cleavage, providing $[M{-}H{-}H_2O{-}CH_2O]^-$ (calculated *m/z* 327.1235) and A^- (calculated *m/z* 195.0657), where A is the moiety from the phenolic end group. The ^{1}H NMR and ^{13}C NMR experiments of compounds **3** and **4** showed major similarities (**Figure 35**), except for the proton signal H−C(7) with no coupling constant observed for **3** and a coupling constant of *J* = 5.8 for **4** (**Table 6**). Their chemical structures were unequivocally identified as *erythro*-guaiacylglycerol-β-O-4'-coniferyl ether (**3**) and *threo*-guaiacylglycerol-β-O-4'-coniferyl ether (**4**), respectively, by comparing the data of LC-MS, TOF-MS, and NMR spectroscopy with those reported in leterature (*Han et al., 2008,* and *Lourith et al., 2005*).

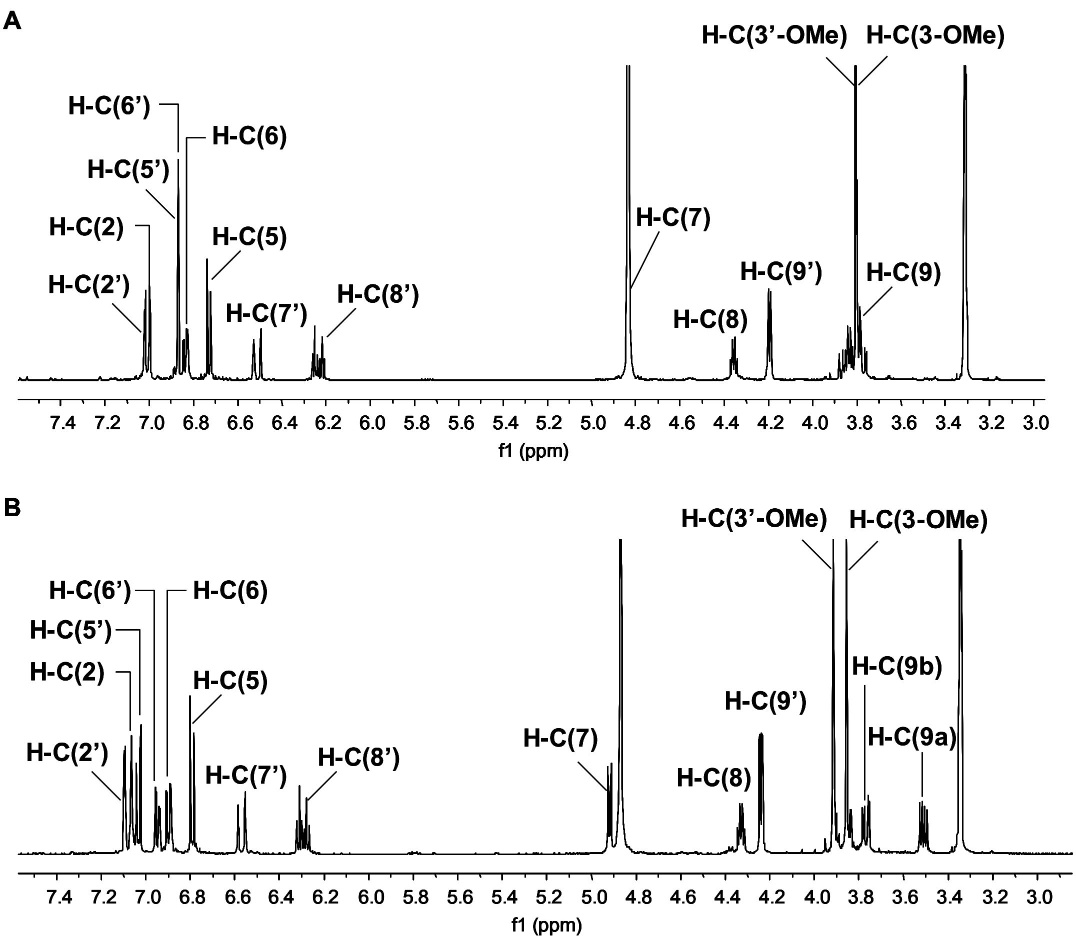

Figure 35: ^{1}H NMR spectra of synthesized compounds (500 MHz, methanol-*d4*). **A**: *erythro*-Guaiacylglycerol-β-O-4'-coniferyl ether (**3**). **B**: *threo*-Guaiacylglycerol-β-O-4'-coniferyl ether (**4**).

Table 6: ^{1}H and ^{13}C NMR data of compounds **3** and **4**.

Position	*erythro*-guaiacylglycerol-β-O-4'-coniferyl ether (**3**)		*threo*-guaiacylglycerol-β-O-4'-coniferyl ether (**4**)	
	^{1}H NMR	^{13}C NMR	^{1}H NMR	^{13}C NMR
1	–	134.10	–	133.79
2	7.02 (1H, d, *J* = 1.9 Hz)	111.90	7.06 (1H, d, *J* = 1.9 Hz)	111.76
3	–	148.72	–	148.84
3-OMe	3.80 (3H, s)	56.52	3.86 (3H, s)	56.55
4	–	147.04	–	147.20
5	6.73 (1H, d, *J* = 8.1 Hz)	115.66	6.79 (1H, d, *J* = 8.1 Hz)	115.85
6	6.84 (1H, dd, *J* = 1.8, 8.1 Hz)	121.04	6.90 (1H, dd, *J* = 1.9, 8.1 Hz)	120.75
7	4.82 (1H, overlapped)	74.12	4.92 (1H, d, *J* = 5.8)	74.04
8	4.35 (1H, m)	86.22	4.33 (1H, m)	87.14
9	3.80 (2H, m)	62.23	3.77 (1H, dd, *J* = 4.0, 11.9 Hz)	61.92
	–	–	3.51 (1H, dd, *J* = 5.3, 11.9 Hz)	–
1'	–	133.07	–	133.17
2'	7.00 (1H, s)	111.40	7.09 (1H, d, *J* = 1.9 Hz)	111.30
3'	–	151.93	–	151.77
3'-OMe	3.80 (3H, s)	56.34	3.91 (3H, s)	56.55
4'	–	148.96	–	149.27
5'	6.87 (1H, brs)	118.92	7.03 (1H, d, *J* = 8.3 Hz)	118.87
6'	6.87 (1H, brs)	120.66	6.95 (1H, dd, *J* = 1.9, 8.3 Hz)	120.81
7'	6.51 (1H, dt, *J* = 1.4, 15.9 Hz)	131.46	6.57 (1H, d, *J* = 15.9 Hz)	131.42
8'	6.24 (1H, dt, *J* = 5.8, 15.9 Hz)	128.51	6.30 (1H, dt, *J* = 5.7, 15.9 Hz)	128.63
9'	4.19 (2H, dd, *J* = 1.4, 5.8 Hz)	63.76	4.24 (2H, dd, *J* = 1.4, 5.7 Hz)	63.75

In order to investigate the presence of compounds **3** and **4** in AGE, the MS/MS parameters were tuned for each individual compound, and then AGE and its fractions were analyzed to screen these dilignols by means of UPLC-ESI-MS/MS. This MS screening, followed by cochromatography with the corresponding reference compounds led to the unequivocal identification of *erythro*-guaiacylglycerol-β-O-4'-coniferyl ether (**3**) and *threo*-guaiacylglycerol-β-O-4'-coniferyl ether (**4**) in AGE (**Figure 36**). Moreover, MS analysis revealed compound **3** and **4** to exist in fractions 4-12 and 4-13, respectively, indicating that these compounds contribute to the antioxidant activity of the fractions (**Figure 36**). Although these compounds were well known as major dehydrogenation products of coniferyl alcohol and identified in several plants, such as *Campylotropis hirtella* (*Han et al., 2008*) and *Brucea Javanica* (*Li et al., 1998*), this is the first report to show the presence of dilignols **3** and **4** in garlic.

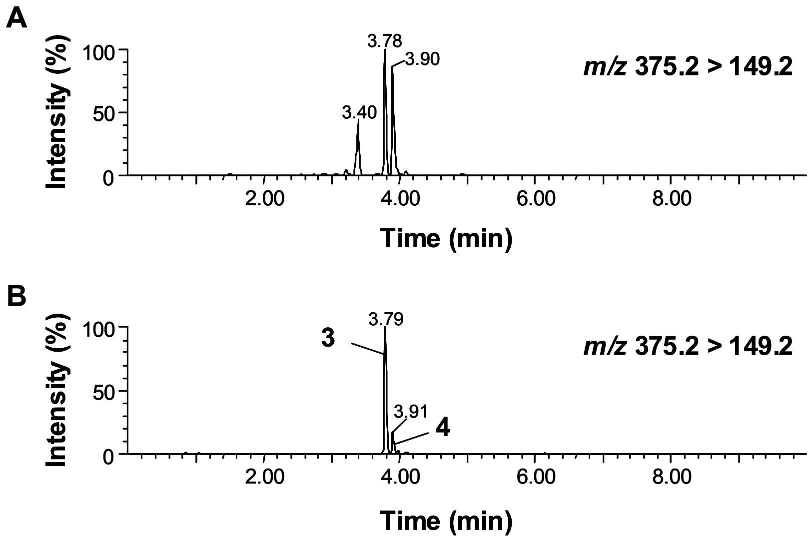

Figure 36: UPLC-MS/MS chromatogram for screening of *erythro*-guaiacylglycerol-β-O-4'-coniferyl ether (**3**) and *threo*-guaiacylglycerol-β-O-4'-coniferyl ether (**4**). **A**: AGE. **B**: Reference mixture of **3** and **4**.

2.2 Identification of antioxidants in AGE by targeted screening based on educated guess

2.2.1 Maillard reaction products

The non-enzymatic reaction between amino acids and reducing sugars, known as the Maillard reaction, occurs during food processing and storage. It leads to the formation of reaction products, which play a major role in food properties, such as flavor, taste and color, as well as in its nutritional and health aspects (*Labuza et al., 1994*). There are plenty of reports on biological activities of Maillard reaction products, such as *in vitro* antioxidant activity (*Delgado-Andrade et al., 2005* and *Martin et al., 2009*), antimicrobial activity (*Rurián-Henares et al., 2008*), and anticancer effect (*Yamabe et al., 2013*) as well as *in vivo* properties to suppress lipid peroxidation and to increase antioxidant activity of plasma (*Seiquer et al., 2008*).

*N*α-(1-Deoxy-D-fructos-1-yl)-L-arginine (**1'**, **Figure 12**), an antioxidant previously identified in AGE (*Ryu et al., 2001*), is an Amadori compound generated through the Maillard reaction (**Figure 37**). This compound was proved to be a product formed through the reaction of glucose with arginine during the aging process of garlic. Since a garlic and AGE are abundant in sugars and containing a large variety of amino acids, diverse Amadori compounds could be present in AGE and might be potent antioxidants. Therefore, the non-enzymatic reactions were carried out with glucose and amino acids present in AGE.

The reactions of glucose with characteristic sulfur-containing amino acids *S*-allyl-L-cysteine and γ-glutamyl-*S*-allyl-L-cysteine were carried out in glacial acetic acid under heating to prepare two Amadori compounds of the corresponding amino acids. UPLC-TOF-MS analysis of the former product in negative ionization mode (ESI^-) revealed a pseudo molecular ion $[M-H]^-$ of *m/z* 322.0965, being in accordance with the molecular formula of $[C_{12}H_{21}NO_7S-H]^-$ (calculated *m/z* 322.0960) as shown in **Figure 38-A**. Moreover, the presence of the corresponding amino acid residue was verified since the fragment ion of *m/z* 160.0438 was observed, having the empirical formula of $[C_6H_{11}NO_2S-H]^-$ (calculated *m/z* 160.0438). The chemical structure of this product was confirmed as *N*α-(1-deoxy-D-fructos-1-yl)-*S*-allyl-L-cysteine (**5**) by means of 1D- and 2D-NMR. UPLC-TOF-MS experiment of the latter product resulted in a pseudo molecular ion of *m/z* 451.1389 for $[M-H]^-$, being in agreement with the exact mass of *m/z* 451.1386, calculated for the elemental composition of $[C_{17}H_{28}N_2O_{10}S-H]^-$ (**Figure 38-B**). NMR spectra led to the identification of this product as *N*α-(1-deoxy-D-fructos-1-yl)-γ-glutamyl-*S*-allyl-L-cysteine (**6**). Another Amadori compound, *trans*-*N*α-(1-deoxy-D-fructos-1-yl)-γ-glutamyl-*S*-1-propenyl-L-cysteine (**7**), was courteously provided by the Chair of Food Chemistry and Molecular Sensory Science (Technische Universität München). Their structures were shown in **Figure 39**.

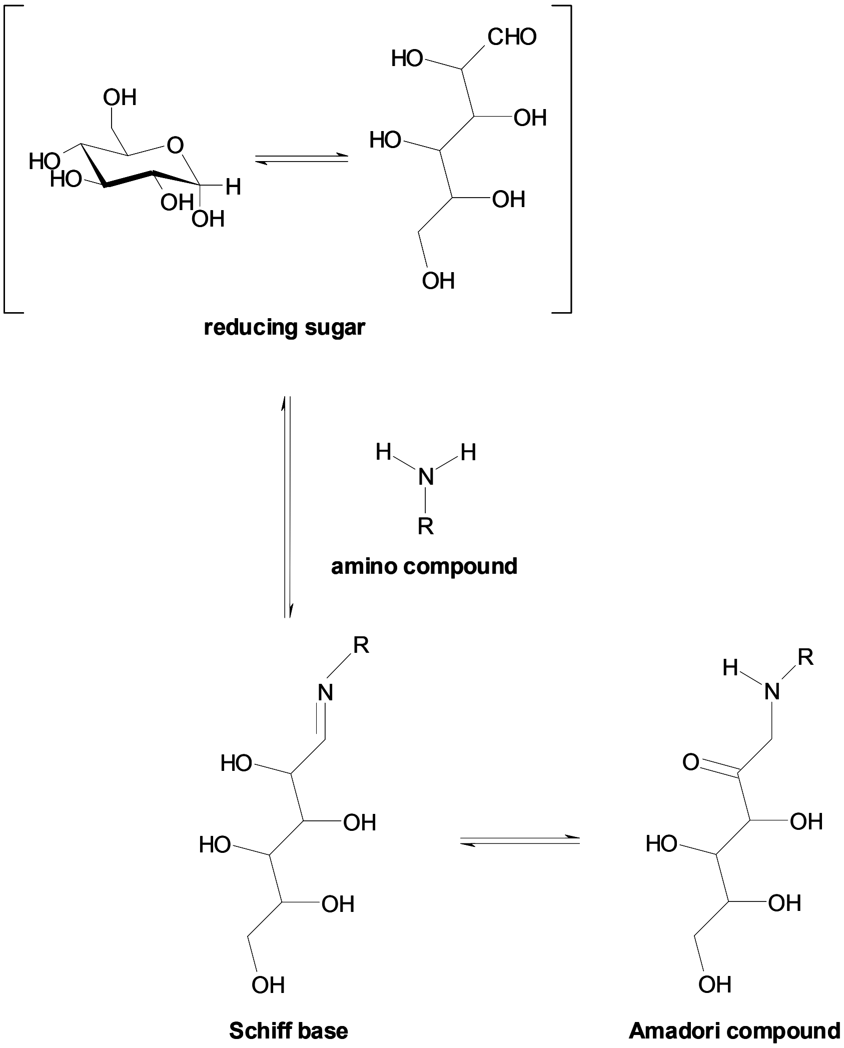

Figure 37: Schematic representation for generation of Amadori compound in the non-enzymatic Maillard reaction (taken from *Adrover et al., 2008*).

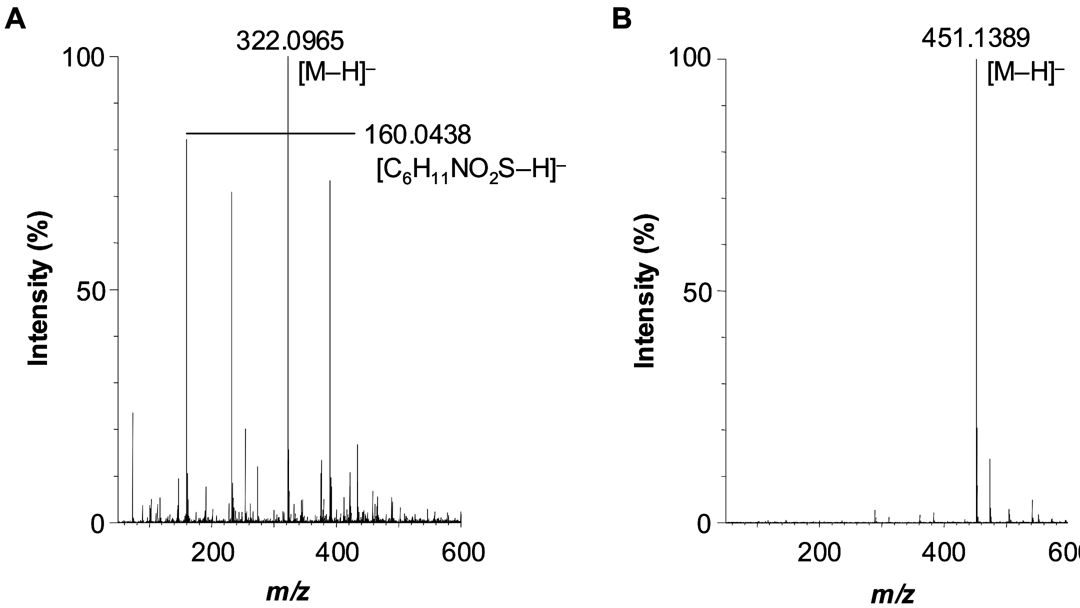

Figure 38: UPLC-ESI-HRMS spectra of synthesized Amadori compounds. **A:** *N*a-(1-Deoxy-D-fructos-1-yl)-*S*-allyl-L-cysteine (**5**). **B**: *N*a-(1-Deoxy-D-fructos-1-yl)-γ-glutamyl-*S*-allyl-L-cysteine (**6**).

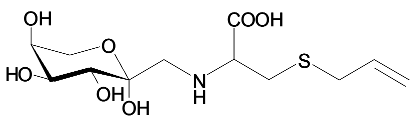

5

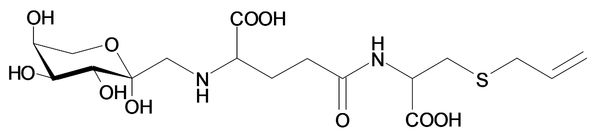

6

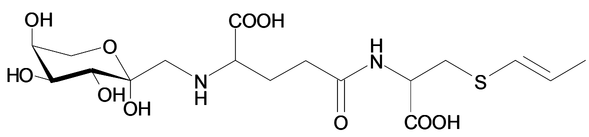

7

Figure 39: Chemical structures of *N*α-(1-deoxy-D-fructos-1-yl)-*S*-allyl-L-cysteine (**5**), *N*α-(1-deoxy-D-fructos-1-yl)-γ-glutamyl-*S*-allyl-L-cysteine (**6**), and *trans*-*N*α-(1-deoxy-D-fructos-1-yl)-γ-glutamyl-*S*-1-propenyl-L-cysteine (**7**).

In order to clarify whether the compounds **5**-**7** exist in AGE, the MS/MS parameters were tuned for each individual compound, and then AGE was screened by means of UPLC-ESI-MS/MS. This MS screening, followed by cochromatography with the corresponding reference compounds, led to the unequivocal identification of Amadori products **5**-**7** in AGE (**Figure 40**).

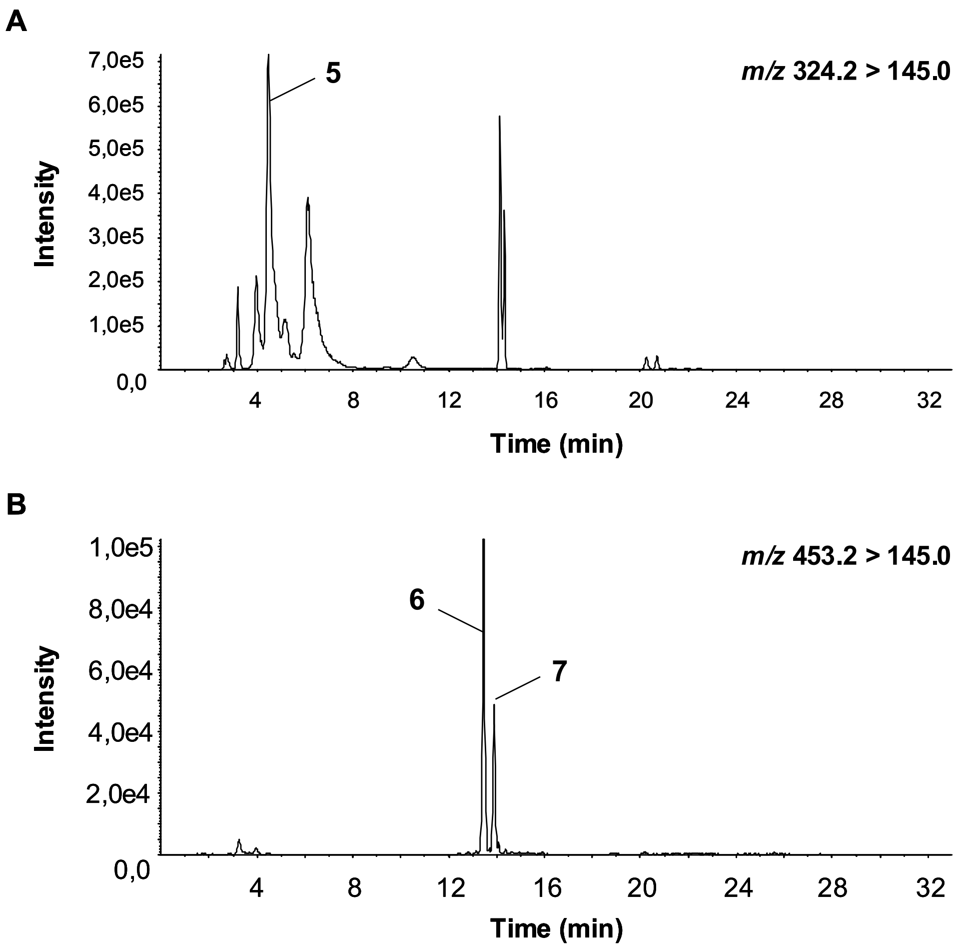

Figure 40: MS chromatograms of AGE recording the selective mass transitions for (**A**) *N*α-(1-deoxy-D-fructos-1-yl)-*S*-allyl-L-cysteine (**5**), and (**B**) *N*α-(1-deoxy-D-fructos-1-yl)-γ-glutamyl-*S*-allyl-L-cysteine (**6**) and *trans*-*N*α-(1-deoxy-D-fructos-1-yl)-γ-glutamyl-*S*-1-propenyl-L-cysteine (**7**).

Moreover, the reactions between glucose and several common amino acids (L-phenylalanine, L-tyrosine, and L-tryptophan) led to generation of the Amadori compounds, *N*α-(1-deoxy-D-fructos-1-yl)-L-phenylalanine (**8**), *N*α-(1-deoxy-D-fructos-1-yl)-L-tyrosine (**9**), *N*α-(1-deoxy-D-fructos-1-yl)-L-tryptophan (**10**), and, in addition, *trans*-1-[(*1R*,*2R*,*3S*,*4S*)-1,2,3,4,5-pentahydroxypent-1-yl]-1,2,3,4-tetrahydro-β-carboline-3-carboxylic acid (**11**) and *cis*-1-[(*1R*,*2R*,*3S*,*4S*)-1,2,3,4,5-pentahydroxypent-1-yl]-1,2,3,4-tetrahydro-β-carboline-3-carboxylic acid (**12**). The latter two polyol-tetrahydro-β-carbolines were obtained as by-products in the reaction mixture of glucose and L-tryptophan, which were reported in the literature (*Gutsche et al., 1999*).

The 1-methyl-1,2,3,4-tetrahydro-β-carboline-3-carboxylic acids **2'** and **3'** (**Figure 12**), identified as antioxidants in AGE (*Ichikawa et al., 2002*), were putatively formed by the reaction of tryptophan and acetaldehyde. Since the reaction product of tryptamine, which is produced by decarboxylation of tryptophan, and acetaldehyde could be present in AGE, tryptamine was reacted with acetaldehyde to give 1-methyl-1,2,3,4-tetrahydro-β-carboline (**13**).

The chemical structures of compounds **8**-**13** (**Figure 41**) were confirmed by means of LC-MS, UPLC-ESI-TOF-MS, and NMR experiments, thus confirming literature data (*Huo et al., 2004* for **8**, *Manini et al., 2001* for **9**, *Gutsche et al., 1999* for **10, 11,** and **12**, and *Fiot et al., 2006* for **13**).

In order to investigate the possible presence of the compounds **8**-**13** in AGE, AGE was screened for the analytes by means of UPLC-ESI-MS/MS after tuning of their respective MS/MS parameters. This MS screening, followed by cochromatography with the corresponding reference compounds, indicated that each of the compounds **9**-**13** exist in AGE (**Figure 42**).

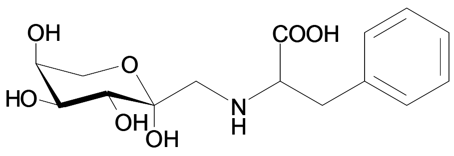

8

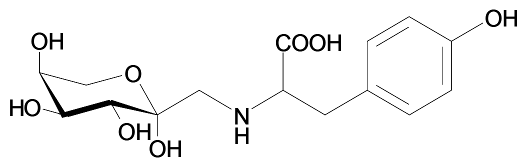

9

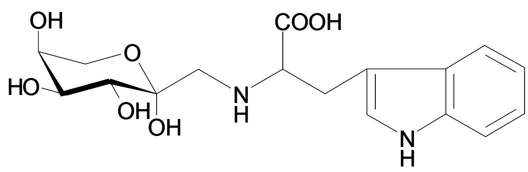

10

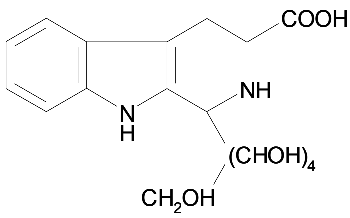

11, 12

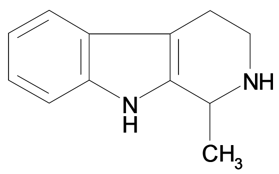

13

Figure 41: Chemical structures of *N*α-(1-deoxy-D-fructos-1-yl)-L-phenylalanine (**8**), *N*α-(1-deoxy-D-fructos-1-yl)-L-tyrosine (**9**), *N*α-(1-deoxy-D-fructos-1-yl)-L-tryptophan (**10**), *trans*-1-[(*1R*,*2R*,*3S*,*4S*)-1,2,3,4,5-pentahydroxypent-1-yl]-1,2,3,4-tetrahydro-β-carboline-3-carboxylic acid (**11**), *cis*-1-[(*1R*,*2R*,*3S*,*4S*)-1,2,3,4,5-pentahydroxypent-1-yl]-1,2,3,4-tetrahydro-β-carboline-3-carboxylic acid (**12**), and 1-methyl-1,2,3,4-tetrahydro-b-carboline (**13**).

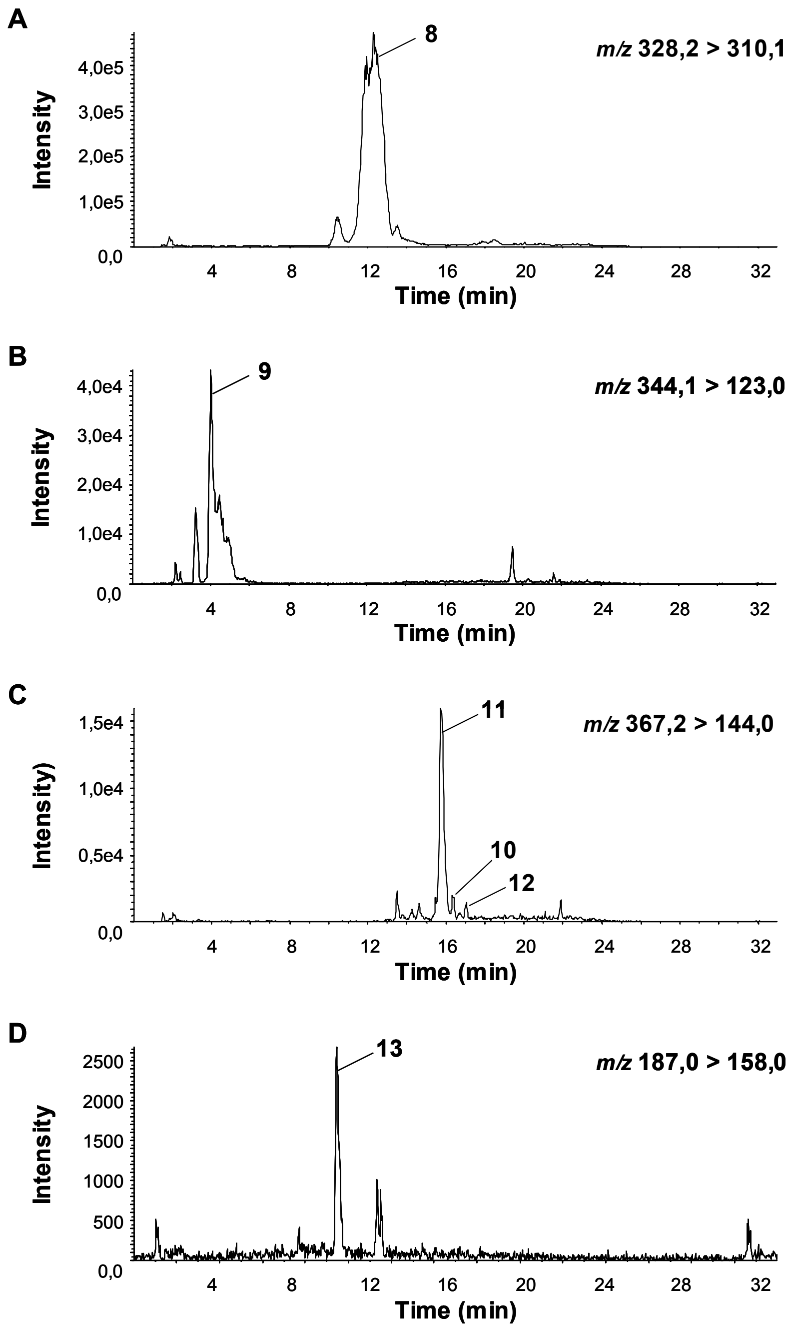

Figure 42: MS chromatograms of AGE recording the selective mass transitions for (**A**) *N*α-(1-deoxy-D-fructos-1-yl)-L-phenylalanine (**8**), (**B**) *N*α-(1-deoxy-D-fructos-1-yl)-L-tyrosine (**9**), (**C**) *N*α-(1-deoxy-D-fructos-1-yl)-L-tryptophan (**10**), *trans*-1-[(*1R*,*2R*,*3S*,*4S*)-1,2,3,4,5-pentahydroxypent-1-yl]-1,2,3,4-tetrahydro-β-carboline-3-carboxylic acid (**11**), and *cis*-1-[(*1R*,*2R*,*3S*,*4S*)-1,2,3,4,5-pentahydroxypent-1-yl]-1,2,3,4-tetrahydro-β-carboline-3-carboxylic acid (**12**), and (**D**) 1-methyl-1,2,3,4-tetrahydro-β-carboline (**13**).

2.2.2 *N*-Phenylpropenoic acid amides

N-*trans*-Feruloyltyramine isolated as the P-selectin expression suppressor from garlic (*Park, 2009*), had been reported to show significant antioxidant and anti-inflammatory activities (*Al-Taweel et al., 2012*). To investigate the role of such *N*-phenylpropenoic acid amides as antioxidants in AGE, a total of five amides, namely *N*-*trans*-feruloyltyramine (**14**), *N*-*trans*-feruloylphenetylamine (**15**), *N*-*trans*-*p*-coumaroyltyramine (**16**), *N*-*trans*-coumaroylphenetyramine (**17**), and *N*-*trans*-*p*-cinnamoyltyramine (**18**), were kindly provided by the Chair of Food Chemistry and Molecular Sensory Science (Technische Universität München) were screened in AGE by means of UPLC-ESI-MS/MS (**Figure 43**). This MS screening, followed by cochromatography with the corresponding reference compounds, unequivocally proved the presence of all of the compounds in AGE (**Figure 44**).

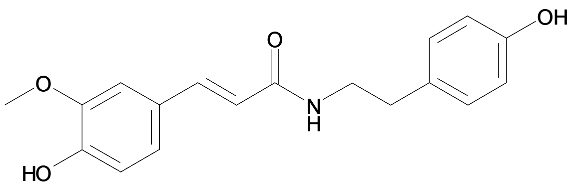

14

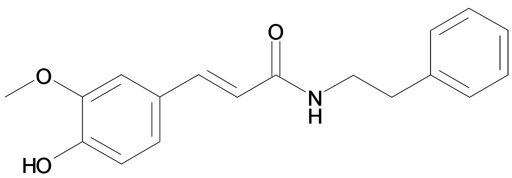

15

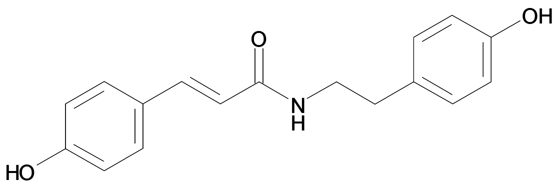

16

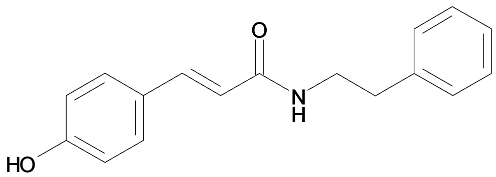

17

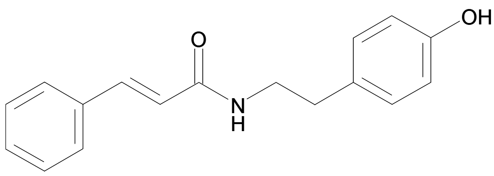

18

Figure 43: Chemical structures of *N*-*trans*-feruloyltyramine (**14**), *N*-*trans*-feruloylphenetylamine (**15**), *N*-*trans*-coumaroyltyramine (**16**), *N*-*trans*-coumaroylphenetyramine (**17**), and *N*-*trans*-cinnamoyltyramine (**18**).

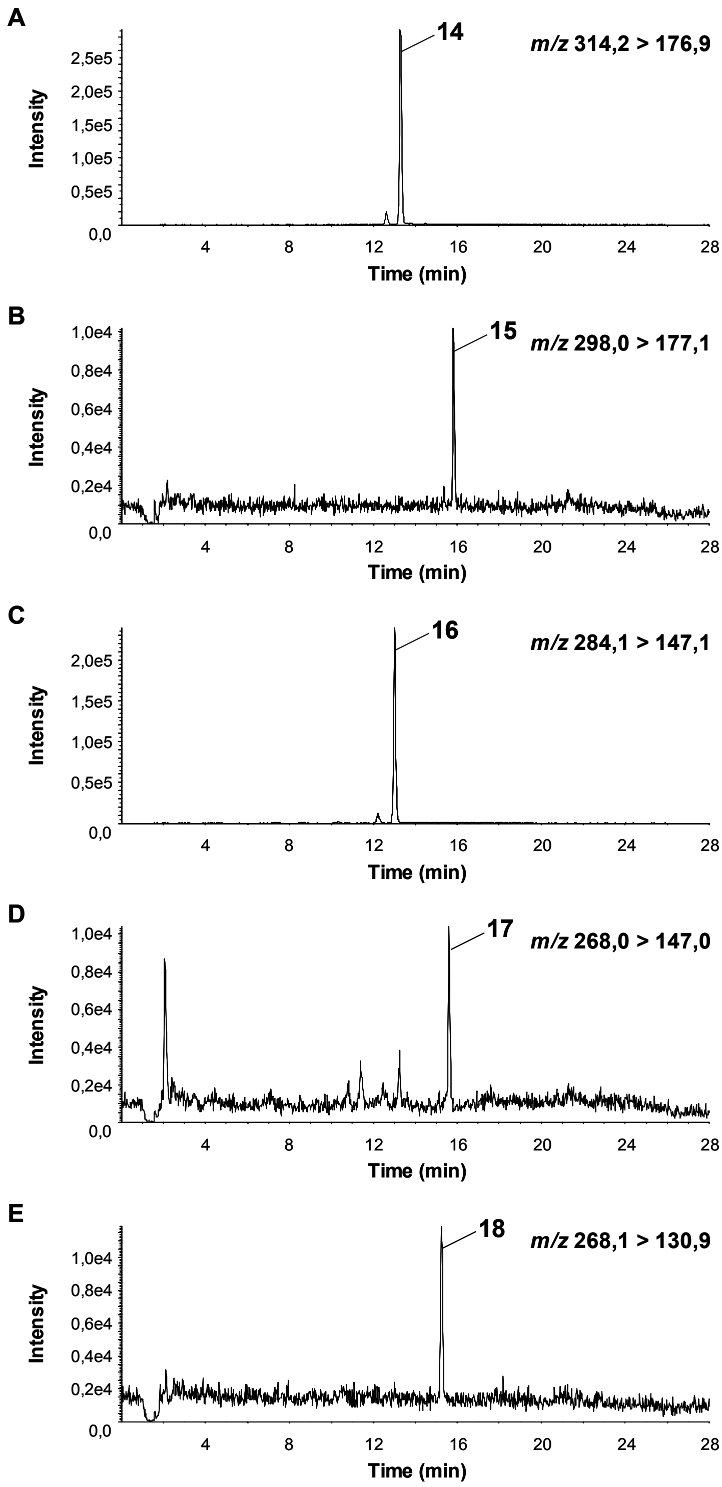

Figure 44: MS chromatograms of AGE recording the selective mass transitions for (**A**) *N-trans*-feruloyltyramine (**14**), (**B**) *N-trans*-feruloylphenetylamine (**15**), (**C**) *N-trans*-coumaroyltyramine (**16**), (**D**) *N-trans*-coumaroylphenetyramine (**17**), and (**E**) *N-trans*-cinnamoyltyramine (**18**).

2.2.3 *N*-Phenylpropenoic acid ethyl esters and benzoic acid ethyl esters

As AGE was manufactured by soaking sliced garlic cloves in a water/ethanol mixture for more than 10 months at room temperature, it was reasonable to suppose that *N*-phenylpropenoic acids from garlic react to form *N*-phenylpropenoic acid ethyl esters during aging.

Thus, two products from the reaction of *N*-phenylpropenoic acid and ethanol, such as ethyl ferulate (**19**) and ethyl *p*-coumarate (**20**), and two products of the corresponding benzoic acid and ethanol, such as ethyl vanillate (**21**) and ethyl *p*-hydroxybenzoate (**22**), were prepared (**Figure 45**). Ethyl *p*-coumarate (**20**) was synthesized from the reaction of *p*-coumaric acid dissolved in ethanol using sulfuric acid (cf. chapter **3.5.5**). Its chemical structure was confirmed by means of LC-MS, TOF-MS, and NMR experiments, indicating the data in agreement with that reported in the literature (*Barbosa-Filho et al., 2004*). Other compounds were purchased from suppliers.

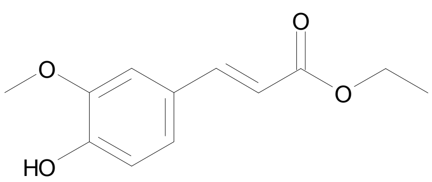

19

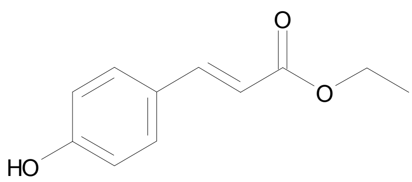

20

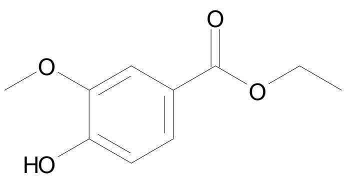

21

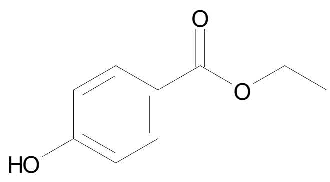

22

Figure 45: Chemical structures of ethyl ferulate (**19**), ethyl *p*-coumarate (**20**), ethyl vanillate (**21**), and ethyl *p*-hydroxybenzoate (**22**).

Subsequently, AGE was screened for the compounds **19**-**22** by means of UPLC-ESI-MS/MS to clarify their existence in AGE. The MS screening and cochromatography with the corresponding standard compounds led to the identification of all the compounds in AGE (**Figure 46**).

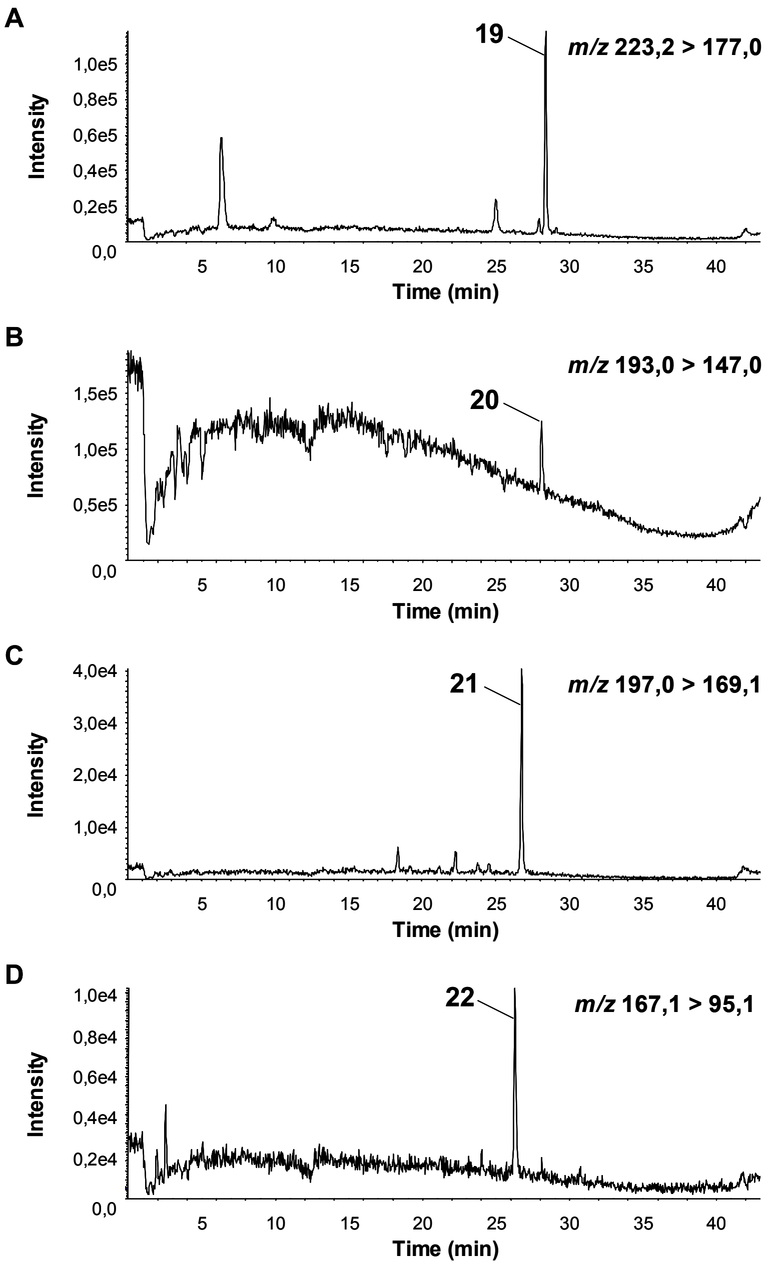

Figure 46: MS chromatograms of AGE recording the selective mass transitions for (**A**) ethyl ferulate (**19**), (**B**) ethyl *p*-coumarate (**20**), (**C**) ethyl vanillate (**21**), and (**D**) ethyl *p*-hydroxybenzoate (**22**).

2.3 Quantitation of antioxidants in aged garlic extract (AGE)

In order to investigate the concentration of the antioxidants identified in AGE, UPLC-ESI-MS/MS methods were developed and quantitative experiments were carried out for (–)-(*2R*,*3S*)-dihydrodehydrodiconiferyl alcohol (**1**), (+)-(*2S*,*3R*)-dehydrodiconiferyl alcohol (**2**) (**Figure 31**), *erythro*-guaiacylglycerol-β-O-4'-coniferyl ether (**3**), *threo*-guaiacylglycerol-β-O-4'-coniferyl ether (**4**) (**Figure 32**), *N*α-(1-deoxy-D-fructos-1-yl)-*S*-allyl-L-cysteine (**5**), *N*α-(1-deoxy-D-fructos-1-yl)-γ-glutamyl-*S*-allyl-L-cysteine (**6**), *trans*-*N*α-(1-deoxy-D-fructos-1-yl)- γ-glutamyl-*S*-1-propenyl-L-cysteine (**7**) (**Figure 39**), *N*α-(1-deoxy-D-fructos-1-yl)-L-phenylalanine (**8**), *N*α-(1-deoxy-D-fructos-1-yl)-L-tyrosine (**9**), *N*α-(1-deoxy-D-fructos-1-yl)-L-tryptophan (**10**), *trans*-1-[(*1R*,*2R*,*3S*,*4S*)-1,2,3,4,5-pentahydroxypent-1-yl]-1,2,3,4-tetrahydro-β-carboline-3-carboxylic acid (**11**), *cis*-1-[(*1R*,*2R*,*3S*,*4S*)-1,2,3,4,5-pentahydroxypent-1-yl]-1,2,3,4-tetrahydro-β-carboline-3-carboxylic acid (**12**), and 1-methyl-1,2,3,4-tetrahydro-β-carboline (**13**) (**Figure 41**), *N*-*trans*-feruloyltyramine (**14**), *N*-*trans*-feruloylphenetylamine (**15**), *N*-*trans*-coumaroyltyramine (**16**), *N*-*trans*-coumaroylphenetyramine (**17**), and *N*-*trans*-cinnamoyltyramine (**18**) (**Figure 43**), ethyl ferulate (**19**), ethyl coumarate (**20**), ethyl vanillate (**21**), and ethyl 4-hydroxybenzoate (**22**) (**Figure 45**).

2.3.1 Quantitative analysis of dilignols 1-4

The concentrations of compounds **1**-**4** were determined by means of UPLC-MS/MS analysis. After optimization of the mass transitions for each compounds, a reference mixture was injected and separated on a RP-18 column prior to MS/MS analysis using the MRM mode. A respective LC-MS/MS chromatogram is shown in **Figure 47**.

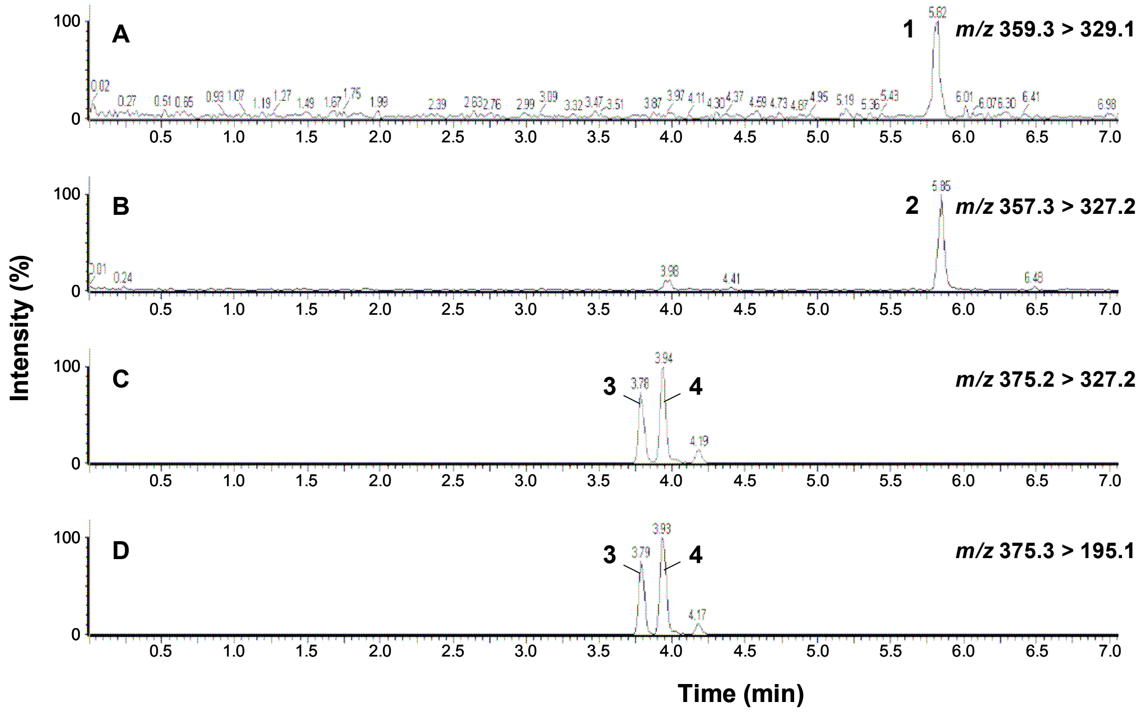

Figure 47: LC-MS/MS chromatogram of a standard mixture of dilignols using the characteristic mass transition for each compound: (**A**) (–)-(*2R*,*3S*)-dihydrodehydrodiconiferyl alcohol (**1**), (**B**) (+)-(*2S*,*3R*)-dehydrodiconiferyl alcohol (**2**), (**C**) *erythro*-guaiacylglycerol-β-O-4'-coniferyl ether (**3**), and (**D**) *threo*-guaiacylglycerol-β-O-4'-coniferyl ether (**4**).

Using defined standard solutions of each reference compound, calibration curves were obtained by linear regression analysis of the peak area versus concentration (approximately 5.0-10,000 ng/mL, seven points), which indicated a good linear response (>0.999). The linear range of the calibration curves covered the amounts of the analyte compounds in AGE. The limit of quantitation (LOQ) of these compounds were 4.3-5.9 ng/mL for β-5 linkaged dilignols (**1** and **2**) and 0.1-0.5 ng/mL for β-O-4 linkaged dilignols (**3** and **4**). The results are shown in **Table 7**.

Moreover, a recovery experiment was carried out by spiking aliquots of AGE with increasing amounts of the purified dilignols (three points). Each experiment was repeated three times. The recovery was in the range 97.8-104.0%, indicating good accuracy of the method (**Table 8**). Relative standard deviation (RSD) was less than 7%, thus demonstrating excellent precision.

Table 7: Linear equation of calibration curves, linear range and limit of quantitation (LOQ) for compounds **1-4**.

Compound	Equation	r^2	Linear range (ng/mL)	LOQ (ng/mL)
(–)-(*2R*,*3S*)-dihydrodehydrodiconiferyl alcohol (**1**)	y = 103.64x + 4.01	0.9995	11.7-11,700	5.9
(+)-(*2S*,*3R*)-dehydrodiconiferyl alcohol (**2**)	y = 254.98x - 107.88	0.9994	53.5-10,700	4.3
erythro-guaiacylglycerol-β-O-4'-coniferyl ether (**3**)	y = 18985x + 6212	0.9994	2.1-4,200	0.1
threo-guaiacylglycerol-β-O-4'-coniferyl ether (**4**)	y = 5453.4x + 1679.3	0.9997	5.2-10,400	0.5

Table 8: Recovery rates of quantitative analysis of four lignols **1-4** in aged garlic extract. Recovery was calculated by dividing concentration determined by concentration calculated. RSD was determined by 3 independent workups with 2 analytical replicates.

Compound	Amount added (µg/g)	Conc calculated (µg/g)	Conc determined (µg/g)	Recovery (%)	RSD (%)
(–)-(*2R*,*3S*)- dihydrodehydrodiconiferyl			235.45		
dihydrodehydrodiconiferyl	31.91	267.36	275.25	103.0	5.45
alcohol (**1**)	124.10	359.55	363.38	101.1	3.79
	248.20	483.65	494.56	102.3	6.94
(+)-(*2S*,*3R*)-			205.81		
dehydrodiconiferyl	36.14	241.95	238.35	98.5	0.57
alcohol (**2**)	90.35	296.16	289.61	97.8	3.18
	180.71	386.52	382.66	99.0	2.37
erythro-guaiacylglycerol-			13.02		
β-O-4'-coniferyl ether (**3**)	4.42	17.43	17.54	100.6	3.99
	8.83	21.85	22.41	102.6	2.52
	22.08	35.10	35.69	101.7	1.70
threo-guaiacylglycerol-			44.96		
β-O-4'-coniferyl ether (**4**)	5.82	50.78	49.67	97.8	2.95
	29.12	74.08	74.13	100.1	0.73
	58.23	103.19	107.36	104.0	0.71

For the quantification of the dilignol antioxidants **1**-**4**, aliquots of AGE were analyzed by reversed phase UPLC with MS/MS using the developed method. Tthe concentrations of **1**-**4** in AGE were 235.5, 205.8, 13.0, and 45.0 µg/g of dried AGE, respectively (**Table 9**). The highest concentration observed for (–)-(*2R*,*3S*)-dihydrodehydrodiconiferyl alcohol (**1**) is approximately one-tenth of the concentration of *N*α-(1-deoxy-D-fructos-1-yl)-L-arginine and twice the concentration of tetrahydro-β-carboline derivatives identified in AGE as antioxidants (*Ryu et al., 2001* and *Ichikawa et al., 2002*).

Table 9: Concentration of dilignols **1**-**4** in AGE. RSD was determined by 3 independent workups with 2 analytical replicates.

Compound	Concentration (µg/g-dry)	RSD (%)
(–)-(*2R*,*3S*)-dihydrodehydrodiconiferyl alcohol (**1**)	235.5	7.8
(+)-(*2S*,*3R*)-dehydrodiconiferyl alcohol (**2**)	205.8	2.7
erythro-guaiacylglycerol-β-O-4'-coniferyl ether (**3**)	13.0	5.3
threo-guaiacylglycerol-β-O-4'-coniferyl ether (**4**)	45.0	1.7

2.3.2 Quantitative analysis of Amadori compounds and tetrahydro-β-carbolines

The compounds **5**-**13** were quantified by UPLC-MS/MS analysis by means of a stable isotope dilution assays (SIDA). As the first step, stable isotope labeled analogues of **5** and **6** were synthesized using ^{13}C-labeled glucose following the methods developed for the unlabeled compounds (cf. chapter **3.5.6**), giving *N*a-(1-deoxy-D-fructos-1-yl)-*S*-allyl-L-cysteine-$^{13}C_6$ (**5-^{13}C$_6$**) and *N*a-(1-deoxy-D-fructos-1-yl)-γ-glutamyl-*S*-allyl-L-cysteine-$^{13}C_6$ (**6-^{13}C$_6$**) (**Figure 48**).

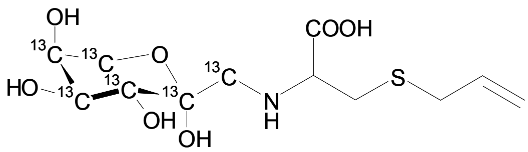

5-^{13}C$_6$

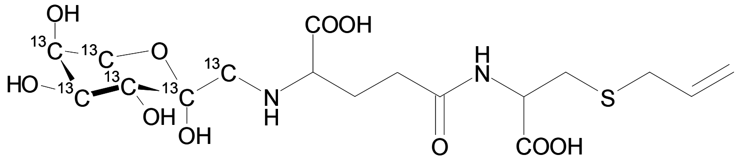

6-^{13}C$_6$

Figure 48: Chemical structures of *N*α-(1-deoxy-D-fructos-1-yl)-*S*-allyl-L-cysteine-$^{13}C_6$ (**5-^{13}C$_6$**) and *N*α-(1-deoxy-D-fructos-1-yl)-γ-glutamyl-*S*-allyl-L-cysteine-$^{13}C_6$ (**6-^{13}C$_6$**).

The mass spectra of these synthesized compounds showed *m/z* 328.1163 and 457.1580 as the molecular mass peaks, which are well in accordance with the calculated exact mass of $[^{12}C_6{}^{13}C_6H_{21}NO_7S-H]^-$ (*m/z* 328.1162) and $[^{12}C_{11}{}^{13}C_6H_{28}N_2O_{10}S-H]^-$ (*m/z* 457.1588), respectively (**Figure 42**). By comparing the data of the synthesized compounds with those for unlabeled compounds obtained by means of LC-MS, TOF-MS, and NMR spectroscopy, the chemical structures of the labeled twin molecules were unequivocally confirmed (cf. chapter **3.5.6**).

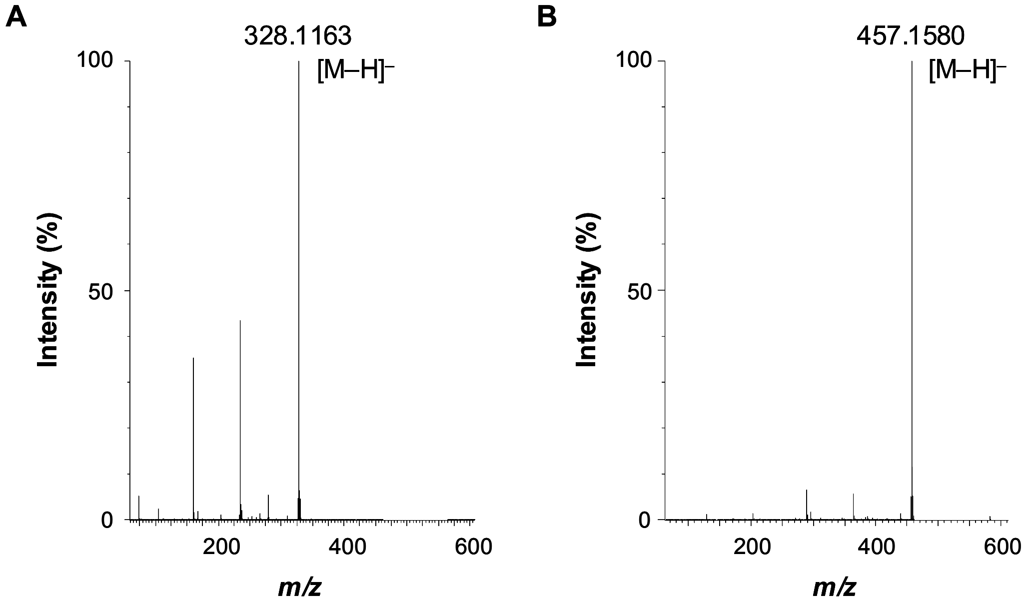

Figure 49: UPLC-HRMS spectra of the stable isotope labeled internal standard. **A:** *N*a-(1-Deoxy-D-fructos-1-yl)-*S*-allyl-L-cysteine-$^{13}C_6$ (**5-^{13}C$_6$**). **B:** *N*a-(1-Deoxy- D-fructos-1-yl)-γ-glutamyl-*S*-allyl-L-cysteine-$^{13}C_6$ (**6-^{13}C$_6$**).

The calibration mixtures of the Amadori compounds and their ^{13}C-labeled internal standards were prepared by mixing varying concentrations of unlabeled standards with the corresponding labeled standards in the constant concentrations over a range of ratios from 0.05 to 20.00. These mixtures were analyzed by means of LC-MS/MS using MRM mode. The calibration curves were obtained by plotting the exact concentration ratios of labeled compounds to unlabeled compounds versus the respective area ratios, which indicated good linear responses (>0.99) (**Figure 50** and cf. chapter **3.6.2**).

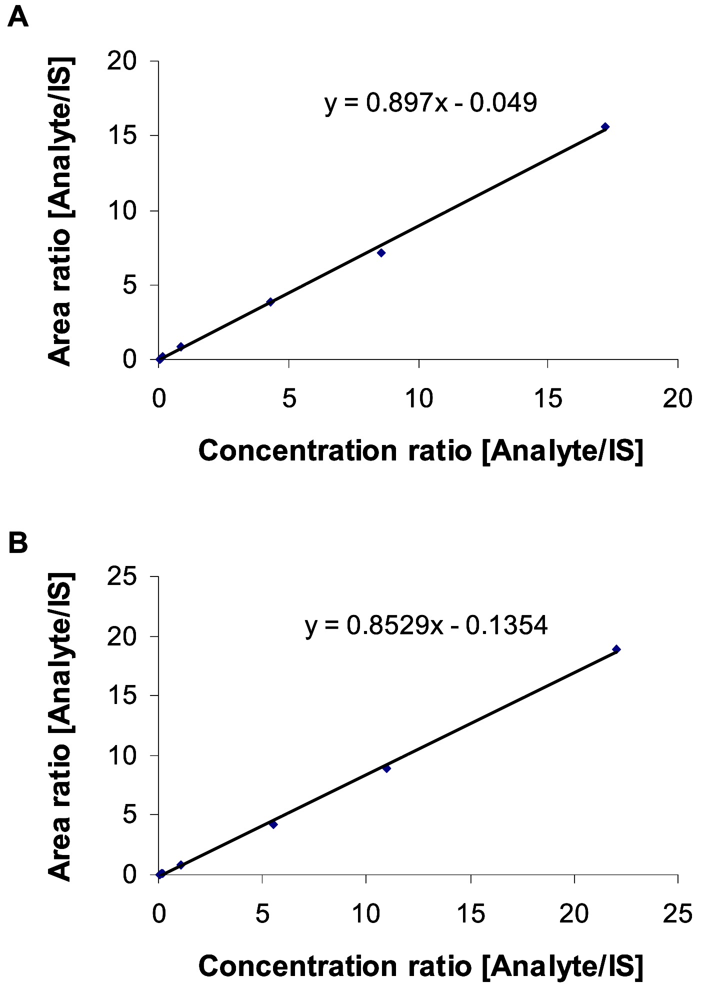

Figure 50: Calibration curves of the Amadori compounds using their corresponding $^{13}C_6$-labeled internal standard for quantification of (**A**) *N*α-(1-deoxy-D-fructos-1-yl)-*S*-allyl-L-cysteine (**5**) and (**B**) *N*α-(1-deoxy-D-fructos-1-yl)-γ-glutamyl-*S*-allyl-L-cysteine (**6**).

Consequently, ^{13}C-labeled analogues of the compounds **8**-**12** were synthesized using a similar procedure to give *N*α-(1-deoxy-D-fructos-1-yl)-L-phenylalanine-$^{13}C_6$ (**8-$^{13}C_6$**), *N*α-(1-deoxy-D-fructos-1-yl)-L-tyrosine-$^{13}C_6$ (**9-$^{13}C_6$**), *N*α-(1-deoxy-D-fructos-1-yl)-L-tryptophan-$^{13}C_6$ (**10-$^{13}C_6$**), *trans*-1-[(*1R*,*2R*,*3S*,*4S*)-1,2,3,4,5-pentahydroxypent-1-yl]-1,2,3,4-tetrahydro-β-carboline-3-carboxylic acid-$^{13}C_6$ (**11-$^{13}C_6$**), and *cis*-1-[(*1R*,*2R*,*3S*,*4S*)-1,2,3,4,5-pentahydroxypent-1-yl]-1,2,3,4-tetrahydro-β-carboline-3-carboxylicacid-$^{13}C_6$ (**12-$^{13}C_6$**) (**Figure 51**). Their chemical structures were unequivocally identified by means of LC-MS, TOF-MS, and NMR spectroscopy (cf. chapter **3.5.6**). The calibration curves obtained using the LC-MS/MS data of unlabeled compounds and labeled internal standards showed good linear responses (>0.99) (cf. chapter **3.6.2** and **3.6.3**).

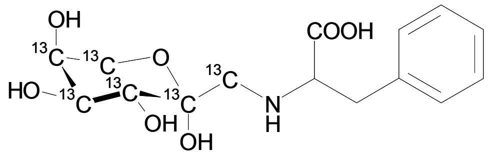

8-$^{13}C_6$

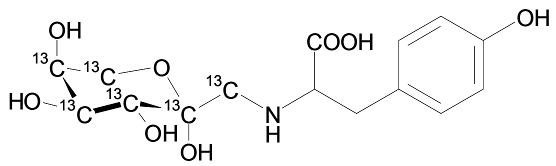

9-$^{13}C_6$

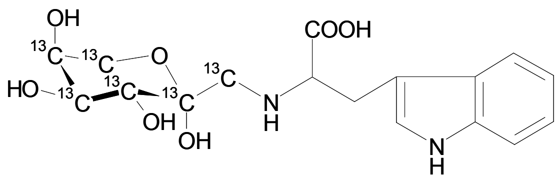

10-$^{13}C_6$

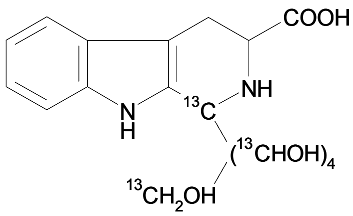

11-$^{13}C_6$, 12-$^{13}C_6$

Figure 51: Chemical structures of the internal standards, *N*α-(1-deoxy-D-fructos-1-yl)-L-phenylalanine-$^{13}C_6$ (**8-$^{13}C_6$**), *N*α-(1-deoxy-D-fructos-1-yl)-L-tyrosine-$^{13}C_6$ (**9-$^{13}C_6$**), *N*α-(1-deoxy-D-fructos-1-yl)-L-tryptophan-$^{13}C_6$ (**10-$^{13}C_6$**), *trans*-1-[(*1R*,*2R*,*3S*,*4S*)-1,2,3,4,5-pentahydroxypent-1-yl]-1,2,3,4-tetrahydro-β-carboline-3-carboxylic acid-$^{13}C_6$ (**11-$^{13}C_6$**), and *cis*-1-[(*1R*,*2R*,*3S*,*4S*)-1,2,3,4,5-pentahydroxypent-1-yl]-1,2,3,4-tetrahydro-β-carboline-3-carboxylic acid-$^{13}C_6$ (**12-$^{13}C_6$**).

In order to quantitatively determine the compounds **5**-**13**, aliquots of AGE was doted with the synthesized $^{13}C_6$-labeled internal standards and analyzed using the developed method, which revealed the concentrations of these compounds **5**-**13** were 84.9, 8.5, 5.7, 42.9, 32.6, 39.5, 0.2, 2.2, and 0.9 µg/g of dried AGE, respectively (**Table 10**).

Table 10: Concentration of six Amadori compounds and three tetrahydro-β-carboline derivatives **5**-**13** in AGE. RSD was determined by 3 independet workups with 2 analytical replicates.

Compound	Concentration (µg/g-dry)	RSD (%)
*N*α-(1-Deoxy-D-fructos-1-yl)-*S*-allyl-L-cysteine (**5**)	84.9	5.2
*N*α-(1-Deoxy-D-fructos-1-yl)-γ-glutamyl-*S*-allyl-L-cysteine (**6**)	8.5	2.9
*N*α-(1-Deoxy-D-fructos-1-yl)-γ-glutamyl-*S*-1-propenyl-L-cysteine (**7**)	5.7	4.3
*N*α-(1-Deoxy-D-fructos-1-yl)-L-phenylalanine (**8**)	42.9	4.8
*N*α-(1-Deoxy-D-fructos-1-yl)-L-tyrosine (**9**)	32.6	5.3
*N*α-(1-Deoxy-D-fructos-1-yl)-L-tryptophan (**10**)	39.5	6.2
trans-1-[(*1R*,*2R*,*3S*,*4S*)-1,2,3,4,5-pentahydroxypent-1-yl]-1,2,3,4-tetrahydro-β-carboline-3-carboxylic acid (**11**)	0.2	9.5
cis-1-[(*1R*,*2R*,3*S*,*4S*)-1,2,3,4,5-pentahydroxypent-1-yl]-1,2,3,4-tetrahydro-β-carboline-3-carboxylic acid (**12**)	2.2	17.7
1-methyl-1,2,3,4-tetrahydro-β-carboline (**13**)	0.9	2.6

2.3.3 Quantitative analysis of *N*-phenylpropenoic acid amides

To get information on the concentrations of *N*-phenylpropenoic acid biogenic amides (**14**-**18**) identified in AGE, *N*-*trans*-isoferuloyltyramine was synthesized as a suitable internal standard (**Figure 52** and cf. chapter **3.5.7**).

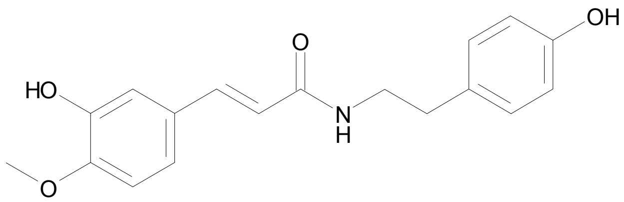

Figure 52: Chemical structure of the internal standard *N*-*trans*-isoferuloyltyramine.

The mass spectrum of the synthesized compound is displayed in **Figure 53**. The molecular mass peak and the sodium adduct mass peak were observed at *m/z* 314.1490 for $[M+H]^+$, and *m/z* 336.1210 for $[M+Na]^+$. The chemical structure was completely verified by means of LC-MS, TOF-MS, and NMR spectroscopy (cf. chapter **3.5.7**). The analyte compounds **14**-**18** and the synthesized internal standard were calibrated by plotting the peak area ratios of analytes to the internal standard in the LC-MS/MS analysis against the concentration ratios of calibration mixtures of known concentration. The calibration curve indicated good linearity for concentration ratios ranging from 0.1 to 10.0 (>0.99) (cf. chapter **3.6.4**).

For quantitative determination of the compounds **14**-**18**, aliquots of AGE was doted with the synthesized internal standard and analyzed using the developed method, which indicated the concentrations of the compounds **14**-**18** were 98.1, 1.1, 23.1, 0.2, and 1.0 µg/g of dried AGE, respectively (**Table 11**).

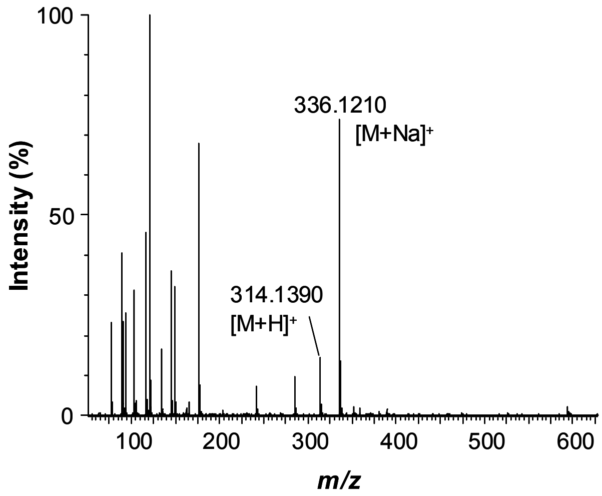

Figure 53: UPLC-HRMS spectrum of *N*-*trans*-isoferuloyltyramine.

Table 11: Concentration of the *N*-phenylpropenoic acid amides **20**-**24** in AGE. RSD was determined by 3 independet workups with 2 analytical replicates.

Compound	Concentration (µg/g-dry)	RSD (%)
N-*trans*-feruloyltyramine (**14**)	98.1	3.2
N-*trans*-feruloylphenetylamine (**15**)	1.1	10.1
N-*trans*-coumaroyltyramine (**16**)	23.1	5.6
N-*trans*-coumaroylphenetyramine (**17**)	0.2	7.0
N-*trans*-cinnamoyltyramine (**18**)	1.0	5.7

2.3.4 Quantitative analysis of *N*-phenylpropenoic acid ethyl esters and benzoic acid ethyl esters

In order to quantify two *N*-phenylpropenoic acid ethyl esters and two benzoic acid ethyl esters (**19**-**22**) identified in AGE, a SIDA method was developed. The stable isotope labeled analogues of the compounds **19**-**22** were synthesized using ^{2}H-labeled ethanol following the methods developed for the unlabeled ethyl p-coumarate (cf. chapter **3.5.8**), giving ethyl ferulate-$^{2}H_5$ (**19-$^{2}H_5$**), ethyl *p*-coumarate-$^{2}H_5$ (**20-$^{2}H_5$**), ethyl vanillate-$^{2}H_5$ (**21-$^{2}H_5$**), and ethyl *p*-hydroxybenzoate-$^{2}H_5$ (**22-$^{2}H_5$**) (**Figure 54**).

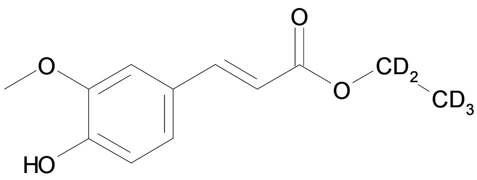

19-$^{2}H_5$

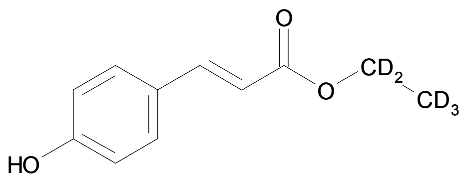

20-$^{2}H_5$

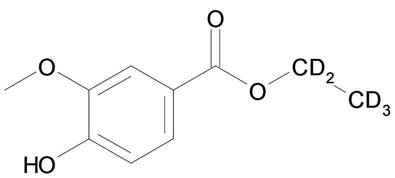

21-$^{2}H_5$

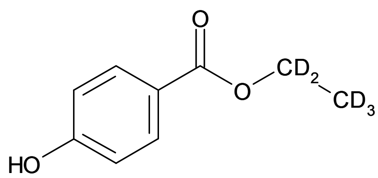

22-$^{2}H_5$

Figure 54: Chemical structures of the internal standards, ethyl ferulate-$^{2}H_5$ (**19-$^{2}H_5$**), ethyl *p*-coumarate-$^{2}H_5$ (**20-$^{2}H_5$**), ethyl vanillate-$^{2}H_5$ (**21-$^{2}H_5$**), and ethyl *p*-hydroxybenzoate-$^{2}H_5$ (**22-$^{2}H_5$**).

Their chemical structures were unequivocally identified by means of LC-MS, TOF-MS, and NMR spectroscopy (cf. chapter **3.5.8**). Good linear responses were found in the calibration curves obtained by plotting the peak area ratios of analyte compounds **19**-**22** to the corresponding internal standards in the LC-MS/MS analysis against the concentration ratios of calibration mixtures of known concentration (cf. chapter **3.6.5**).

Aliquots of AGE were doted with the labeled internal standards and analyzed using the developed method, which clarified the concentrations of the compounds **19**-**22** were 2.9, 2.1, 15.3, and 1.4 µg/g of dried AGE, respectively (**Table 12**).

Table 12: Concentration of two *N*-phenylpropenoic acid ethyl esters and two benzoic acid ethyl esters (**25**-**28**) in AGE. RSD was determined by 3 independet workups with 2 analytical replicates.

Compound	Concentration (µg/g-dry)	RSD (%)
ethyl ferulate (**19**)	2.9	5.6
ethyl *p*-coumarate (**20**)	2.1	2.1
ethyl vanillate (**21**)	15.3	5.8
ethyl *p*-hydroxybenzoate (**22**)	1.4	0.7

2.4 Antioxidant activity of compounds identified in aged garlic extract (AGE)

Since compounds **1** and **2** were isolated using antioxidant activity-guided fractionation (cf. chapter **2.1.1** and **2.1.2**), these two dilignols should be potent antioxidants. *Song et al.* (*2011*) reported dihydrodehydrodiconiferyl alcohol showed strong effect in DPPH radical scavenging assay with the value comparable to that of the positive control, such as ascorbic acid and gallic acid, and significantly inhibited high glucose-induced ROS production in mesangial cells. In addition, dehydrodiconiferyl alcohol exhibited significant superoxide radical scavenging activities compared with standard antioxidant, BHA (*Lee et al., 2009*). DPPH radical scavenging activities of the other two dilignols (**3** and **4**) have been also examined by *Li et al.* (*2012*), which were similar to that of ascorbic acid.

Besides dilignols, several Maillard reaction products have been known to be antioxidants, which have hydrogen peroxide or free radical scavenging activity comparable to ascorbic acid (*Ryu et al., 2001*, *Ichikawa et al., 2002*, and *Herraiz et al., 2003*), Moreover, the antioxidant activities of the *N*-phenylpropenoic acid biogenic amides (*Yang et al., 2011*, and *Orfali et al., 2009*) and ethyl esters (*Kikuzaki et al., 2002*, and *Neudörffer et al., 2004*) have been also studied using various assays.

These authors investigated for the antioxidant activity of the test substances using different assays and different positive controls. In this study, the compounds identified in AGE were examined for their antioxidant activities using two assays differing in the antioxidant mechanisms. Ascorbic acid, quercetin, and (–)-epicatechin were used as positive controls.

To investigate the activity of the compounds identified in AGE, compounds **1**-**22**, compounds **1'**-**5'** previously identified as antioxidants in AGE, several characteristic compounds in AGE, and the three reference substances known as antioxidants were studied for their antioxidant activity using the ORAC and the HPS assay (**Table 13**). *Ichikawa et al.* (*2002*) reported on the HPS activity of tetrahydro-b-carboline derivatives, revealing the compounds **2'** and **3'** showed similar values, which were much lower than those of the compounds **4'** and **5'**. Therefore, the mixture of the compounds **2'** and **3'** were prepared without separation and assayed. The reference substances ascorbic acid, quercetin, and (–)-epicatechin, showed high activities comparable with that reported in the literature (*Ou et al., 2001* and *Wolfe et al., 2008*).

As expected, dilignol compounds **1**-**4** showed high antioxidant activities with 2.60-3.65 µmol TE/µmol in the ORAC assay and 0.92-1.08 µmol-H_2O_2 scavenged/µmol in the HPS assay. Their activities, which were about one third of reference substances in ORAC assay and about half of them in HPS assay, were about twice or more times higher than the compounds known as antioxidants in AGE (**1'**-**5'**).

Among the Amadori compounds and tetrahydro-β-carbolines, the Amadori compounds of γ-glutamyl-*S*-1-propenyl-L-cysteine (**7**), L-tyrosine (**9**), and L-tryptophan (**10**) as well as all of tetrahydro-β-carboline derivatives (**11**-**13**) showed comparable activities to the antioxidant Amadori compound and tetrahydro-β-carbolines known in AGE (**1'**-**5'**).

Almost all of the *N*-phenylpropenoic acid amides and ethyl esters showed high activities ranging from 1.10 to 6.31 µmol TE/µmol in the ORAC assay and from 0.20-1.31 µmol-H_2O_2 scavenged/µmol in the HPS assay. Some of them such as, e.g. *N*-*trans*-feruloyltyramine (**14**) and *N*-*trans*-coumaroyltyramine (**16**), were even comparable to the reference antioxidants, and showed stronger antioxidant activity than their precursor pnenylpropenoic acids especially in ORAC assay.

Table 13: Antioxidant activity of AGE compounds and reference substances.

Compound	ORAC assay [a] (µmol TE/µmol)	HPS assay [b] (µmol-H_2O_2 scavenged/µmol)
(–)-(*2R*,*3S*)-dihydrodehydrodiconiferyl alcohol (**1**)	2.60 ± 0.20	1.08 ± 0.01
(+)-(*2S*,*3R*)-dehydrodiconiferyl alcohol (**2**)	3.65 ± 0.37	0.95 ± 0.02
erythro-guaiacylglycerol-β-O-4'-coniferyl ether (**3**)	3.27 ± 0.14	0.92 ± 0.03
threo-guaiacylglycerol-β-O-4'-coniferyl ether (**4**)	3.53 ± 0.09	0.97 ± 0.02
*N*α-(1-deoxy-D-fructos-1-yl)-*S*-allyl-L-cysteine (**5**)	0.30 ± 0.01	0.05 ± 0.00
*N*α-(1-deoxy-D-fructos-1-yl)-γ-glutamyl-*S*-allyl-L-cysteine (**6**)	0.39 ± 0.01	0.03 ± 0.00
trans-*N*α-(1-deoxy-D-fructos-1-yl)-γ-glutamyl-*S*-1-propenyl-L-cysteine (**7**)	0.90 ± 0.04	0.12 ± 0.00
*N*α-(1-deoxy-D-fructos-1-yl)-L-phenylalanine (**8**)	<0.02	0.04 ± 0.00
*N*α-(1-deoxy-D-fructos-1-yl)-L-tyrosine (**9**)	0.98 ± 0.01	0.65 ±0.01
*N*α-(1-deoxy-D-fructos-1-yl)-L-tryptophan (**10**)	1.72 ± 0.07	0.32 ± 0.00
trans-1-[(1R,2R,3S,4S)-1,2,3,4,5-pentahydroxypent-1-yl]-1,2,3,4-tetrahydro-β-carboline-3-carboxylic acid (**11**)	1.56 ± 0.10	0.34 ± 0.01
cis-1-[(1R,2R,3S,4S)-1,2,3,4,5-pentahydroxypent-1-yl]-1,2,3,4-tetrahydro-β-carboline-3-carboxylic acid (**12**)	1.69 ± 0.11	0.23 ± 0.00
1-methyl-1,2,3,4-tetrahydro-β-carboline (**13**)	1.74 ± 0.04	0.03 ± 0.00
N-*trans*-feruloyltyramine (**14**)	5.62 ± 0.65	1.31 ± 0.09
N-*trans*-feruloylphenetylamine (**15**)	4.19 ± 0.39	0.70 ± 0.05
N-*trans*-coumaroyltyramine (**16**)	6.31 ± 0.74	0.47 ± 0.00
N-*trans*-coumaroylphenetyramine (**17**)	3.19 ± 0.14	0.88 ± 0.01
N-*trans*-cinnamoyltyramine (**18**)	1.10 ± 0.10	0.20 ± 0.00
ethyl ferulate (**19**)	1.86 ± 0.04	1.28 ± 0.03

Table 13: Continued.

Compound	ORAC assay [a] (μmol TE/μmol)	HPS assay [b] (μmol-H_2O_2 scavenged/μmol)
ethyl *p*-coumarate (**20**)	3.25 ± 0.15	0.99 ± 0.03
ethyl vanillate (**21**)	4.32 ± 0.12	1.07 ± 0.02
ethyl *p*-hydroxybenzoate (**22**)	1.12 ± 0.07	0.56 ± 0.03
*N*α-(1-deoxy-D-fructos-1-yl)-L-arginine (**1'**)	<0.02	0.10 ± 0.00
Mixture of 1-methyl-1,2,3,4-tetrahydro-β-carboline-3-carboxylic acids (**2'** and **3'**)	1.48 ± 0.06	0.08 ± 0.00
(*1R*,*3S*)-1-methyl-1,2,3,4-tetrahydro-β-carboline-1,3-dicarboxylic acid (**4'**)	1.68 ± 0.08	0.66 ± 0.01
(*1S*,*3S*)-1-methyl-1,2,3,4-tetrahydro-β-carboline-1,3-dicarboxylic acid (**5'**)	1.73 ± 0.09	0.27 ± 0.00
S-allyl-L-cysteine	0.10 ± 0.00	<0.01
γ-glutamyl-*S*-allyl-L-cysteine	0.91 ± 0.01	<0.01
γ-glutamyl-*S*-1-propenyl-L-cysteine	1.00 ± 0.01	0.10 ± 0.00
trans-ferulic acid	2.91 ± 0.10	1.15 ± 0.07
trans-*p*-coumaric acid	2.01 ± 0.19	0.95 ± 0.02
trans-cinnamic acid	0.08 ± 0.00	<0.01
ascorbic acid	0.33 ± 0.01	0.83 ± 0.02
quercetin	7.13 ± 0.22	1.69 ± 0.02
(−)-epicatechin	9.65 ± 0.53	1.89 ± 0.03

[a] The value represents mean ± SD by four independent repetitions.
[b] The value represents mean ± SD by three independent repetitions.

From the results of quantitative analyses (**Table 9-12**) and the results of the

ORAC assay (**Table 13**), the antioxidant activity in the individual original concentration in AGE was calculated to gain the contribution to the activity of the whole AGE extract (**Table 14**).

Among the identified compounds, (–)-(*2R*,*3S*)-dihydrodehydrodiconiferyl alcohol (**1**), (+)-(*2S*,*3R*)-dehydrodiconiferyl alcohol (**2**), and *N*-*trans*-feruloyltyramine (**14**) showed the highest contribution in the range of 1.6-2.0%. This contribution value is higher than that of *S*-allyl-L-cysteine, which has the largest contribution among the constituents previously identified in AGE. In addition, the contribution of *threo*-guaiacylglycerol-β-O-4'-coniferyl ether (**4**) and *N*-*trans*-coumaroyltyramine (**16**) (0.4% and 0.5%, respectively) was comparable to that of the known antioxidants. These results verified the great importance of the above identified compounds in AGE.

The calculated sum of the contribution of the compounds **1**-**22** was 6.9%, which is almost equal to that of the combination mixture of **1**-**22** (7.0%), indicating the legitimacy of the above calculation. Since the sum of the contribution of all the compounds identified in AGE is approximately 30%, a vast number of trace components with high antioxidant activity remain unidentified. In section 2.1, (–)-(*2R*,*3S*)-dihydrodehydrodiconiferyl alcohol (**1**) and (+)-(*2S*,*3R*)-dehydrodiconiferyl alcohol (**2**) were isolated from fraction 4-14 and no antioxidant could be obtained in the other active fraction, such as fraction 4-12, 4-15, and 4-16. Thus the unidentified antioxidants are presumed to be present in such fractions.

Table 14: Contribution of AGE compounds to the activity of the whole AGE extract.

Compound	ORAC assay [a] (nmol TE/g-dry)	Contribution [b] (%)
AGE	104.86	100.0
(–)-(*2R*,*3S*)-dihydrodehydrodiconiferyl alcohol (**1**)	1.70	1.6
(+)-(*2S*,*3R*)-dehydrodiconiferyl alcohol (**2**)	2.10	2.0
erythro-guaiacylglycerol-β-O-4'-coniferyl ether (**3**)	0.11	0.1
threo-guaiacylglycerol-β-O-4'-coniferyl ether (**4**)	0.42	0.4
*N*α-(1-deoxy-D-fructos-1-yl)-*S*-allyl-L-cysteine (**5**)	0.08	0.1
*N*α-(1-deoxy-D-fructos-1-yl)-γ-glutamyl-*S*-allyl-L-cysteine (**6**)	0.01	<0.1
trans-*N*α-(1-deoxy-D-fructos-1-yl)-γ-glutamyl-*S*-1-propenyl-L-cysteine (**7**)	0.01	<0.1
*N*α-(1-deoxy-D-fructos-1-yl)-L-phenylalanine (**8**)	<0.01	<0.1
*N*α-(1-deoxy-D-fructos-1-yl)-L-tyrosine (**9**)	0.09	0.1
*N*α-(1-deoxy-D-fructos-1-yl)-L-tryptophan (**10**)	0.19	0.2
trans-1-[(1R,2R,3S,4S)-1,2,3,4,5-pentahydroxypent-1-yl]-1,2,3,4-tetrahydro-β-carboline-3-carboxylic acid (**11**)	<0.01	<0.1
cis-1-[(1R,2R,3S,4S)-1,2,3,4,5-pentahydroxypent-1-yl]-1,2,3,4-tetrahydro-β-carboline-3-carboxylic acid (**12**)	0.01	<0.1
1-methyl-1,2,3,4-tetrahydro-β-carboline (**13**)	0.01	<0.1
N-*trans*-feruloyltyramine (**14**)	1.76	1.7
N-*trans*-feruloylphenetylamine (**15**)	0.01	<0.1
N-*trans*-coumaroyltyramine (**16**)	0.51	0.5
N-*trans*-coumaroylphenetyramine (**17**)	<0.01	<0.1
N-*trans*-cinnamoyltyramine (**18**)	<0.01	<0.1

Table 14: Continued.

Compound	ORAC assay [a] (nmol TE/g-dry)	Contribution [b] (%)
ethyl ferulate (**19**)	0.01	<0.1
ethyl *p*-coumarate (**20**)	0.01	<0.1
ethyl vanillate (**21**)	0.13	0.1
ethyl *p*-hydroxybenzoate (**22**)	<0.01	<0.1
Sum of **1-22**	7.18	6.9
Combination of **1-22**	7.33	7.0
*N*α-(1-deoxy-D-fructos-1-yl)-L-arginine (**1’**)	0.08	0.1
Mixture of 1-methyl-1,2,3,4-tetrahydro-β-carboline-3-carboxylic acids (**2’** and **3’**)	1.05	1.0
(*1R*,*3S*)-1-methyl-1,2,3,4-tetrahydro-β-carboline-1,3-dicarboxylic acid (**4’**)	0.60	0.6
(*1S*,*3S*)-1-methyl-1,2,3,4-tetrahydro-β-carboline-1,3-dicarboxylic acid (**5’**)	0.61	0.6
S-allyl-L-cysteine	1.27	1.2
γ-glutamyl-*S*-allyl-L-cysteine	0.96	0.9
γ-glutamyl-*S*-1-propenyl-L-cysteine	0.54	0.5

[a] The value is calculated by multiplying the concentraion (**Table 9-12**) with the ORAC activity (**Table 13**).

[b] The value represents the percentage of individual activity against the activity of AGE.

2.5 Discussion

As a result, four dilignols, six Amadori compounds, three tetrahydro-β-carbolines, five *N*-phenylpropenoic acid amides, and four ethyl esters were identified in AGE for the first time, namely (–)-(*2R*,*3S*)-dihydrodehydrodiconiferyl alcohol (**1**), (+)-(*2S*,*3R*)-dehydrodiconiferyl alcohol (**2**), *erythro*-guaiacylglycerol-β-O-4'-coniferyl ether (**3**), *threo*-guaiacylglycerol-β-O-4'-coniferyl ether (**4**), *N*α-(1-deoxy-D-fructos-1-yl)-*S*-allyl-L-cysteine (**5**), *N*α-(1-deoxy-D-fructos-1-yl)-γ-glutamyl-*S*-allyl-L-cysteine (**6**), *trans*-*N*α-(1-deoxy-D-fructos-1-yl)-γ-glutamyl-*S*-1-propenyl-L-cysteine (**7**), *N*α-(1-deoxy-D-fructos-1-yl)-L-phenylalanine (**8**), *N*α-(1-deoxy-D-fructos-1-yl)-L-tyrosine (**9**), *N*α-(1-deoxy-D-fructos-1-yl)-L-tryptophan (**10**), *trans*-1-[(1R,2R,3S,4S)-1,2,3,4,5-pentahydroxypent-1-yl]-1,2,3,4-tetrahydro-β-carboline-3-carboxylic acid (**11**), *cis*-1-[(1R,2R,3S,4S)-1,2,3,4,5-pentahydroxypent-1-yl]-1,2,3,4-tetrahydro-β-carboline-3-carboxylic acid (**12**), 1-methyl-1,2,3,4-tetrahydro-β-carboline (**13**), *N*-*trans*-feruloyltyramine (**14**), *N*-*trans*-feruloylphenetylamine (**15**), *N*-*trans*-coumaroyltyramine (**16**), *N*-*trans*-coumaroylphenetyramine (**17**), *N*-*trans*-cinnamoyltyramine (**18**), ethyl ferulate (**19**), ethyl *p*-coumarate (**20**), ethyl vanillate (**21**) and ethyl *p*-hydroxybenzoate (**22**). This is also the first report on all of these compounds in garlic except **14** and **16**.

Among these identified compounds, (–)-(*2R*,*3S*)-dihydrodehydrodiconiferyl alcohol (**1**), (+)-(*2S*,*3R*)-dehydrodiconiferyl alcohol (**2**), *threo*-guaiacylglycerol-β-O-4'-coniferyl ether (**4**), *N*-*trans*-feruloyltyramine (**14**), and *N*-*trans*-coumaroyltyramine (**16**) were found to be one of the major antioxidants in AGE because of their contribution to the whole AGE regarding antioxidant activity (**Figure 55**).

Two dilignols (**1** and **2**) isolated using the activity-guided fractionation are produced by β-5 linked dimerization of coniferyl alcohol. Since the compounds **1** and **2** have different configuration at C2 and C3, their diastereomers might exist as well. In addition, *Adler* (*1977*) reported coniferyl alcohol easily dimerize to form several dilignols with a β-O-4 linkage in nature. Therefore, two β-O-4 linked dilignols (**3** and **4**) were synthesized by oxidative coupling of coniferyl alcohol, and then identified in AGE by means of LC-MS/MS analysis. Monolignols, such as coniferyl alcohol and sinapyl alcohol, can be polymerized to form various lignin compounds. It is suggested that some of such lignins would be present as important antioxidants in AGE because the antioxidant activity of such compounds has been reported in literature (*Lee et al., 2009* and *Li et al., 2012*).

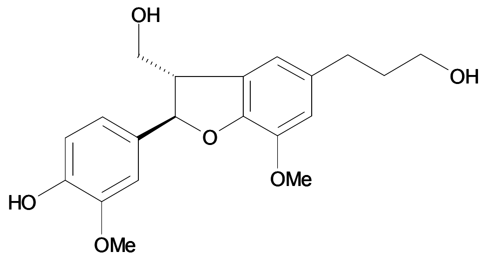

1

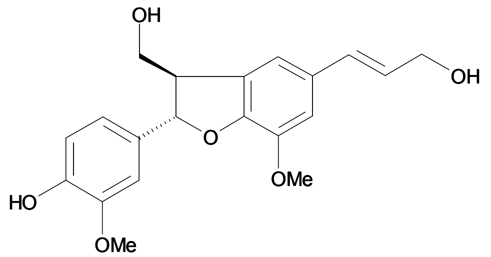

2

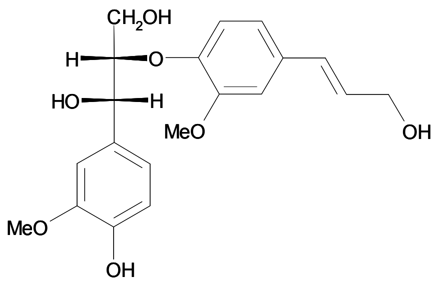

4

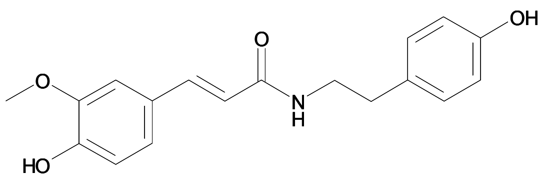

14

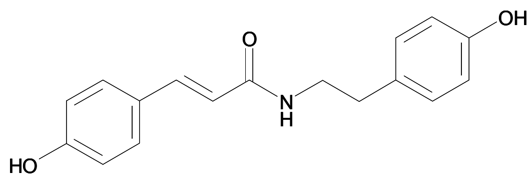

16

Figure 55: Chemical structures of antioxidants contributing largely to the activity of the whole AGE.

The Maillard reaction occurs during the aging process of AGE, which results in formation of the Amadori compounds and tetrahydro-β-carbolines (*Ryu et al., 2001*, and *Ichikawa et al., 2002*). In the present study, the Amadori compounds of *S*-allyl-L-cysteine, γ-glutamyl-*S*-allyl-L-cysteine, and γ-glutamyl-*S*-1-propenyl-L-cysteine (**5**-**7**) were identified in AGE. To the best of my knowledge, these Amadori compounds were found in natural food products for the first time. γ-Glutamyl-*S*-alk(en)yl-L-cysteines are relatively abundant in garlic (cf. chapter **1.2.2**), and *S*-allyl-L-cysteine, which is enzymatically formed by hydrolysis of γ-glutamyl-S-allyl-L-cysteine during the aging process, is unique and beneficial compound of AGE (*Colín-González et al., 2012*). The Amadori compounds derived from such sulfur-containing amino acids through the Maillard reaction during the aging process are expected to be characteristic compounds in AGE (**Figure 56**).

There is a substantial bulk of literatures, which reported on the identification and biological property of phenylpropanoids. *p*-Coumaric acid, remaining a crossroad in the biosynthesis of most phenylpropanoids, is formed by two enzymatic pathways; the primal one by the transformation of cinnamic acid derived from phenylalanine through phenylalanine ammonia-lyase, and another one by the direct deamination of tyrosine through tyrosine ammonia-lyase (*Rösler et al., 1997*). Caffeic acid and ferulic acid are formed from *p*-coumaric acid by hydroxylation and methyltransration. Monolignols, such as coniferyl alcohol and *p*-coumaryl alcohol, are formed from these phenylpropanoids and lead to formation of lignans and lignins.

It can be assumed that AGE contains a range of phenylpropanoid related compounds although their amounts are low. In deed, three ferulic acid derivatives, three *p*-coumaric acid derivatives, and one cinnamic acid derivative were found in AGE. Interestingly, no caffeic acid derivatives, however, could be identified (data not shown).

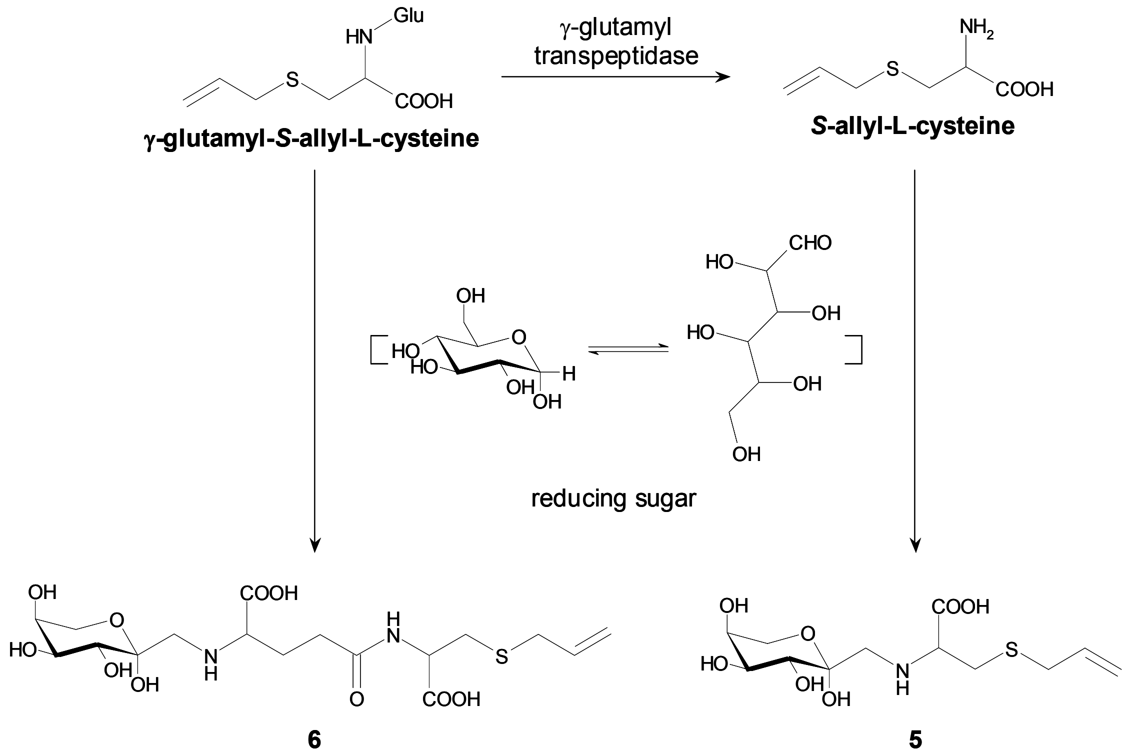

Figure 56: Formation pathway proposed for the generation of *S*-allyl-L-cysteine, *N*α-(1-deoxy-D-fructos-1-yl)-*S*-allyl-L-cysteine (**5**), and *N*α-(1-deoxy-D-fructos-1-yl)-γ-glutamyl-*S*-allyl-L-cysteine (**6**) through the Maillard reaction during the aging process.

3 Materials and methods

3.1 Chemicals

The following chemicals were purchased from the suppliers:

(±)-6-Hydroxy-2,5,7,8-tetramethylchromane-2-carboxylic acid (Trolox), Sigma-Aldrich, Steinheim, Germany
(−)-Epicatechin, Sigma-Aldrich, Steinheim, Germany
2,2'-Azino-bis(3-ethylbenzothiazoline-6-sulfonic acid) diammonium salt (ABTS), Sigma-Aldrich, Steinheim, Germany
2,2'-Azobis(2-methylpropionamidine) dihydrochloride (AATS), Sigma-Aldrich, Steinheim, Germany
Acetaldehyde, Sigma-Aldrich, Steinheim, Germany
Acetonitrile, J.T.Baker, Deventer, Netherlands
Ascorbic acid, Sigma-Aldrich, Steinheim, Germany
Coniferyl alcohol, Sigma-Aldrich, Steinheim, Germany
D-Glucose, Fluka, Buchs, Switzerland
Ethanol, Merck KGaA, Darmstadt, Germany
Ethyl ferulate (**19**), Alfa Aesar, Karlsruhe, Germany
Ethyl vanillate (**21**), Alfa Aesar, Karlsruhe, Germany
Ethyl *p*-hydroxybenzoate (**22**), Fluka, Buchs, Switzerland
Ferulic acid, Sigma-Aldrich, Steinheim, Germany
Fluorescein sodium salt, Sigma-Aldrich, Steinheim, Germany
Formic acid, Merck KGaA, Darmstadt, Germany
Glacial acetic acid, Merck KGaA, Darmstadt, Germany
Hydrogen chloride, Merck KGaA, Darmstadt, Germany
Hydrogen peroxid, Merck, Hohenbrunn, Germany
Isoferulic acid, Sigma-Aldrich, Steinheim, Germany
L-Phenylalanine, Sigma-Aldrich, Steinheim, Germany
L-Tryptophan, Sigma-Aldrich, Steinheim, Germany
L-Tyrosine, Sigma-Aldrich, Steinheim, Germany
Methanol, J.T.Baker, Deventer, Netherlands
p-Coumaric acid, Sigma-Aldrich, Steinheim, Germany
p-Hydroxybenzoic acid, Sigma-Aldrich, Steinheim, Germany
Peroxidase from horseradish, Sigma-Aldrich, Steinheim, Germany
Pyruvic acid, Merck KGaA, Darmstadt, Germany
Quercetin, Sigma-Aldrich, Steinheim, Germany

Sodium hydroxide, Merck KGaA, Darmstadt, Germany
Sulfuric acid, Merck KGaA, Darmstadt, Germany
Tetrahydrofuran, Merck KGaA, Darmstadt, Germany
Thionyl chloride, Sigma-Aldrich, Steinheim, Germany
Tryptamine hydrochloride, Fluka, Buchs, Switzerland
Vanillic acid, Sigma-Aldrich, Steinheim, Germany

The following NMR solvents and labeled chemicals were purchased from Euriso-Top (Giv-sur-Yvette, France):
Acetone-d_6
Chloroform-*d* ($CDCl_3$)
Dimethyl sulfoxide-d_6 (DMSO-d_6)
D-Glucose-$^{13}C_6$
Ethanol-d_5
Methanol-d_4

The following chemicals were kindly provided by the Chair of Food Chemistry and Molecular Sensory Science (Technische Universität München):
γ-Glutamyl-*S*-1-propenyl-L-cysteine
trans-*N*α-(1-deoxy-D-fructos-1-yl)-γ-glutamyl-*S*-1-propenyl-L-cysteine (**7**)
N-*trans*-Feruloyltyramine (**14**)
N-*trans*-Feruloylphenetylamine (**15**)
N-*trans*-*p*-Coumaroyltyramine (**16**)
N-*trans*-*p*-Coumaroylphenetyramine (**17**)
N-*trans*-Cinnamoyltyramine (**18**)

The following chemicals were provided by Wakunaga Pharmaceutical Co., Ltd.:
*N*α-(1-Deoxy-D-fructos-1-yl)-L-arginine (**1’**)
S-Allyl-L-cysteine
γ-Glutamyl-*S*-allyl-L-cysteine

Water was purified by a Milli-Q Gradient A10 system (Millipore, Schwalbach, Germany), and solvents used were of HPLC-grade (Merck, Darmstadt, Germany).

3.2 Aged garlic extract (AGE)

Aged garlic extract was provided by Wakunaga Pharmaceutical Co., Ltd., which was manufactured under a license issued by the Ministry of Health and Welfare of Japan, and formulated as follows; sliced, fresh raw garlic cloves (*Allium sativum* L.) was dipped into the aqueous ethanol in a stainless steel tank, and extracted for more than 10 months at room temperature. AGE used for these experiments contained *S*-allylcysteine in the range of 1.6-2.4 mg/g dry weight (*Morihara et al., 2011*).

3.3 *In vitro* antioxidant assays

3.3.1 ORAC assay

Following a literature protocol (*Ou et al., 2001*) with some modification, the ORAC assay was carried out. The sample solutions of AGE and its fractions were prepared in phosphate buffer (10 mM, pH 7.4) in the concentration ratios naturally occurring in AGE. The sample solutions of test substances were prepared in the same phosphate buffer in the appropriate concentration. A series of Trolox solutions (200, 100, 50, 25, 12.5 µM) was prepared by diluting an ethanolic solution of Trolox (2 mM) with phosphate buffer. Sample solution, Trolox dilution (25 µL), or phosphate buffer (10 mM, pH 7.4) used as blank was placed in wells of a 96-well black microplate (VWR, Ismaning, Germany). Then fluorescein sodium salt (10 nM in phosphate buffer, 150 µL) was added to each well, and the microplate was incubated at 37°C for 30 min. Thereafter, the decay of fluorescence was measured every 90 s at the excitation wavelength of 485 nm and the emission wavelength of 520 nm using a FLUOstar OPTIMA plate reader (BMG LABTECH, Offenburg, Germany). The first three cycles were taken to determine the background signal. After 3 cycles, AAPH (240 mM in phosphate buffer, 25 µL) was added, and then the measurement was resumed and continued up to 90 min (60 cycles in total).

The ORAC values were calculated according to the method of *Cao et al.* (*1993*). Briefly, a standard curve was obtained from the area under the fluorescence versus time curve (AUC) for Trolox dilutions minus the AUC for blank. Then the AUC for the sample solution minus the AUC for the blank was calculated and compared to the standard curve. ORAC values were expressed as Trolox equivalents (µmol TE/µmol).

3.3.2 Hydrogen peroxide scavenging (HPS) assay

The hydrogen peroxide scavenging (HPS) assay was performed according to a literature protocol with a slight modification (*Ryu et al., 2001*). The sample solutions were prepared in the same way as in the ORAC assay using phosphate buffer (100 mM, pH 6.0). An aliquot (100 µL) of the sample solution or phosphate buffer used for control was placed in each well of a 96-well clear microplate (VWR, Ismaning, Germany). Then, phosphate buffer (30 µL) and aqueous hydrogen peroxide solution (500 µM in water, 10 µL, final concentration: 5×10^{-9} mol in each well) or phosphate buffer used for blank were added in each well. Thereafter, a solution of peroxidase (150 U/mL in water, 40 µL) and a solution of ABTS (0.1% in water, 40 µL) were added. After incubation for 15 min at 37 °C, the absorbance of each well was measured at 414 nm by means of a FLUOstar OPTIMA equipment (BMG LABTECH, Offenburg, Germany).

Using the following measured absorbance value, the absorbance of the sample solution (AS), the sample-blank solution (ASB, without hydrogen peroxide), the control solution (AC, without sample solution), and control-blank solution (ACB, without sample solution and hydrogen peroxide), the percentage of scavenged hydrogen peroxide for the sample solutions of AGE and its frations was calculated as the HPS activity (P) as follows:

$$P\ (\%) = [(AC-ACB)-(AS-ASB)]/(AC-ACB)\times100$$

For the sample solutions of test substances, the molar concentration of scavenged hydrogen peroxide was calculated as the HPS activity (C) using the final molar concentration of substances (C_S) as follows:

$$C\ (\mu mol\text{-}H_2O_2\ scavenged/\mu mol) = 5\times10^{-9}\times P/100/C_S$$

3.4 Fractionation of aged garlic extract (AGE)

3.4.1 Fractionation of aged garlic extract (AGE) into four fractions

An aliquot of AGE (80 g, dry weight) was fractionated by a preparative HPLC system (cf. chapter **3.7.1**). The effluent was separated and fractions were concentrated under reduced pressure at 40°C, and then freeze-dried to yield fraction 1 (28.3 g), 2 (0.3 g), 3 (6.7 g), and 4 (43.5 g) (**Figure 15**).

3.4.2 Fractionation of fraction 4 into sixteen fractions

An aliquot (10 g) of fraction 4 was further separated on a semipreparative HPLC system (cf. chapter **3.7.2**, system 1-1, gradient 1). Monitoring the effluent at 220 nm, a total of 16 subfractions were collected, separated from solvent under vacuum, and then freeze-dried to obtain fractions 4-1 (286 mg), 4-2 (47 mg), 4-3 (86 mg), 4-4 (455 mg), 4-5 (1542 mg), 4-6 (3129 mg), 4-7 (153 mg), 4-8 (46 mg), 4-9 (115 mg), 4-10 (9 mg), 4-11 (11 mg), 4-12 (25 mg), 4-13 (21 mg), 4-14 (6 mg), 4-15 (39 mg), and 4-16 (90 mg) with the yields given in parentheses (**Figure 12**).

3.4.3 Fractionation of fraction 4-14 into eleven fractions

Fraction 4-14 (6 mg) of was further separated by means of semipreparative HPLC system (cf. chapter **3.7.2**, system 2-1). Monitoring the effluent at 220 nm, a total of 11 subfractions were separated to obtain fractions 4-14.1 (<0.1 mg), 4-14.2 (<0.1 mg), 4-14.3 (<0.1 mg), 4-14.4 (0.2 mg), 4-14.5 (0.4 mg), 4-14.6 (<0.1 mg), 4-14.7 (<0.1 mg), 4-14.8 (<0.1 mg), 4-14.9 (0.6 mg), 4-14.10 (<0.1 mg), 4-14.11 (0.7 mg) with the yields given in parentheses (**Figure 16**).

3.4.4 Fractionation to obtain fraction 4-14.6 from ethyl acetate extract of aged garlic extract (AGE)

An aliquot of AGE (1250 g, dry weight) was extracted with 2.5 L of ethyl acetate twice followed by the HPLC separation described in chapter **3.4.2** to lead 534.6 mg of fraction 4-14. Then, an aliquot (200 mg) of fraction 4-14 was fractionated using the HPLC separation described in chapter **3.4.3** to give 63.8 mg of fraction 4-14.6.

3.4.5 Fractionation of fraction 4-14.6 and isolation of dilignol compounds

An aliquot (30 mg) of fraction 4-14.6 was then further separated using the same semipreparative HPLC system (cf. chapter **3.7.2**, system 2-2). Monitoring the HPLC effluent at 220 nm showed two main compounds, which were isolated, freed from solvent under vacuum, and freeze-dried to afford compounds **1** (14.7 mg) and **2** (11.7 mg) as white, amorphous powders in yields (**Figure 18**).

Spectroscopic data of (–)-(2R,3S)-dihydrodehydrodiconiferyl alcohol (1)

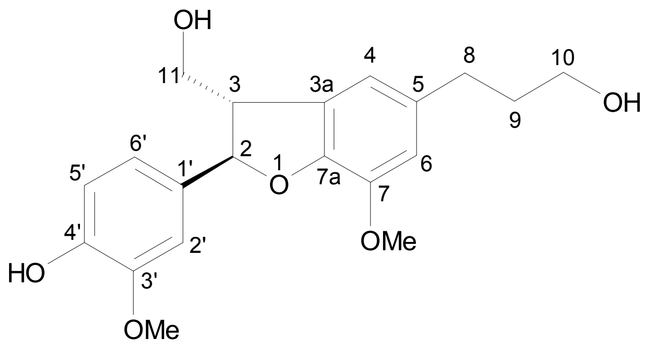

UV/vis (MeOH/H_2O, 5:5, v/v): λmax = 232, 281 nm. **UPLC-TOF-MS (ESI$^-$)**: *m/z* 359.1497 ($[M-H]^-$, measured; *m/z* 359.1495, calculated for $[C_{20}H_{24}O_6-H]^-$). **CD (MeOH, 0.28 mmol/L)**: λmax ($\Delta\varepsilon$) = 294 (-1.1), 242 (-2.8), 224 (+1.4). **^{1}H NMR (400 MHz, acetone-*d_6*, COSY)**: δ/ppm 7.04 [d, 1H, *J* = 1.9 Hz, H-C(2')], 6.89 [dd, 1H, *J* = 1.9, 8.2 Hz, H-C(6')], 6.81 [d, 1H, *J* = 8.2 Hz, H-C(5')], 6.75 [d, 1H, *J* = 1.6 Hz, H-C(4)], 6.73 [d, 1H, *J* = 1.6 Hz, H-C(6)], 5.52 [d, 1H, *J* = 6.6 Hz, H-C(2)], 3.83 [s, 3H, H-C(7-OMe)], 3.82 [s, 3H, H-C(3'-OMe)], 3.76-3.92 [m, 2H, H-C(11)], 3.57 [t, 2H, *J*= 6.4 Hz, H-C(10)], 3.51 [m, 1H, *J* = 6.4, 6.6 Hz, H-C(3)], 2.62 [t, 2H, *J* = 7.7 Hz, H-C(8)], 1.79 [m, 2H, *J* = 6.4, 7.7 Hz, H-C(9)]. **^{13}C NMR (100 MHz, acetone-*d_6*, HSQC, HMBC)**: δ/ppm 148.35 [C(3')], 147.35 [C(7a)], 147.19 [C(4')], 144.89 [C(7)], 136.30 [C(5)], 134.70 [C(1')], 130.00 [C(3a)], 119.54 [C(6')], 117.57 [C(4)], 115.64 [C(5')], 113.89 [C(6)], 110.45 [C(2')], 88.18 [C(2)], 64.78 [C(11)], 61.84 [C(10)], 56.42 [C(7-OMe)], 56.27 [C(3'-OMe)], 55.10 [C(3)], 36.00 [C(9)], 32.70 [C(8)].

Spectroscopic data of (+)-(*2S*,*3R*)-dehydrodiconiferyl alcohol (2)

UV/vis (MeOH/H_2O, 5:5, v/v): λmax = 225, 275 nm. **UPLC-TOF-MS (ESI$^-$)**: *m/z* 357.1350 ($[M-H]^-$, measured; *m/z* 357.1338, calculated for $[C_{20}H_{22}O_6-H]^-$).

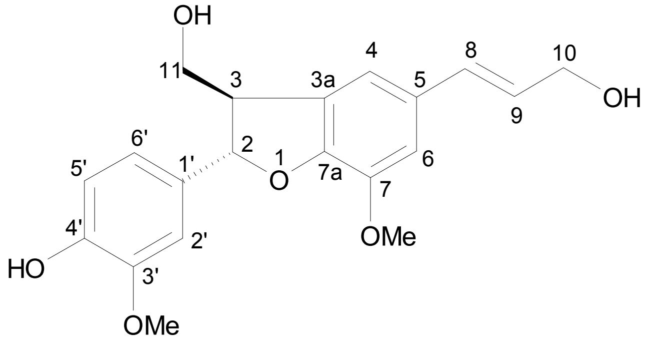

CD (MeOH, 0.28 mmol/L): λ max ($\Delta\varepsilon$) = 286 (+1.4), 231 (-1.2). **^{1}H NMR (400 MHz, acetone-d_6, COSY)**: δ/ppm 7.04[d, 1H, *J* = 1.9 Hz, H-C(2')], 6.98 [d, 1H, *J* = 1.6 Hz, H-C(4)], 6.95 [d, 1H, *J* = 1.6 Hz, H-C(6)], 6.89 [dd, 1H, *J* = 1.9, 8.1 Hz, H-C(6')], 6.81 [d, 1H, *J* = 8.2 Hz, H-C(5')], 6.53 [d, 1H, *J* = 15.9 Hz, H- C(8)], 6.25 [dt, 1H, *J* = 5.3, 15.9 Hz, H-C(9)], 5.57 [d, 1H, *J* = 6.5 Hz, H-C(2)], 4.20 [d, 2H, *J* = 5.3 Hz, H-C(10)], 3.87 [s, 3H, H-C(7-OMe)], 3.82 [s, 3H, H-C(3'-OMe)], 3.93-3.79 [m, 2H, H-C(11)], 3.54 [dd, 1H, *J* = 6.3, 6.5 Hz, H-C(3)]. **^{13}C NMR (100 MHz, acetone-d_6, HSQC, HMBC)**: δ/ppm 151.77 [C(3')], 149.27 [C(4')], 148.84 [C(3)], 147.20 [C(4)], 133.79 [C(1)], 133.17 [C(1')], 131.42 [C(7')], 128.63 [C(8')], 120.81 [C(6')], 120.75 [C(6)], 118.87 [C(5')], 115.85 [C(5)], 111.76 [C(2)], 111.30 [C(2')], 87.14 [C(8)], 74.04 [C(7)], 63.75 [C(9')], 61.92 [C(9)], 56.55 [C(3'-OMe)], 56.35 [C(3-OMe)].

3.5 Synthetic experiments and model reactions

3.5.1 Synthesis of *erythro*- and *threo*-guaiacylglycerol-β-*O*-4'-coniferyl ether

Following a literature protocol (*Ito et al., 2002*) with some modifications, the compounds **3** and **4** were synthesized. Coniferyl alcohol (0.56 mmol) was dissolved in phosphate buffer (85 mL; 100 mM, pH 6.0), and a solution (5 mL) of horseradish peroxidase (3.4 µg/mL) in phosphate buffer and an aqueous solution (85 mL) of hydrogen peroxide (0.01% in water) were added to the solution dropwise within 30 min while stirring at room temperature. After continued stirring for 5 h, the reaction was stopped by the addition of hydrogen chloride (2 mL, 1 M). Then the reaction mixture was extracted with ethyl acetate (2 × 200 mL), the combined organic layers were separated from solvent under vacuum.

The residue was redissolved in methanol/water (75/25, v/v; 15 mL), and then the target compounds **3** and **4** were isolated by means of semipreparative HPLC system (cf. chapter **3.7.2**, system 1-2, gradient 1). Monitoring the effluent at 220 nm, the effluent of the peaks detected at 16.2 and 16.8 min, respectively, were collected individually and freed from solvent under vacuum to give compounds 3 (4.0 µmol) and 4 (7.2 µmol) as white, amorphous powders after freeze-drying (**Figure 26**).

Spectroscopic data of *erythro*-guaiacylglycerol-β-*O*-4'-coniferyl ether (3)

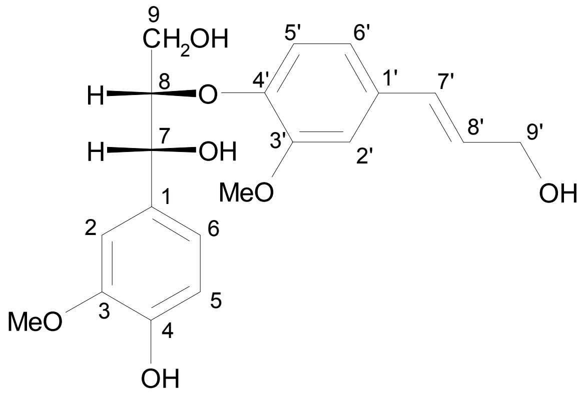

UV/vis (MeOH/H_2O, 5:5, v/v): λ max = 265 nm. **UPLC-TOF-MS (ESI$^-$)**: *m/z* 375.1446 ([M−H]$^-$, measured; *m/z* 375.1444, calculated for [$C_{20}H_{24}O_7$−H]$^-$). **^{1}H NMR (500 MHz, methanol-*d₄*, COSY)**: δ/ppm 3.80 [s, 3H, H-C(3-OMe)], 3.80 [s, 3H, H-C(3'-OMe)], 3.80 [m, 2H, H-C(9)], 4.19 [dd, 2H, *J* = 1.4, 5.8 Hz, H-C(9')], 4.35 [m, 1H, H-C(8)], 4.82 [overlapped, 1H, H-C(7)], 6.24 [dt, 1H, *J* = 5.8, 15.9 Hz, H-C(8')], 6.51 [dt, 1H, *J* = 1.4, 15.9 Hz, H-C(7')], 6.73 [d, 1H, *J* = 8.1 Hz, H-C(5)], 6.84 [dd, 1H, *J* = 1.8, 8.1 Hz, H-C(6)], 6.87 [brs, 2H, H-C(5', 6')], 7.00 [s, 1H, H-C(2')], 7.02 [d, 1H, *J* = 1.9 Hz, H-C(2)]. **^{13}C NMR (125 MHz, methanol-*d₄*, HSQC, HMBC)**: δ/ppm 56.34 [C(3'-OMe)], 56.52 [C(3-OMe)], 62.23 [C(9)], 63.76 [C(9')], 74.12 [C(7)], 86.22 [C(8)], 111.40 [C(2')], 111.90 [C(2)], 115.66 [C(5)], 118.92 [C(5')], 120.66 [C(6')], 121.04 [C(6)], 128.51 [C(8')], 131.46 [C(7')], 133.07 [C(1')], 134.10 [C(1)], 147.04 [C(4)], 148.72 [C(3)], 148.96 [C(4')], 151.93 [C(3')].

Spectroscopic data of *threo*-guaiacylglycerol-β-*O*-4'-coniferyl ether (4)

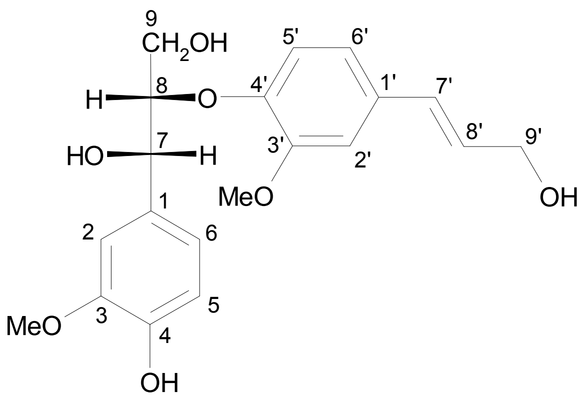

UV/vis (MeOH/H_2O, 5:5, v/v): λ max = 264 nm. **UPLC-TOF-MS (ESI$^-$)**: *m/z* 375.1447 ([M−H]$^-$, measured; *m/z* 375.1444, calculated for [$C_{20}H_{24}O_7$−H]$^-$). **^{1}H NMR (500 MHz, methanol-*d₄*, COSY)**: δ/ppm 3.51 [dd, 2H, *J* = 5.3, 11.9 Hz, H-C(9b)], 3.77 [dd, 1H, *J* = 4.0, 11.9 Hz, H-

C(9a)], 3.86 [s, 3H, H-C(3-OMe)], 3.91 [s, 3H, H-C(3'-OMe)], 4.24 [dd, 2H, *J* = 1.4, 5.7 Hz, H-C(9')], 4.33 [m, 1H, H-C(8)], 4.92 [d, 1H, *J* = 5.8 Hz, H-C(7)], 6.30 [dt, 1H, *J* = 5.7, 15.9 Hz, H-C(8')], 6.57 [d, 1H, *J* = 15.9 Hz, H-C(7')], 6.79 [d, 1H, *J* = 8.1 Hz, H-C(5)], 6.90 [dd, 1H, *J* = 1.9, 8.1 Hz, H-C(6)], 6.95 [dd, 1H, *J* = 1.9, 8.3 Hz, H-C(6')], 7.03 [d, 1H, *J* = 8.3 Hz, H-C(5')], 7.06 [d, 1H, *J* = 1.9 Hz, H-C(2)], 7.09 [d, 1H, *J* = 1.9 Hz, H-C(2')]. **^{13}C NMR (125 MHz, methanol-*d_4*, HSQC, HMBC)**: δ/ppm 56.35 [C(3-OMe)], 56.55 [C(3'-OMe)], 61.92 [C(9)], 63.75 [C(9')], 74.04 [C(7)], 87.14 [C(8)], 111.30 [C(2')], 111.76 [C(2)], 115.85 [C(5)], 118.87 [C(5')], 120.75 [C(6)], 120.81 [C(6')], 128.63 [C(8')], 131.42 [C(7')], 133.17 [C(1')], 133.79 [C(1)], 147.20 [C(4)], 148.84 [C(3)], 149.27 [C(4')], 151.77 [C(3')].

3.5.2 Synthesis of tetrahydro-β-carboline derivatives

3.5.2.1 Preparation of the mixture of 1-methyl-1,2,3,4-tetrahydro-β-carboline-3-carboxylic acids (2' and 3')

Following a literature protocol (*Ichikawa et al., 2002*) with a slight modification, L-tryptophan (1.0 g, 4.9 mmol) was dissolved in 10 mL of water. After addition of 0.1 mL of sulfuric acid and acetaldehyde (0.5 mL, 8.9 mmol), the reaction mixture was stirred at room temperature for 12 h. The pH was adjusted to 5 with 1N sodium hydroxide. Then the filtrate obtained after filtration was analyzed, and the mixture of compounds **2'** and **3'** was isolated by semipreparative HPLC system (cf. chapter **3.7.2**, system 1-2, gradient 2). Monitoring the effluent at 220 nm, the effluent of the peak detected around 11-12 min was collected and freed from solvent under vacuum to give the mixture of compounds **2'** and **3'** (3.4 mmol) as white, amorphous powders after freeze-drying.

Spectroscopic data of the mixture of 1-methyl-1,2,3,4-tetrahydro-β-carboline-3-carboxylic acids (2' and 3')

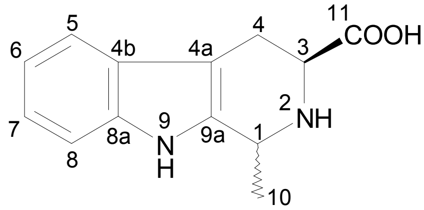

LC-MS (ESI$^+$): *m/z* 231.2 ([M+H]$^+$). **^{1}H NMR (400 MHz, DMSO-*d_6*, COSY)**: δ/ppm 1.60 [d, 3H, *J* = 6.8 Hz, H-C(10)], 2.97 [dd, 1H, *J* = 7.9, 15.9 Hz, H-C(4α)], 3.12 [dd, 1H, *J* = 5.5, 16.2 Hz, H-C(4β)], 3.68 [dd, 1H, *J* = 5.5, 7.9 Hz, H-

C(3)], 4.67 [d, 1H, J = 6.8 Hz, H-C(1)], 6.99 [m, 1H, H-C(6)], 7.08 [m, 1H, H-C(7)], 7.34 [t, 1H, J = 7.6 Hz, H-C(8)], 7.44 [t, 1H, J = 7.3 Hz, H-C(5)], 11.13 [s, 1H, H-N(9)]. **^{13}C NMR (100 MHz, DMSO-d_6, HSQC, HMBC)**: δ/ppm 18.24 [C(10)], 23.20 [C(4)], 46.54 [C(1)], 52.78 [C(3)], 106.59 [C(4a)], 111.27 [C(8)], 118.03 [C(5)], 118.85 [C(6)], 121.36 [C(7)], 126.11 [C(4b)], 132.38 [C(9a)], 136.41 [C(8a)], 169.83 [C(11)].

3.5.2.2 Synthesis of 1-methyl-1,2,3,4-tetrahydro-β-carboline-1,3-dicarboxylic acids (4' and 5')

Following a literature protocol (*Ichikawa et al., 2002*) with a slight modification, L-Tryptophan (1.0 g, 4.9 mmol) was dissolved in 10 mL of water. After addition of 0.1 mL of sulfuric acid and pyruvic acid (0.5 g, 5.7 mmol), the reaction mixture was stirred at room temperature for 12 h. The pH was adjusted to 5 with 1N sodium hydroxide. Then the filtrate obtained after filtration was analyzed, and the compounds **4'** and **5'** were isolated by semipreparative HPLC system (cf. chapter **3.7.2**, system 1-2, gradient 2). Monitoring the effluent at 220 nm, the effluent of the peaks detected around 11-12 min and around 13-14 was collected and freed from solvent under vacuum to give the compounds **4'** (1.1 mmol) and **5'** (0.2 mmol), respectively, as white and amorphous powders after freeze-drying.

Spectroscopic data of (*1R*,*3S*)-1-methyl-1,2,3,4-tetrahydro-β-carboline-1,3-dicarboxylic acid (4')

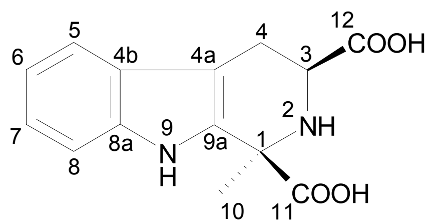

LC-MS (ESI$^+$): m/z 275.1 ([M+H]$^+$). **^{1}H NMR (500 MHz, DMSO-d_6, COSY)**: δ/ppm 1.75 [s, 3H, H-C(10)], 2.90 [dd, 1H, J = 11.5, 15.5 Hz, H-C(4α)], 3.16 [dd, 1H, J = 4,8, 15.5 Hz, H-C(4β)], 4.14 [dd, 1H, J = 4.8, 11.5 Hz, H-C(3)], 6.96 [dd, 1H, J = 7.4, 7.7 Hz, H-C(6)], 7.05 [dd, 1H, J = 7.4, 8.0 Hz, H-C(7)], 7.40 [d, 1H, J = 7.7 Hz, H-C(5)], 7.41 [d, 1H, J = 8.0 Hz, H-C(8)], 10.71 [s, 1H, H-N(9)]. **^{13}C NMR (125 MHz, DMSO-d_6, HSQC, HMBC)**: δ/ppm 23.22 [C(4)], 23.91 [C(10)], 51.73 [C(3)], 60.32 [C(1)], 104.24 [C(4a)], 111.69 [C(8)], 117.63 [C(5)], 118.51 [C(6)], 121.14 [C(7)], 125.56 [C(4b)], 132.90 [C(9a)], 136.11 [C(8a)], 170.41 [C(11)], 171.42 [C(12)].

Spectroscopic data of (*1S*,*3S*)-1-methyl-1,2,3,4-tetrahydro-β-carboline-1,3-dicarboxylic acid (5')

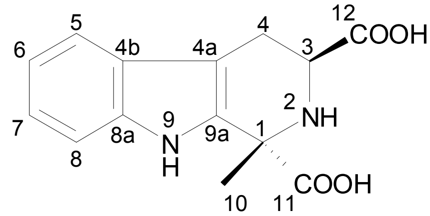

LC-MS (ESI$^+$): *m/z* 275.1 ([M+H]$^+$). **^{1}H NMR (500 MHz, DMSO-*d$_6$*, COSY)**: δ/ppm 1.71 [s, 3H, H-C(10)], 2.74 [dd, 1H, *J* = 11.7, 15.5 Hz, H-C(4α)], 3.07 [dd, 1H, *J* = 4,5, 15.5 Hz, H-C(4β)], 4.02 [dd, 1H, *J* = 4.5, 11.7 Hz, H-C(3)], 6.96 [dd, 1H, *J* = 7.1, 7.2 Hz, H-C(6)], 7.05 [dd, 1H, *J* = 7.1, 7.2 Hz, H-C(7)], 7.33 [d, 1H, *J* = 8.0 Hz, H-C(8)], 7.41 [d, 1H, *J* = 7.8 Hz, H-C(5)], 11.05 [s, 1H, H-C(9)]. **^{13}C NMR (125 MHz, DMSO-*d$_6$*, HSQC, HMBC)**: δ/ppm 23.46 [C(4)], 24.50 [C(10)], 53.99 [C(3)], 60.45 [C(1)], 105.28 [C(4a)], 111.11 [C(8)], 117.68 [C(5)], 118.32 [C(6)], 120.91 [C(7)], 125.50 [C(4b)], 133.50 [C(9a)], 136.27 [C(8a)], 171.82 [C(11)] , 171.94 [C(12)].

3.5.3 Synthesis of Amadori compounds and tetrahydro-β-carbolines

3.5.3.1 *N*α-(1-Deoxy-D-fructos-1-yl)-*S*-allyl-L-cysteine (5)

Following a method of *Ryu et al.* (*2001*) with a slight modification, *S*-allyl-L-cysteine (100 mg, 0.62 mmol) and D-glucose (620 mg, 3.44 mmol) were dissolved in 5 mL of glacial acetic acid, and the mixture was stirred at 80ºC for 1h. The reaction mixture was neutralized with sodium hydroxide, and the filtrate obtained after filtration was analyzed by semipreparative HPLC system (cf. chapter **3.7.2**, system 1-2, gradient 3). Monitoring the effluent at 220 nm, the effluent of the peak detected around 15.0 min was collected and freed from solvent under vacuum to give the compound **5** (80.5 mg, 0.25 mmol, 40.1%) as white, amorphous powders after freeze-drying.

Spectroscopic data of *N*α-(1-deoxy-D-fructos-1-yl)-*S*-allyl-L-cysteine (5)

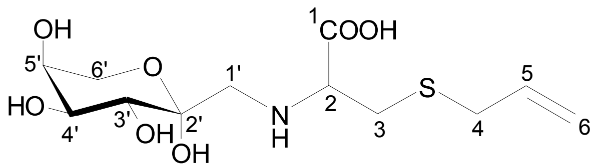

UPLC-TOF-MS (ESI$^-$): *m/z* 322.0965 ([M−H]$^-$, measured; *m/z* 322.0960, calculated for [$C_{12}H_{21}NO_7S$−H]$^-$). **^{1}H NMR (500**

MHz, methanol-*d*$_4$, COSY): δ/ppm 2.91 [m, 1H, H-C(3α)], 3.16 [m, 1H, H-C(3β)], 3.25 [d, 2H, *J* = 6.9 Hz, H-C(4)], 3.40 [m, 2H, H-C(1')], 3.70 [m, 1H, H-C(6'α)], 3.77 [m, 1H, H-C(2)], 3.80 [m, 1H, H-C(5')], 3.99 [m, 1H, H-C(4')], 4.01 [m, 1H, H-C(6'β)], 4.12 [m, 1H, H-C(3')], 5.20 [dd, 2H, *J* = 10.0, 16.9 Hz, H-C(6)], 5.82 [m, 1H, H-C(5)]. **^{13}C NMR (125 MHz, methanol-*d*$_4$, HSQC, HMBC)**: δ/ppm 31.87 [C(3)], 35.27 [C(4)], 54.70 [C(1')], 62.92 [C(2)], 65.36 [C(6')], 72.16 [C(5')], 77.83 [C(4')], 84.27 [C(3')], 96.80 [C(2')], 118.80 [C(6)], 135.00 [C(5)], 171.97 [C(1)].

3.5.3.2 *N*α-(1-Deoxy-D-fructos-1-yl)-γ-glutamyl-*S*-allyl-L-cysteine (6)

*N*α-(1-Deoxy-D-fructos-1-yl)-γ-glutamyl-*S*-allyl-L-cysteine (**6**) was prepared following the same procedure described in chapter **3.5.3** using γ-glutamyl-*S*-allyl-L-cysteine (100 mg, 0.34 mmol) instead of *S*-allyl-L-cysteine. The reaction mixture was analyzed by semipreparative HPLC system (cf. chapter **3.7.2**, system 1-2, gradient 4) after neutralization and filtration. Monitoring the effluent at 220 nm, the effluent of the peak detected around 10.5 min was collected and freed from solvent under vacuum to give the compound **6** (66.3 mg, 0.15 mmol, 42.5%) as white, amorphous powders after freeze-drying.

Spectroscopic data of *N*α-(1-deoxy-D-fructos-1-yl)-γ-glutamyl-*S*-allyl-L-cysteine (6)

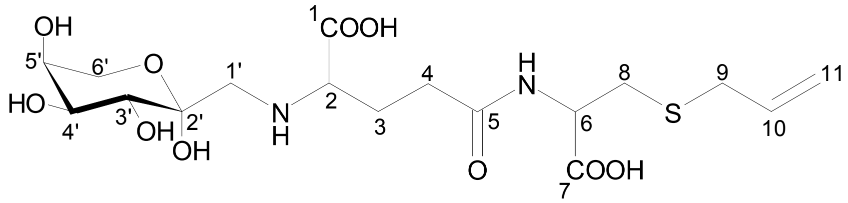

UPLC-TOF-MS (ESI$^-$): *m/z* 451.1389 ([M−H]$^-$, measured; *m/z* 451.1386, calculated for $[C_{17}H_{28}N_2O_{10}S-H]^-$). **^{1}H NMR (500 MHz, methanol-*d*$_4$, COSY)**: δ/ppm 2.19 [dd, 2H, *J* = 6.0, 12.1 Hz, H-C(3)], 2.62 [m, 2H, H-C(4)], 2.78 [dd, 2H, *J* = 8.4, 13.9 Hz, H-C(8α)], 2.99 [m, 1H, H-C(8β)], 3.18 [d, 2H, *J* = 7.3 Hz, H-C(9)], 3.28 [m, 2H, H-C(1')], 3.68 [m, 1H, H-C(2)], 3.70 [m, 1H, H-C(6'α)], 3.79 [m, 1H, H-C(5')], 3.99 [m, 1H, H-C(4')], 4.02 [m, 1H, H-C(6'β)], 4.08 [m, 1H, H-C(3')], 4.57 [m, 1H, H-C(6)], 5.13 [m, 2H, H-C(11)], 5.79 [m, 1H, H-C(10)]. **^{13}C NMR (125 MHz, methanol-*d*$_4$, HSQC, HMBC)**: δ/ppm 31.87 [C(3)], 35.27 [C(4)], 54.70 [C(1')], 62.92 [C(2)], 65.36 [C(6')], 72.16 [C(5')], 77.83 [C(4')], 84.27

[C(3')], 96.80 [C(2')], 118.80 [C(6)], 135.00 [C(5)], 171.97 [C(1)].

3.5.3.3 *N*α-(1-Deoxy-D-fructos-1-yl)-L-phenylalanine (8)

*N*α-(1-Deoxy-D-fructos-1-yl)-L-phenylalanine (**8**) was prepared following the same procedure described in chapter **3.5.3** using L-phenylalanine (100 mg, 0.61 mmol) instead of *S*-allyl-L-cysteine. The reaction mixture was analyzed by semipreparative HPLC system (cf. chapter **3.7.2**, system 1-2, gradient 5) after neutralization and filtration. Monitoring the effluent at 220 nm, the effluent of the peak detected around 6.5 min was collected and freed from solvent under vacuum to give the compound **8** (65.4 mg, 0.20 mmol, 32.8%) as white, amorphous powders after freeze-drying.

Spectroscopic data of *N*α-(1-deoxy-D-fructos-1-yl)-L-phenylalanine (8)

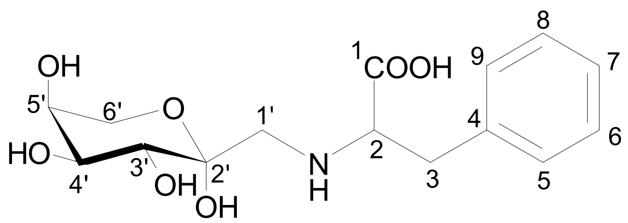

LC-MS (ESI$^+$): *m/z* 328.2 ($[M+H]^+$). **^{1}H NMR (400 MHz, methanol-*d₄*, COSY)**: δ/ppm 3.05 [m, 1H, H-C(1'α)], 3.18 [m, 2H, H-C(3)], 3.31 [m, 1H, H-C(1'β)], 3.62 [m, 1H, H-C(3')], 3.64 [m, 1H, H-C(6'α)], 3.73 [m, 1H, H-C(4)], 3.83 [m, 1H, H-C(5')], 3.88 [m, 1H, H-C(6'β)], 3.93 [m, 1H, H-C(2)], 7.25-7.37 [m, 5H, H-C(5, 6, 7, 8, 9)]. **^{13}C NMR (100 MHz, methanol-d_4, HSQC, HMBC)**: δ/ppm 37.36 [C(3)], 54.81 [C(1')], 65.26 [C(6')], 65.91 [C(2)], 70.83 [C(5')], 72.13 [C(4')], 84.36 [C(3')], 96.59 [C(2')], 128.68 [C(7)], 130.07 [C(6, 8)], 130.63 [C(5, 9)], 137.23 [C(4)], 172.84 [C(1)].

3.5.3.4 *N*α-(1-Deoxy-D-fructos-1-yl)-L-tyrosine (9)

*N*α-(1-Deoxy-D-fructos-1-yl)-L-tyrosine (**9**) was prepared following the same procedure described in chapter **3.5.3** using L-tyrosine (100 mg, 0.55 mmol) instead of *S*-allyl-L-cysteine. The reaction mixture was analyzed by semipreparative HPLC system (cf. chapter **3.7.2**, system 1-2, gradient 6) after neutralization and filtration. Monitoring the effluent at 220 nm, the effluent of the peak detected around 7.5 min was collected and freed from solvent under vacuum to give the compound **9** (44.6 mg, 0.13 mmol, 23.6%) as white, amorphous powders after freeze-drying.

Spectroscopic data of *N*α-(1-deoxy-D-fructos-1-yl)-L-tyrosine (9)

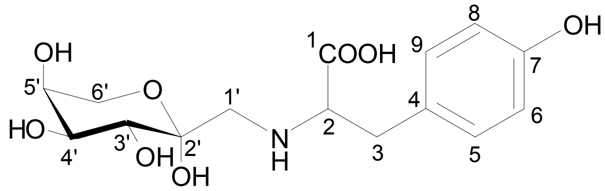

LC-MS (ESI^+): *m/z* 344.1 ($[M+H]^+$). **^{1}H NMR (400 MHz, methanol-*d_4*, COSY)**: δ/ppm 3.05 [m, 1H, H-C(1'α)], 3.23 [m, 2H, H-C(3)], 3.31 [m, 1H, H-C(1'β)], 3.61 [m, 1H, H-C(3')], 3.64 [m, 1H, H-C(6'α)], 3.72 [m, 1H, H-C(2)], 3.82 [m, 1H, H-C(4')], 3.93 [m, 1H, H-C(6'β)], 3.99 [m, 1H, H-C(5')], 6.73-6.79 [m, 2H, H-C(5, 9)] , 7.11-7.17 [m, 2H, H-C(6, 8)]. **^{13}C NMR (100 MHz, methanol-*d_4*, HSQC, HMBC)**: δ/ppm 36.73 [C(3)], 54.92 [C(1')], 62.35 [C(6')], 66.17 [C(2)], 70.82 [C(5')], 77.91 [C(4')], 84.86 [C(3')], 96.57 [C(2')], 116.87 [C(6)], 117.00 [C(8)], 127.44 [C(4)], 131.64 [C(5)], 131.68 [C(9)], 158.05 [C(7)], 173.00 [C(1)].

3.5.3.5 *N*α-(1-Deoxy-D-fructos-1-yl)-L-tryptophan (10), *trans*-1-[(*1R*,*2R*,*3S*,*4S*)-1,2,3,4,5-pentahydroxypent-1-yl]-1,2,3,4-tetrahydro-β-carboline-3-carboxylic acid (11), and *cis*-1-[(*1R*,*2R*,*3S*,*4S*)-1,2,3,4,5-pentahydroxypent-1-yl]-1,2,3,4-tetrahydro-β-carboline-3-carboxylic acid (12)

*N*α-(1-Deoxy-D-fructos-1-yl)-L-tryptophan (**10**), *trans*-1-[(*1R*,*2R*,*3S*,*4S*)-1,2,3,4,5-pentahydroxypent-1-yl]-1,2,3,4-tetrahydro-β-carboline-3-carboxylic acid (**11**), and *cis*-1-[(*1R*,*2R*,*3S*,*4S*)-1,2,3,4,5-pentahydroxypent-1-yl]-1,2,3,4-tetrahydro-β-carboline-3-carboxylic acid (**12**) were prepared following the same procedure described in chapter **3.5.3** using L-tryptophan (100 mg, 0.49 mmol) instead of *S*-allyl-L-cysteine. The reaction mixture was analyzed by semipreparative HPLC system (cf. chapter **3.7.2**, system 1-2, gradient 5) after neutralization and filtration. Monitoring the effluent at 220 nm, the effluent of the peaks detected around 10.5 min, 11.5 min, and 13.5 min were collected separately and freed from solvent under vacuum to give the compounds **11** (29.8 mg, 0.08 mmol, 16.3%), **10** (6.0 mg, 0.02 mmol, 4.1%), and **12** (10.5 mg, 0.03 mmol, 6.1%), respectively, as white, amorphous powders after freeze-drying.

Spectroscopic data of *N*α-(1-deoxy-D-fructos-1-yl)-L-tryptophan (10)

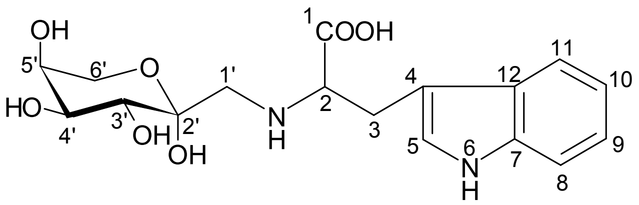

LC-MS (ESI$^+$): *m/z* 367.2 ($[M+H]^+$). **^{1}H NMR (400 MHz, methanol-*d$_4$*, COSY)**: δ/ppm 2.95 [m, 1H, H-C(1'α)], 3.23 [m, 2H, H-C(3)], 3.45 [m, 1H, H-C(1'β)], 3.54 [m, 1H, H-C(6'α)], 3.56 [m, 1H, H-C(3')], 3.68 [m, 1H, H-C(4')], 3.77 [m, 1H, H-C(6'β)], 3.82 [m, 1H, H-C(5')], 3.92 [m, 1H, H-C(2)], 7.06 [m, 1H, H-C(10)], 7.13 [m, 1H, H-C(9)], 7.22 [m, 1H, H-C(5)], 7.37 [m, 1H, H-C(8)], 7.70 [m, 1H, H-C(11)]. **^{13}C NMR (100 MHz, methanol-*d$_4$*, HSQC, HMBC)**: δ/ppm 27.65 [C(3)], 54.74 [C(1')], 62.28 [C(2)], 65.12 [C(6')], 71.11 [C(5')], 77.98 [C(4')], 84.26 [C(3')], 96.50 [C(2')], 102.76 [C(4)], 112.50 [C(8)], 119.53 [C(11)], 120.34 [C(9)], 123.00 [C(10)], 125.38 [C(5)], 128.41 [C(12)], 138.47 [C(7)], 173.21 [C(1)].

Spectroscopic data of *trans*-1-[(1R,2R,3S,4S)-1,2,3,4,5-pentahydroxypent-1-yl]-1,2,3,4-tetrahydro-β-carboline-3-carboxylic acid (11)

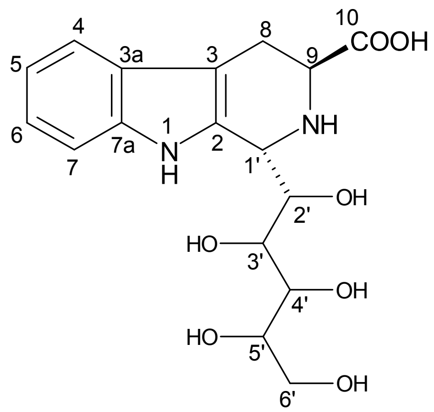

LC-MS (ESI$^+$): *m/z* 367.2 ($[M+H]^+$). **^{1}H NMR (500 MHz, methanol-*d$_4$*, COSY)**: δ/ppm 3.06 [dd, 1H, J = 10.8, 16.2 Hz, H-C(8α)], 3.46 [dd, 1H, J = 5.2, 16.2 Hz, H-C(8β)], 3.68 [dd, 1H, J = 5.4, 10.9 Hz, H-C(6'α)], 3.75 [m, 1H, H-C(5')], 3.81 [dd, 1H, J = 4.1, 10.9 Hz, H-C(6'β)], 4.05 [d, 1H, J = 7.5 Hz, H-C(4')], 4.11 [d, 1H, J = 3.8 Hz, H-C(3')], 4.17 [dd, 1H, J = 5.2, 10.8 Hz, H-C(9)], 4.20 [dd, 1H, J = 3.8, 9.1 Hz, H-C(2')], 4.98 [d, 1H, J = 9.1 Hz, H-C(1')], 7.03 [pt, 1H, J = 7.1, 7.9 Hz, H-C(5)], 7.12 [pt, 1H, J = 7.1, 8.1 Hz, H-C(6)], 7.36 [d, 1H, J = 8.1 Hz, H-C(7)], 7.50 [d, 1H, J = 7.9 Hz, H-C(4)]. **^{13}C NMR (125 MHz, methanol-*d$_4$*, HSQC, HMBC)**: δ/ppm 24.03 [C(8)], 55.82 [C(1')], 56.21 [C(9)], 64.64 [C(6')], 70.81 [C(4')], 72.14 [C(2')], 73.00 [C(3')], 73.23 [C(5')], 107.84 [C(3)], 112.40 [C(7)], 119.15 [C(4)], 120.33 [C(5)], 123.35 [C(6)], 127.27 [C(3a)], 130.02 [C(2)], 138.58 [C(7a)], 173.82 [C(10)].

Spectroscopic data of *cis*-1-[(1R,2R,3S,4S)-1,2,3,4,5-pentahydroxypent-1-yl]-1,2,3,4-tetrahydro-β-carboline-3-carboxylic acid (12)

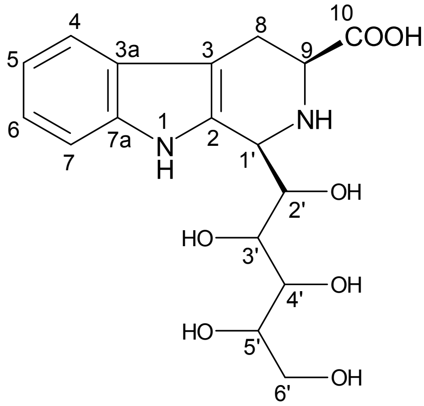

LC-MS (ESI$^+$): *m/z* 367.2 ([M+H]$^+$). **^{1}H NMR (500 MHz, methanol-*d*$_4$, COSY)**: δ/ppm 3.12 [m, 1H, H-C(8α)], 3.40 [dd, 1H, *J* = 4.4, 12.1 Hz, H-C(8β)], 3.73 [dd, 1H, *J* = 5.7, 10.5 Hz, H-C(6'α)], 3.78 [m, 1H, H-C(5')], 3.80 [m, 1H, H-C(6'β)], 3.91 [dd, 1H, *J* = 1.9, 7.5 Hz, H-C(4')], 4.00 [dd, 1H, *J* = 5.0, 12.1 Hz, H-C(9)], 4.23 [dd, 1H, *J* = 1.9, 3.8 Hz, H-C(3')], 4.57 [dd, 1H, *J* = 1.8, 3.8 Hz, H-C(2')], 5.02 [brs, 1H, H-C(1')], 7.05 [pt, 1H, *J* = 7.8 Hz, H-C(5)], 7.14 [pt, 1H, *J* = 7.8 Hz, H-C(6)], 7.36 [d, 1H, *J* = 8.1 Hz, H-C(7)], 7.49 [d, 1H, *J* = 7.8 Hz, H-C(4)]. **^{13}C NMR (125 MHz, methanol-*d*$_4$, HSQC, HMBC)**: δ/ppm 23.71 [C(8)], 57.53 [C(1')], 59.38 [C(9)], 64.64 [C(6')], 71.76 [C(2')], 72.40 [C(3')], 72.47 [C(4')], 72.97 [C(5')], 110.17 [C(3)], 112.38 [C(7)], 119.08 [C(4)], 120.56 [C(5)], 123.40 [C(6)], 127.75 [C(3a)], 129.06 [C(2)], 138.68 [C(7a)], 173.50 [C(10)].

3.5.4 Synthesis of 1-methyl-1,2,3,4-tetrahydro-β-carboline

1-Methyl-1,2,3,4-tetrahydro-β-carboline (**13**) was synthesized by the method of *Ichikawa et al.* (*2002*) with a slight modification. Tryptamine hydrochloride (1.0 g, 6.2 mmol) was dissolved in 10 mL of water, followed by adding 0.1 mL of sulfuric acid and 0.5 mL of acetaldehyde (8.9 mmol). The reaction mixture was stirred at room temperature for 12 h. After the pH was adjusted to 5 with sodium hydroxide, the reaction mixture was filtrated and analyzed by means of semipreparative HPLC system (cf. chapter **3.7.2**, system 1-1, gradient 2). The target compound eluted around 9.5 min was isolated, freed from the solvent in a vacuum, and feeze-dried, leading to amorphous powder of the compound **13** (949 mg, 5.1 mmol, 82.3%).

Spectroscopic data of 1-methyl-1,2,3,4-tetrahydro-β-carboline (13)

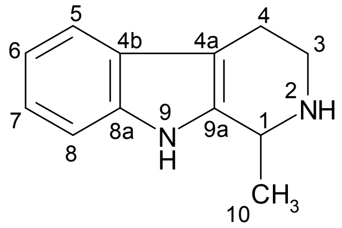

LC-MS (ESI$^+$): *m/z* 187.0 ($[M+H]^+$). **^{1}H NMR (400 MHz, methanol-*d$_4$*, COSY)**: δ/ppm 1.74 [d, 3H, *J* = 6.8 Hz, H-C(10)], 3.06 [m, 2H, H-C(4)], 3.43 [ddd, 1H, *J* = 5.6, 9.1, 12.7 Hz, H-C(3α)], 3.71 [ddd, 1H, *J* = 4.2, 5.6, 12.7 Hz, H-C(3β)], 4.76 [qt, 1H, *J* = 6.8 Hz, H-C(1)], 7.06 [dt, 1H, *J* = 1.0, 7.1, 7.9 Hz, H-C(6)], 7.15 [t, 1H, *J* = 7.1, 8.2 Hz, H-C(7)], 7.37 [d, 1H, *J* = 8.2 Hz, H-C(8)], 7.48 [d, 1H, *J* = 7.9 Hz, H-C(5)]. **^{13}C NMR (100 MHz, methanol-*d$_4$*, HSQC, HMBC)**: δ/ppm 18.06 [C(10)], 19.69 [C(4)], 42.68 [C(3)], 50.71 [C(1)], 106.92 [C(4a)], 112.50 [C(8)], 119.26 [C(5)], 120.70 [C(6)], 123.54 [C(7)], 127.54 [C(4b)], 131.40 [C(9a)], 138.34 [C(8a)].

3.5.5 Synthesis of ethyl *p*-coumarate

p-Coumaric acid (328.0 mg, 2.0 mmol) was dissolved in 1 mL of ethanol (17.1 mmol), followed by adding 100 µL of concentrated sulfuric acid to the solution. The mixture was maintained under argon at 70˚C while stirring. After 20 h, the reaction mixture was neutralized with sodium hydroxide and was analyzed by means of MPLC system (cf. chapter **3.7.3**, gradient 1). The target compound eluted around 6.0 min was isolated, concentrated, and feeze-dried under vacuum, giving amorphous powder of the compound **20** (102.0 mg, 0.53 mmol, 26.6%).

Spectroscopic data of ethyl *p*-coumarate (20)

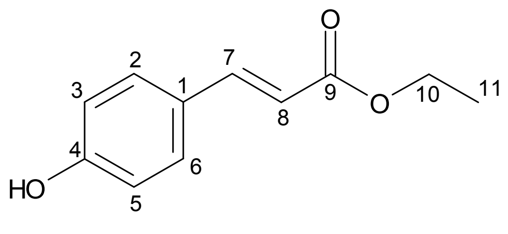

LC-MS (ESI$^+$): *m/z* 193.0 ($[M+H]^+$). **^{1}H NMR (400 MHz, methanol-*d$_4$*, COSY)**: δ/ppm 1.31 [t, 3H, *J* = 7.1 Hz, H-C(11)], 4.21 [q, 2H, *J* = 7.1 Hz, H-C(10)], 6.31 [d, 1H, *J* = 15.9 Hz, H-C(8)], 6.80 [m, 2H, H-C(3, 5)], 7.45 [m, 2H, H-C(2, 6)], 7.60 [d, 1H, *J* = 15.9 Hz, H-C(7)]. **^{13}C NMR (100 MHz, methanol-*d$_4$*, HSQC, HMBC)**: δ/ppm 14.45 [C(11)], 61.45 [C(10)], 115.37 [C(8)], 116.85 [C(3, 5)], 127.20 [C(1)], 131.15 [C(2, 6)], 146.38 [C(7)], 161.30 [C(4)], 169.35 [C(9)].

3.5.6 Synthesis of ^{13}C-labeled Amadori compounds and tetrahydro-β-carbolines

The ^{13}C-labeled analogues of Amadori compounds and tetrahydro-β-carbolines were synthesized by the same protocol as their unlabeled compounds using D-glucose-$^{13}C_6$ instead of D-Glucose.

3.5.6.1 *N*α-(1-Deoxy-D-fructos-1-yl)-*S*-allyl-L-cysteine-$^{13}C_6$ (5-$^{13}C_6$)

The reaction of *S*-allyl-L-cysteine (50 mg, 0.31 mmol) and D-glucose-$^{13}C_6$ (100 mg, 0.54 mmol) led to the compound **5-$^{13}C_6$** (55.8 mg, 0.17 mmol, 54.6%).

Spectroscopic data of *N*α-(1-deoxy-D-fructos-1-yl)-*S*-allyl-L-cysteine-$^{13}C_6$ (5-$^{13}C_6$)

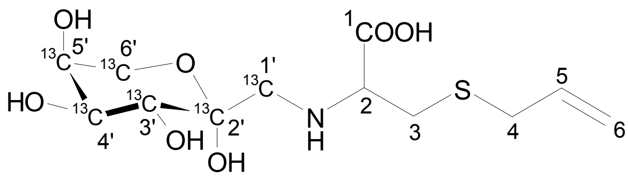

UPLC-TOF-MS (ESI$^-$): *m/z* 328.1163 ([M−H]$^-$, measured; *m/z* 328.1162, calculated for [$^{12}C_6{}^{13}C_6H_{21}NO_7S$−H]$^-$). **^{1}H NMR (500 MHz, methanol-*d$_4$*)**: δ/ppm 2.93 [m, 1H, H-C(3α)], 3.16 [m, 1H, H-C(3β)], 3.24 [m, 2H, H-C(4)], 3.47 [m, 2H, H-C(1')], 3.72 [m, 1H, H-C(6'α)], 3.79 [m, 1H, H-C(2)], 3.86 [m, 1H, H-C(5')], 3.95 [m, 1H, H-C(4')], 4.01 [m, 1H, H-C(6'β)],4.14 [m, 1H, H-C(3')], 5.19 [m, 2H, H-C(6)], 5.82 [m, 1H, H-C(5)].

3.5.6.2 *N*α-(1-Deoxy-D-fructos-1-yl)-γ-glutamyl-*S*-allyl-L-cysteine-$^{13}C_6$ (6-$^{13}C_6$)

The reaction of γ-glutamyl-*S*-allyl-L-cysteine (50 mg, 0.17 mmol) and D-glucose-$^{13}C_6$ (100 mg, 0.54 mmol) led to the compound **6-$^{13}C_6$** (31.1 mg, 0.07 mmol, 39.4%).

Spectroscopic data of *N*α-(1-deoxy-D-fructos-1-yl)-γ-glutamyl-*S*-allyl-L-cysteine-$^{13}C_6$ (6-$^{13}C_6$)

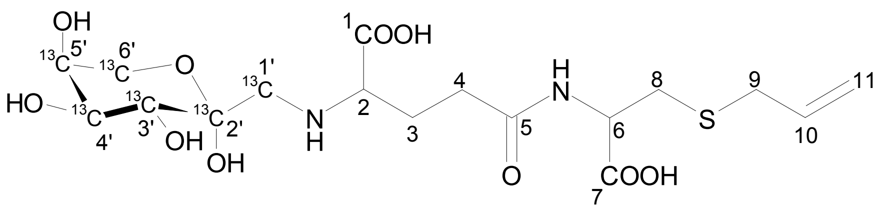

UPLC-TOF-MS (ESI$^-$): *m/z* 457.1580 ([M−H]$^-$, measured; *m/z* 457.1588, calculated for [$^{12}C_{11}{}^{13}C_6H_{28}N_2O_{10}S{-}H]^-$). **^{1}H NMR (500 MHz, methanol-*d₄*)**: δ/ppm 2.18 [m, 2H, *J* = 6.0, 12.1 Hz, H-C(3)], 2.61 [m, 2H, H-C(4)], 2.77 [dd, 2H, *J* = 8.4, 14.0 Hz, H-C(8α)], 2.98 [m, 1H, H-C(8β)], 3.17 [m, 2H, H-C(9)], 3.38 [m, 2H, H-C(1')], 3.65 [m, 1H, H-C(2)], 3.72 [m, 1H, H-C(6'α)], 3.79 [m, 1H, H-C(5')], 3.87 [m, 1H, H-C(4')], 3.94 [m, 1H, H-C(6'β)], 4.17 [m, 1H, H-C(3')], 4.57 [m, 1H, H-C(6)], 5.13 [m, 2H, H-C(11)], 5.79 [m, 1H, H-C(10)].

3.5.6.3 *N*α-(1-Deoxy-D-fructos-1-yl)-L-phenylalanine-$^{13}C_6$ (8-$^{13}C_6$)

The reaction of L-phenylalanine (50 mg, 0.30 mmol) and D-glucose-$^{13}C_6$ (100 mg, 0.54 mmol) led to the compound **8-$^{13}C_6$** (46.3 mg, 0.14 mmol, 45.9%).

Spectroscopic data of *N*α-(1-deoxy-D-fructos-1-yl)-L-phenylalanine-$^{13}C_6$ (8-$^{13}C_6$)

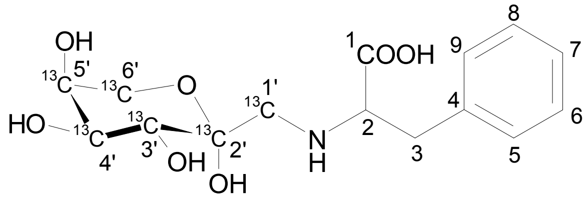

LC-MS (ESI⁻): *m/z* 332.1 ([M−H]⁻). **^{1}H NMR (500 MHz, methanol-*d₄*)**: δ/ppm 3.05 [m, 1H, H-C(1'α)], 3.17 [m, 1H, H-C(1'β)], 3.31 [d, 2H, H-C(3)], 3.47 [m, 1H, H-C(3')], 3.60 [m, 1H, H-C(6'α)], 3.69 [m, 1H, H-C(4)], 3.79 [m, 1H, H-C(5')], 3.88 [m, 1H, H-C(6'β)], 3.93 [m, 1H, H-C(2)], 7.23-7.37 [m, 5H, H-C(5, 6, 7, 8, 9)].

3.5.6.4 *N*α-(1-Deoxy-D-fructos-1-yl)-L-tyrosine-$^{13}C_6$ (9-$^{13}C_6$)

The reaction of L-tyrosine (50 mg, 0.28 mmol) and D-glucose-$^{13}C_6$ (100 mg, 0.54 mmol) led to the compound **9-$^{13}C_6$** (21.1 mg, 0.06 mmol, 21.9%).

Spectroscopic data of *N*α-(1-deoxy-D-fructos-1-yl)-L-tyrosine-$^{13}C_6$ (9-$^{13}C_6$)

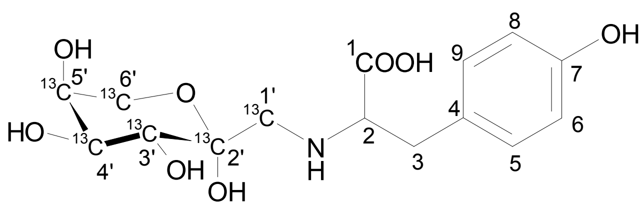

LC-MS (ESI⁻): *m/z* 348.1 ([M−H]⁻). **^{1}H NMR (400 MHz, methanol-*d₄*)**: δ/ppm 3.06 [m, 1H, H-C(1'α)], 3.28 [m, 2H, H-C(3)], 3.31 [m, 1H, H-C(1'β)], 3.45 [m, 1H, H-C(3')], 3.59 [m, 1H, H-C(6'α)], 3.68 [m, 1H, H-C(2)], 3.80 [m, 1H, H-C(4')], 3.83 [m, 1H, H-C(6'β)], 3.97 [m, 1H, H-C(5')], 6.73-6.79 [m, 2H, H-C(5, 9)] , 7.12-7.17 [m, 2H, H-C(6, 8)]. **^{13}C NMR (100 MHz, methanol-*d_4*)**: δ/ppm 36.64 [C(3)], 55.05 [C(1')], 62.43 [C(6')], 65.33 [C(2)], 71.17 [C(5')], 77.87 [C(4')], 84.79 [C(3')], 96.49 [C(2')], 116.80 [C(6)], 116.93 [C(8)], 127.42 [C(4)], 131.54 [C(5)], 131.57 [C(9)], 157.99 [C(7)], 172.83 [C(1)].

3.5.6.5 *N*α-(1-Deoxy-D-fructos-1-yl)-L-tryptophan-$^{13}C_6$ (10-$^{13}C_6$)

The reaction of L-tryptophan (100 mg, 0.49 mmol) and D-glucose-$^{13}C_6$ (200 mg, 1.08 mmol) led to the compounds **10-$^{13}C_6$** (13.2 mg, 0.04 mmol, 7.2%), **11-$^{13}C_6$** (13.9 mg, 0.04 mmol, 7.6%), and **12-$^{13}C_6$** (12.6 mg, 0.03 mmol, 6.9%).

Spectroscopic data of *N*α-(1-deoxy-D-fructos-1-yl)-L-tryptophan-$^{13}C_6$ (10-$^{13}C_6$)

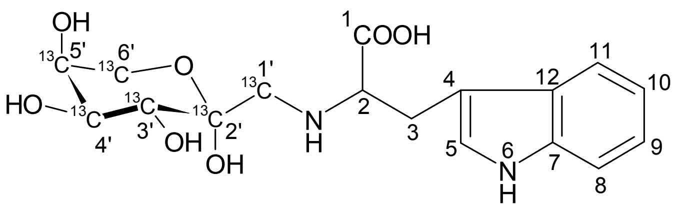

LC-MS (ESI$^+$): *m/z* 373.2 ([M+H]$^+$). **^{1}H NMR (500 MHz, methanol-*d_4*, COSY)**: δ/ppm 2.80 [m, 1H, H-C(1'α)], 3.10 [m, 2H, H-C(3)], 3.45 [m, 1H, H-C(1'β)], 3.55 [m, 1H, H-C(6'α)], 3.57 [m, 1H, H-C(3')], 3.68 [m, 1H, H-C(4')], 3.78 [m, 1H, H-C(6'β)], 3.83 [m, 1H, H-C(5')], 3.96 [m, 1H, H-C(2)], 7.06 [m, 1H, H-C(10)], 7.12 [m, 1H, H-C(9)], 7.24 [m, 1H, H-C(5)], 7.37 [m, 1H, H-C(8)], 7.70 [m, 1H, H-C(11)]. **^{13}C NMR (125 MHz, methanol-*d_4*, HSQC, HMBC)**: δ/ppm 23.94 [C(3)], 40.71 [C(1')], 55.91 [C(2)], 64.72 [C(6')], 70.75 [C(5')], 76.43 [C(4')], 84.20 [C(3')], 98.29 [C(2')], 102.68 [C(4)], 112.34 [C(8)], 119.09 [C(11)], 120.26 [C(9)], 123.29 [C(10)], 127.19 [C(5)], 129.65 [C(12)], 138.48 [C(7)], 173.80 [C(1)].

Spectroscopic data of *trans*-1-[(1R,2R,3S,4S)-1,2,3,4,5-pentahydroxypent-1-yl]-1,2,3,4-tetrahydro-β-carboline-3-carboxylic acid-$^{13}C_6$ (11-$^{13}C_6$)

LC-MS (ESI$^+$): *m/z* 373.2 ([M+H]$^+$). **^{1}H NMR (500 MHz, methanol-*d_4*)**: δ/ppm 3.14 [dd, 1H, *J* = 10.6, 16.3 Hz, H-C(8α)], 3.50 [m, H, H-C(8β)], 3.59 [m, 1H, H-C(6'α)], 3.69 [m, 1H, H-C(5')], 3.87 [m, 1H, H-C(6'β)], 4.00 [m, 1H, H-C(4')], 4.11

[m, 1H, H-C(3')], 4.27 [m, 1H, H-C(9)], 4.32 [m, 1H, H-C(2')], 5.17 [m, 1H, H-C(1')], 7.08 [pt, 1H, *J* = 7.1, 8.0 Hz, H-C(5)], 7.17 [pt, 1H, *J* = 7.1, 8.2 Hz, H-C(6)], 7.40 [d, 1H, *J* = 8.2 Hz, H-C(7)], 7.54 [d, 1H, *J* = 8.0 Hz, H-C(4)].

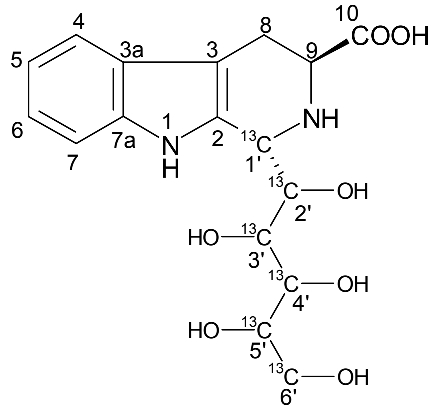

Spectroscopic data of *cis*-1-[(1R,2R,3S,4S)-1,2,3,4,5-pentahydroxypent-1-yl]-1,2,3,4-tetrahydro-β-carboline-3-carboxylic acid-$^{13}C_6$ (12-$^{13}C_6$)

LC-MS (ESI$^+$): *m/z* 373.2 ($[M+H]^+$). **^{1}H NMR (500 MHz, methanol-*d*$_4$)**: δ/ppm 3.12 [m, 1H, H-C(8α)], 3.43 [m, 1H, H-C(8β)], 3.62 [m, 1H, H-C(6'α)], 3.68 [m, 1H, H-C(5')], 3.80 [m, 1H, H-C(6'β)], 3.90 [m, 1H, H-C(4')], 4.02 [dd, 1H, *J* = 5.0, 12.1 Hz, H-C(9)], 4.25 [m, 1H, H-C(3')], 4.46 [m, 1H, H-C(2')], 5.18 [brs, 1H, H-C(1')], 7.07 [pt, 1H, *J* = 7.1, 8.0 Hz, H-C(5)], 7.14 [pt, 1H, *J* = 7.1, 8.2 Hz, H-C(6)], 7.39 [d, 1H, *J* = 8.2 Hz, H-C(7)], 7.52 [d, 1H, *J* = 8.0 Hz, H-C(4)].

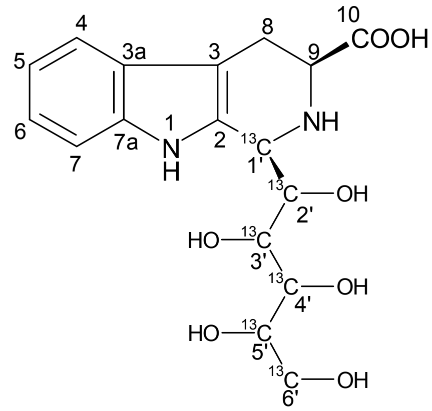

3.5.7 Synthesis of *N-trans*-isoferuloyltyramine

Isoferulic acid (194.0 mg, 1.0 mmol) was mixed with 1 mL of thionyl chloride (13.8 mmol) and was then heated under reflux until no further formation of hydrogen chloride was observable. After cooling to room temperature, the reaction mixture was dried under a stream of nitrogen. Then, tyramine (274 mg, 2 mmol) dissolved in 30 mL of dried tetrahydrofuran was added to the residue, and this solution was stirred for up to 72 h at room temperature. The reaction mixture was dried under a stream of nitrogen, redissolved in the mixture of water and methanol (1:1, v/v), and analyzed by means of semipreparative HPLC system (cf. chapter **3.7.2**, system 2-3). The target compound eluted around 18.5 min was isolated, freed from the solvent in a vacuum, and feeze-dried, giving amorphous powder of the compound (29.8 mg, 0.10 mmol, 9.5%).

Spectroscopic data of *N-trans*-isoferuloyltyramine

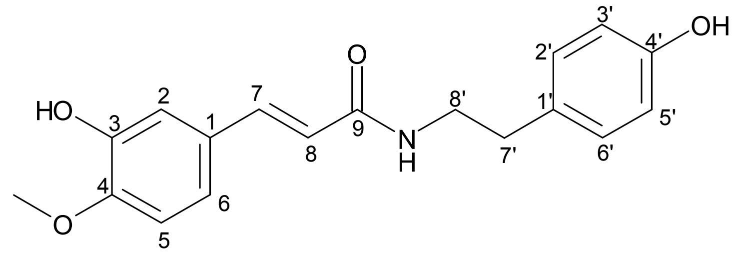

UPLC-TOF-MS (ESI$^+$): *m/z* 314.1390 ($[M+H]^+$, measured; *m/z* 314.1390, calculated for $[C_{18}H_{20}NO_4+H]^+$). **^{1}H NMR (500 MHz, methanol-*d*$_4$, COSY)**: δ/ppm 2.79 [t, 2H, *J* = 7.3 Hz, H-C(7')], 3.49 [t, 2H, *J* = 7.3 Hz, H-C(8')], 3.92 [s, 3H, H-C(4-OMe)], 6.41 [d, 1H, *J* = 15.7 Hz, H-C(8)], 6.75 [d, 2H, *J* = 8.4 Hz, H-C(3', 5')], 6.96 [d, 1H, *J* = 8.4 Hz, H-C(5)], 7.03 [dd, 1H, *J* = 2.1, 8.4 Hz, H-C(6)], 7.07 [d, 1H, *J* = 2.1 Hz, H-C(2)], 7.09 [d, 2H, *J* = 8.4 Hz, H-C(2', 6')], 7.44 [d, 1H, *J* = 15.7 Hz, H-C(7)]. **^{13}C NMR (125 MHz, methanol-*d*$_4$, HSQC, HMBC)**: δ/ppm 35.81 [C(7')], 42.56 [C(8')], 56.38 [C(4-OMe)], 112.53 [C(5)], 114.50 [C(2)], 116.27 [C(3', 5')], 119.40 [C(8)], 122.10 [C(6)], 129.52 [C(1)], 130.73 [C(2', 6')], 131.32 [C(1')], 141.77 [C(7)], 147.95 [C(3)], 150.84 [C(4)], 156.96 [C(4')], 169.08 [C(9)].

3.5.8 Synthesis of ^{2}H-labeled *N*-phenylpropenoic acid ethyl esters and benzoic acid ethyl esters

3.5.8.1 Ethyl ferulate-$^2H_5$ (19-$^2H_5$)

Ferulic acid (100.2 mg, 0.52 mmol) was dissolved in 250 µL of ethanol-*d*$_5$ (4.26 mmol), followed by adding 20 µL of concentrated sulfuric acid to the solution. The mixture was maintained under argon at 70˚C while stirring. After 20 h, the reaction mixture was neutralized with sodium hydroxide and was analyzed by means of semipreparative HPLC system (cf. chapter **3.7.2**, system 1-2, gradient 7). The target compound eluted around 10.5 min was isolated, concentrated, and feeze-dried under vacuum, giving amorphous powder of the compound **19-$^2H_5$** (20.0 mg, 0.09 mmol, 17.1%).

Spectroscopic data of ethyl ferulate-$^2H_5$ (19-$^2H_5$)

LC-MS (ESI$^-$): *m/z* 226.1 ([M−H]$^-$). **^{1}H NMR (400 MHz, CDCl$_3$)**: δ/ppm 3.89 [s, 3H, H-C(3-OMe)], 6.35 [d, 1H, *J* = 15.9 Hz, H-C(8)], 6.80 [d, 1H, *J* = 8.2 Hz, H-C(5)], 7.06 [dd, 1H, *J* = 1.9, 8.2 Hz, H-C(6)], 7.18 [d, 1H, *J* = 1.9 Hz, H-C(2)], 7.59 [d, 1H, *J* = 15.9 Hz, H-C(7)].

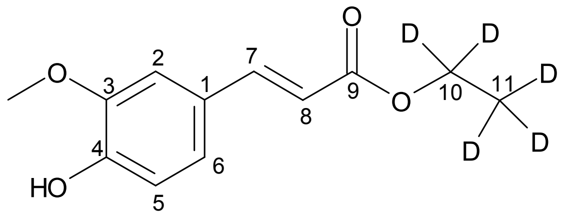

3.5.8.2 Ethyl *p*-coumarate-^{2}H$_5$ (20-^{2}H$_5$)

Ethyl *p*-coumarate-^{2}H$_5$ was synthesized following the same procedure for ethyl ferulate-^{2}H$_5$ (**19-^{2}H$_5$**) using *p*-coumaric acid (100.2 mg, 0.61 mmol) instead of ferulic acid. The reation mixture was analyzed by means of semipreparative HPLC system (cf. chapter **3.7.2**, system 1-2, gradient 8), and the target compound eluted around 17.0 min was isolated, concentrated, and feeze-dried under vacuum, giving amorphous powder of the compound **20-^{2}H$_5$** (23.7 mg, 0.12 mmol, 19.7%).

Spectroscopic data of ethyl *p*-coumarate-^{2}H$_5$ (20-^{2}H$_5$)

LC-MS (ESI$^-$): *m/z* 196.1 ([M−H]$^-$). **^{1}H NMR (400 MHz, CDCl$_3$)**: δ/ppm 6.30 [d, 1H, *J* = 15.9 Hz, H-C(8)], 6.84 [m, 2H, H-C(3, 5)], 7.43 [m, 2H, H-C(2, 6)], 7.63 [d, 1H, *J* = 15.9 Hz, H-C(7)].

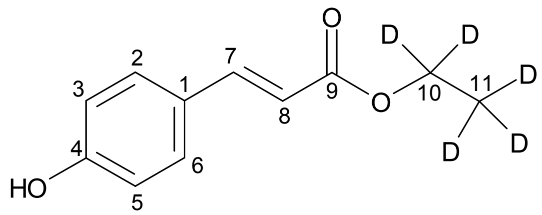

3.5.8.3 Ethyl vanillate-^{2}H$_5$ (21-^{2}H$_5$)

Ethyl vanillate-^{2}H$_5$ was synthesized following the same procedure for ethyl ferulate-^{2}H$_5$ (**19-^{2}H$_5$**) using vanillic acid (100.2 mg, 0.60 mmol) instead of ferulic acid. The reation mixture was analyzed by means of MPLC system (cf. chapter **3.7.3**, gradient 2), and the target compound eluted around 16.5 min was isolated, concentrated, and feeze-dried under vacuum, giving amorphous powder of the compound **21-^{2}H$_5$** (77.0 mg, 0.38 mmol, 64.3%).

Spectroscopic data of ethyl vanillate-^{2}H$_5$ (21-^{2}H$_5$)

LC-MS (ESI$^-$): *m/z* 200.1 ([M−H]$^-$). **^{1}H NMR (400 MHz, CDCl$_3$)**: δ/ppm 3.95 [s, 3H, H-C(3-OMe)], 6.94 [d, 1H, *J* = 8.3 Hz, H-C(5)], 7.55 [d, 1H, *J* = 1.9 Hz, H-C(2)], 7.65 [dd, 1H, *J* = 1.9, 8.3 Hz, H-C(6)].

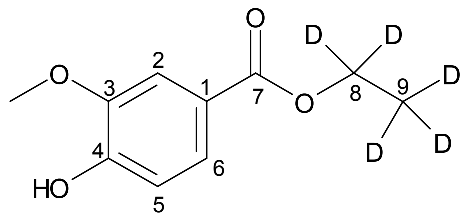

3.5.8.4 Ethyl *p*-hydroxybenzoate-$^2H_5$ (22-$^2H_5$)

Ethyl *p*-coumarate-$^2H_5$ was synthesized following the same procedure for ethyl ferulate-$^2H_5$ (**19-$^2H_5$**) using of *p*-hydroxybenzoic acid (99.8 mg, 0.72 mmol) instead of ferulic acid. The reation mixture was analyzed by means of MPLC system (cf. chapter **3.7.3**, gradient 2), and the target compound eluted around 17.0 min was isolated, concentrated, and feeze-dried under vacuum, giving amorphous powder of the compound **22-$^2H_5$** (43.5 mg, 0.25 mmol, 35.2%).

Spectroscopic data of ethyl *p*-hydroxybenzoate-$^2H_5$ (22-$^2H_5$)

LC-MS (ESI$^-$): *m/z* 170.1 ([M−H]$^-$). **^{1}H NMR (400 MHz, CDCl$_3$)**: δ/ppm 6.86 [m, 2H, H-C(3, 5)], 7.97 [m, 2H, H-C(2, 6)].

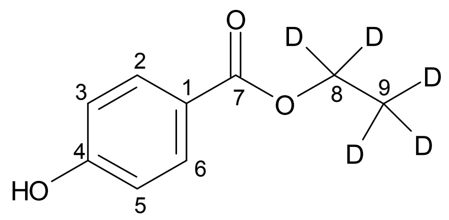

3.6 Quantitative analyses

3.6.1 Quantitation of dilignols

(–)-(*2R*,*3S*)-Dihydrodehydrodiconiferyl alcohol (**1**), (+)-(*2S*,*3R*)-dehydrodiconiferyl alcohol (**2**), *erythro*-guaiacylglycerol-β-O-4'-coniferyl ether (**3**), and *threo*-guaiacylglycerol-β-O-4'-coniferyl ether (**4**) identified in AGE were quantitated by means of UPLC-MS/MS system (cf. chapter **3.8.2**) using absolute calibration method. The MS/MS parameters were tuned for each individual compound, detecting the fragmentation of the $[M-H]^-$ molecular ions into specific product ions after collision with argon. By means of the multiple reaction monitoring (MRM) mode, these dilignol compounds (**1**-**4**) were analyzed using the mass transitions (**Table 15**) monitored for a duration of 20 ms.

Calibration curves were obtained using defined standard solutions (approximately 5.0 – 10,000 ng/mL, seven points) of each reference compound dissolved in methanol/water (20/80, v/v) (**Table 7**). Recovery experiments were performed as follows: An aliquot of AGE was spiked with a standard solution containing defined amounts of analytes dissolved in methanol/water (20/80, v/v), resulting in the sample added approximately 10, 50, or 100% of the initial amounts of analytes (**Table 9**). As the basis for the calculation of the recovery rate, the initial concentration of analytes in unspiked AGE was used.

To determine the concentration of **1**-**4**, an aliquot (1 µL) of 1:10 diluted AGE with methanol/water (20/80, v/v) were analyzed into the UPLC/MS-MS.

Table 15: Mass transitions of AGE compounds and internal standards.

Compound	MW	Ionization mode	Mass transition *m/z*
(–)-(2*R*,3*S*)-dihydrodehydrodiconiferyl alcohol (**1**)	360	ESI^-	359 → 314
(+)-(2*S*,3*R*)-dehydrodiconiferyl alcohol (**2**)	358	ESI^-	357 → 309
erythro-guaiacylglycerol-β-O-4'-coniferyl ether (**3**)	376	ESI^-	375 → 149
threo-guaiacylglycerol-β-O-4'-coniferyl ether (**4**)	376	ESI^-	375 → 150
*N*α-(1-deoxy-D-fructos-1-yl)-*S*-allyl-L-cysteine (**5**)	323	ESI^+	324 → 288
*N*α-(1-deoxy-D-fructos-1-yl)-γ-glutamyl-*S*-allyl-L-cysteine (**6**)	452	ESI^+	453 → 369
trans-*N*α-(1-deoxy-D-fructos-1-yl)-γ-glutamyl-*S*-1-propenyl-L-cysteine (**7**)	452	ESI^+	453 → 369
*N*α-(1-deoxy-D-fructos-1-yl)-L-phenylalanine (**8**)	327	ESI^+	328 → 292
*N*α-(1-deoxy-D-fructos-1-yl)-L-tyrosine (**9**)	343	ESI^+	344 → 326
*N*α-(1-deoxy-D-fructos-1-yl)-L-tryptophan (**10**)	366	ESI^+	367 → 350
trans-1-[(1R,2R,3S,4S)-1,2,3,4,5-pentahydroxypent-1-yl]-1,2,3,4-tetrahydro-β-carboline-3-carboxylic acid (**11**)	366	ESI^+	367 → 156
cis-1-[(1R,2R,3S,4S)-1,2,3,4,5-pentahydroxypent-1-yl]-1,2,3,4-tetrahydro-β-carboline-3-carboxylic acid (**12**)	366	ESI^+	367 → 156
1-methyl-1,2,3,4-tetrahydro-β-carboline (**13**)	186	ESI^+	187 → 170
N-*trans*-feruloyltyramine (**14**)	313	ESI^+	314 → 177
N-*trans*-feruloylphenetylamine (**15**)	297	ESI^+	298 → 177
N-*trans*-coumaroyltyramine (**16**)	283	ESI^+	284 → 147
N-*trans*-coumaroylphenetyramine (**17**)	267	ESI^+	268 → 147
N-*trans*-cinnamoyltyramine (**18**)	267	ESI^+	268 → 131
ethyl ferulate (**19**)	222	ESI^-	221 → 106

Table 15: Continued.

Compound	MW	Ionization mode	Mass transition m/z
ethyl *p*-coumarate (**20**)	192	ESI^-	191 → 117
ethyl vanillate (**21**)	196	ESI^-	195 → 107
ethyl *p*-hydroxybenzoate (**22**)	166	ESI^-	165 → 92
*N*α-(1-deoxy-D-fructos-1-yl)-*S*-allyl-L-cysteine-$^{13}C_6$ (**5-$^{13}C_6$**)	329	ESI^+	330 → 294
*N*α-(1-deoxy-D-fructos-1-yl)-γ-glutamyl-*S*-allyl-L-cysteine-$^{13}C_6$ (**6-$^{13}C_6$**)	458	ESI^+	459 → 374
*N*α-(1-deoxy-D-fructos-1-yl)-L-phenylalanine-$^{13}C_6$ (**8-$^{13}C_6$**)	333	ESI^+	334 → 298
*N*α-(1-deoxy-D-fructos-1-yl)-L-tyrosine-$^{13}C_6$ (**9-$^{13}C_6$**)	349	ESI^+	350 → 332
*N*α-(1-deoxy-D-fructos-1-yl)-L-tryptophan-$^{13}C_6$ (**10-$^{13}C_6$**)	372	ESI^+	373 → 355
trans-1-[(1R,2R,3S,4S)-1,2,3,4,5-pentahydroxypent-1-yl]- 1,2,3,4-tetrahydro-β-carboline-3-carboxylic acid-$^{13}C_6$ (**11-$^{13}C_6$**)	372	ESI^+	373 → 158
cis-1-[(1R,2R,3S,4S)-1,2,3,4,5-pentahydroxypent-1-yl]- 1,2,3,4-tetrahydro-β-carboline-3-carboxylic acid-$^{13}C_6$ (**12-$^{13}C_6$**)	372	ESI^+	373 → 158
N-*trans*-isoferuloyltyramine	313	ESI^+	314 → 177
ethyl ferulate-$^2H_5$ (**19-$^2H_5$**)	227	ESI^-	226 → 111
ethyl *p*-coumarate-$^2H_5$ (**20-$^2H_5$**)	197	ESI^-	196 → 117
ethyl vanillate-$^2H_5$ (**21-$^2H_5$**)	201	ESI^-	200 → 107
ethyl *p*-hydroxybenzoate-$^2H_5$ (**22-$^2H_5$**)	171	ESI^-	170 → 92

3.6.2 Quantitation of Amadori compounds

*N*α-(1-Deoxy-D-fructos-1-yl)-*S*-allyl-L-cysteine (**5**), *N*α-(1-deoxy-D-fructos-1-yl)-γ-glutamyl-*S*-allyl-L-cysteine (**6**), *trans*-*N*α-(1-deoxy-D-fructos-1-yl)-γ-glutamyl-*S*-1-propenyl-L-cysteine (**7**), *N*α-(1-deoxy-D-fructos-1-yl)-L-phenylalanine (**8**), and *N*α-(1-deoxy-D-fructos-1-yl)-L-tyrosine (**9**) identified in AGE were quantitated by means of LC-MS/MS system (cf. chapter **3.8.2**) using SIDA method. The MS/MS parameters of the $^{13}C_6$-labeled internal standards of the compounds **5**, **6**, **8**, and **9** were tuned for each reference compound and each internal standard. By means of the multiple reaction monitoring (MRM) mode, these Amadori compounds (**5**-**9**) were analyzed using the mass transitions (**Table 15**).

Solutions of the analytes and the internal standards were prepared in seven concentration ratios from 0.05 to 20.00 (analyte/IS) and analyzed. Calibration curves were prepared by plotting peak area ratios [analyte/IS] against concentration ratios [analyte/IS] using linear regression (**Figure 57**).

To determine the concentration of these Amadori compounds, an aliquot (1 µL) of 1:10 diluted AGE with methanol/water (20/80, v/v) were analyzed by means of LC/MS-MS. *trans*-*N*α-(1-Deoxy-D-fructos-1-yl)-γ-glutamyl-*S*-1-propenyl-L-cysteine (**7**) was quantified using the calibration curve of *N*α-(1-deoxy-D-fructos-1-yl)-γ-glutamyl-*S*-allyl-L-cysteine (**6**).

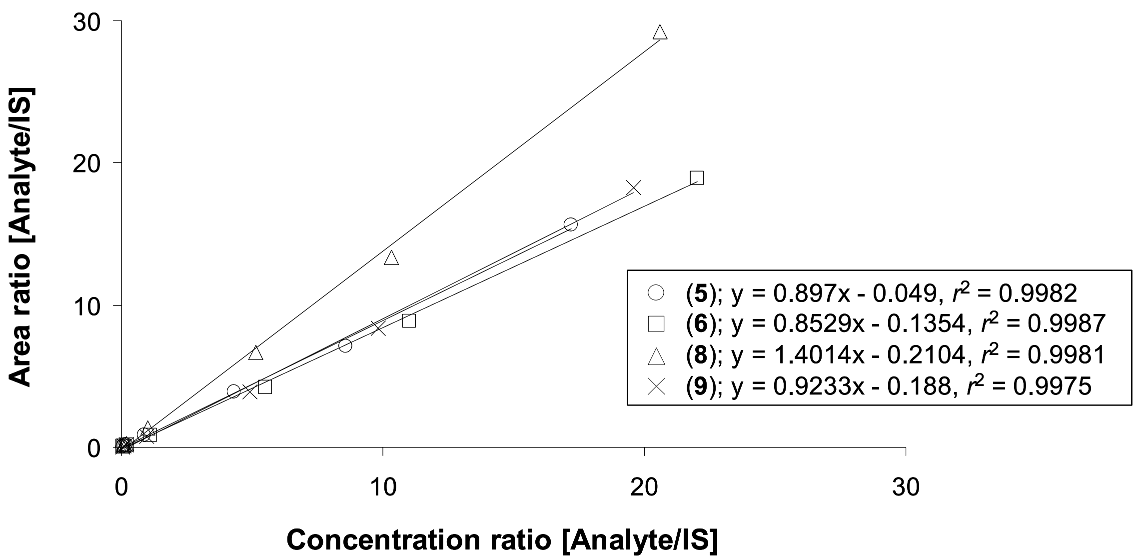

Figure 57: Calibration curves and linear equations of *N*α-(1-deoxy-D-fructos-1-yl)-*S*-allyl-L-cysteine (**5**), *N*α-(1-deoxy-D-fructos-1-yl)-γ-glutamyl-*S*-allyl-L-cysteine (**6**), *N*α-(1-deoxy-D-fructos-1-yl)-L-phenylalanine (**8**), and *N*α-(1-deoxy-D-fructos-1-yl)-L-tyrosine (**9**) using their corresponding $^{13}C_6$-labeled internal standards.

3.6.3 Quantitaon of Amadori compound of tryptophan and tetrahydro-β-carbolines

*N*α-(1-Deoxy-D-fructos-1-yl)-L-tryptophan (**10**), *trans*-1-[(*1R*,*2R*,*3S*,*4S*)-1,2,3,4,5-pentahydroxypent-1-yl]-1,2,3,4-tetrahydro-β-carboline-3-carboxylic acid (**11**), *cis*-1-[(*1R*,*2R*,*3S*,*4S*)-1,2,3,4,5-pentahydroxypent-1-yl]-1,2,3,4-tetrahydro-β-carboline-3-carboxylic acid (**12**), and 1-methyl-1,2,3,4-tetrahydro-β-carboline (**13**) identified in AGE were quantitated by means of UPLC-MS/MS system (cf. chapter **3.8.2**) using SIDA method. The MS/MS parameters were tuned for each reference compound and each $^{13}C_6$-labeled internal standard. By means of the multiple reaction monitoring (MRM) mode, these compounds (**10**-**13**) were analyzed using the mass transitions (**Table 15**). Calibration mixtures of the analytes and the internal standards were prepared in seven concentration ratios from 0.03 to 30.00 (analyte/IS) and analyzed, leading to good linear responses. (**Figure 58**). An aliquot (1 µL) of 1:10 diluted AGE with methanol/water (20/80, v/v) were analyzed by means of the UPLC/MS-MS to determine the concentration of these compounds. 1-Methyl-1,2,3,4-tetrahydro-β-carboline (**13**) was quantified using the calibration curve of *trans*-1-[(*1R*,*2R*,*3S*,*4S*)-1,2,3,4,5-pentahydroxypent-1-yl]-1,2,3,4-tetrahydro-β-carboline-3-carboxylic acid (**11**).

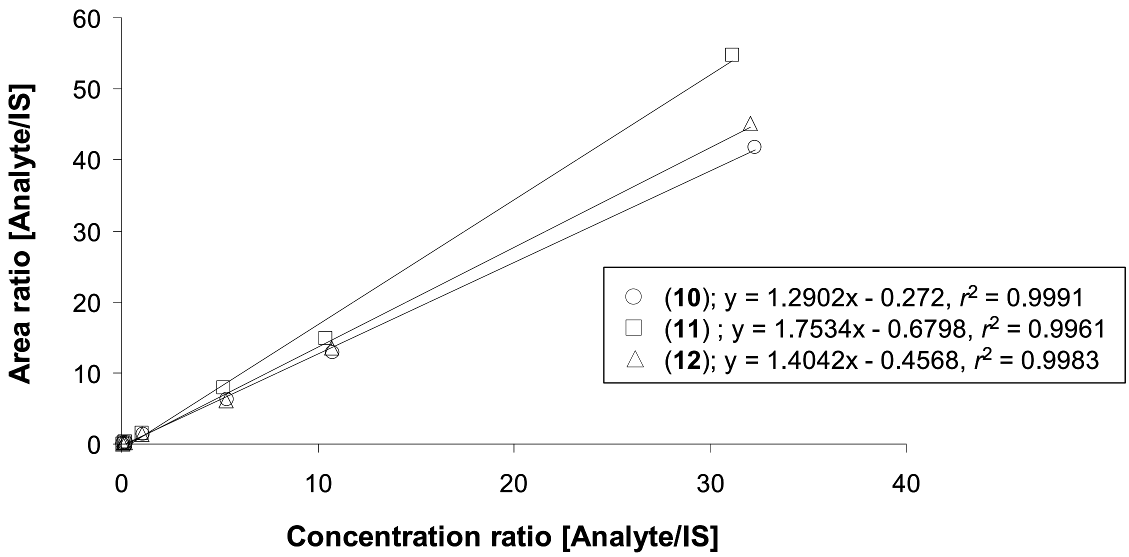

Figure 58: Calibration curves and linear equations of *N*α-(1-deoxy-D-fructos-1-yl)-L-tryptophan (**10**), *trans*-1-[(*1R*,*2R*,*3S*,*4S*)-1,2,3,4,5-pentahydroxypent-1-yl]-1,2,3,4-tetrahydro-β-carboline-3-carboxylic acid (**11**), *cis*-1-[(*1R*,*2R*,*3S*,*4S*)-1,2,3,4,5-pentahydroxypent-1-yl]-1,2,3,4-tetrahydro-β-carboline-3-carboxylic acid (**12**) using their corresponding $^{13}C_6$-labeled internal standards.

3.6.4 Quantitation of *N*-phenylpropenoic acid amides

N-*trans*-Feruloyltyramine (**14**), *N*-*trans*-feruloylphenetylamine (**15**), *N*-*trans*-*p*-coumaroyltyramine (**16**), *N*-*trans*-*p*-coumaroylphenetyramine (**17**), and *N*-*trans*-cinnamoyltyramine (**18**) identified in AGE were quantitated by means of UPLC-MS/MS system (cf. chapter **3.8.2**) using *N*-*trans*-isoferuloyltyramine as an internal standard. The MS/MS parameters were tuned for each reference compound. By means of the multiple reaction monitoring (MRM) mode, these *N*-phenylpropenoic acid amides (**14**-**18**) were analyzed using the mass transitions (**Table 15**). Calibration mixtures of the analytes and the internal standards were prepared in five concentration ratios from 0.1 to 10.0 (analyte/IS) and analyzed, resulting in good linear responses (**Figure 59**). An aliquot (1 µL) of 1:10 diluted AGE with methanol/water (20/80, v/v) were analyzed by means of the UPLC/MS-MS.

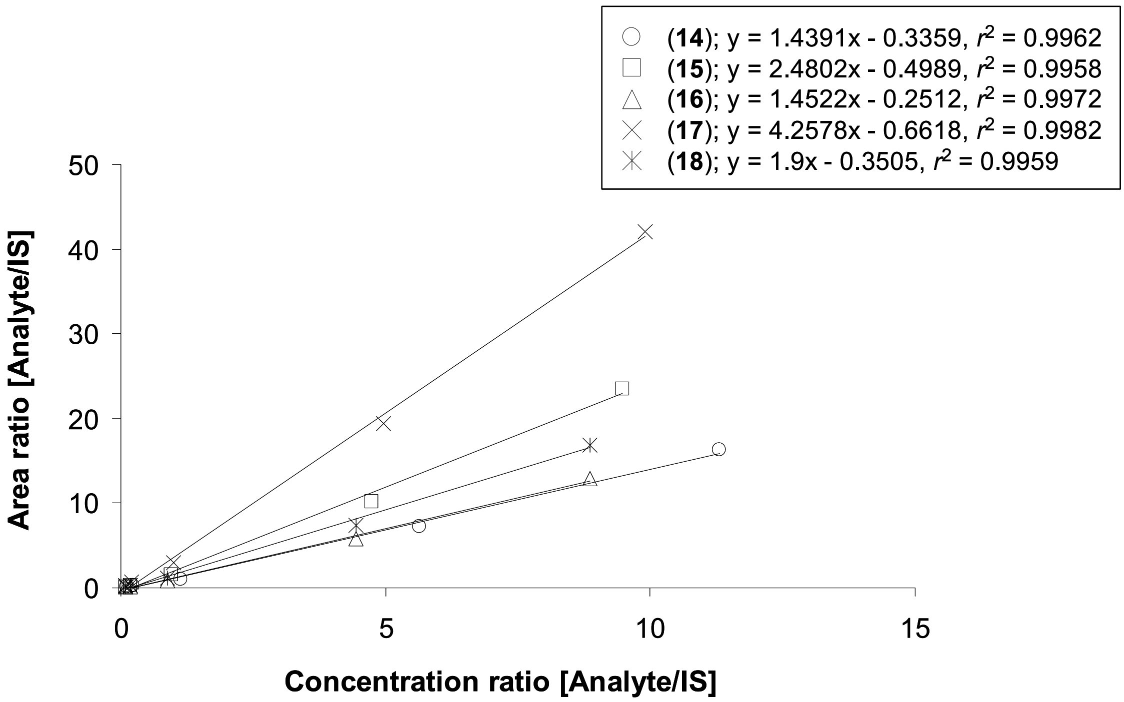

Figure 59: Calibration curves and linear equations of *N*-*trans*-feruloyltyramine (**14**), *N*-*trans*-feruloylphenetylamine (**15**), *N*-*trans*-*p*-coumaroyltyramine (**16**), *N*-*trans*-*p*-coumaroylphenetyramine (**17**), and *N*-*trans*-cinnamoyltyramine (**18**) using *N*-*trans*-isoferuloyltyramine as an internal standard.

3.6.5 Quantitation of *N*-phenylpropenoic acid ethyl esters and benzoic acid ethyl esters

Ethyl ferulate (**19**), ethyl *p*-coumarate (**20**), ethyl vanillate (**21**), and ethyl *p*-hydroxybenzoate (**22**) identified in AGE were quantitated by means of LC-MS/MS system (cf. chapter **3.8.2**) using SIDA method. After $^{2}H_5$-labeled internal standards of the compounds **19**-**22** were synthesized, the MS/MS parameters were tuned for each reference compound and each labeled internal standard. By means of the multiple reaction monitoring (MRM) mode, these *N*-phenylpropenoic acid ethyl esters and benzoic acid ethyl esters (**19**-**22**) were analyzed using the mass transitions (**Table 15**). Solutions of the analytes and the internal standards were prepared in seven concentration ratios from 0.05 to 20.00 (analyte/IS) and analyzed, which gave good calibration curves (**Figure 60**). To determine the concentration of these *N*-phenylpropenoic acid ethyl esters and benzoic acid ethyl esters, an aliquot (1 µL) of 1:10 diluted AGE with methanol/water (20/80, v/v) were analyzed by means of LC/MS-MS.

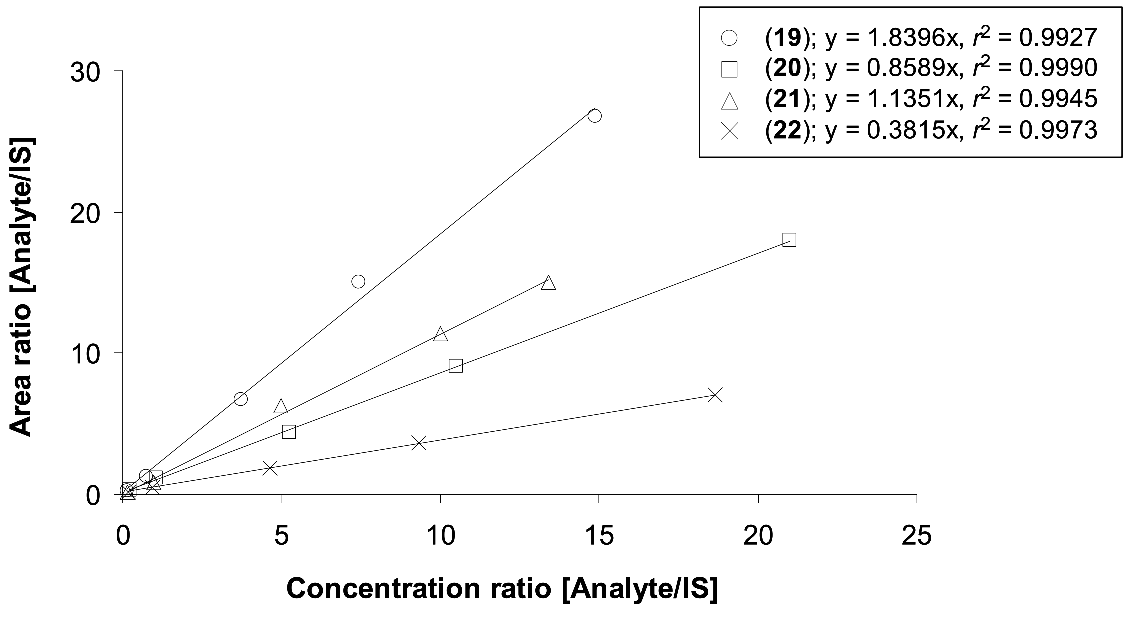

Figure 60: Calibration curves and linear equations of ethyl ferulate (**19**), ethyl *p*-coumarate (**20**), ethyl vanillate (**21**), and ethyl *p*-hydroxybenzoate (**22**) using their corresponding $^{2}H_5$-labeled internal standards.

3.7 Chromatographic methods

3.7.1 Preparative high performance liquid chromatography (preparative HPLC)

pump	PrepStar SD-1 (Varian, Darmstadt, Germany)
UV detector	Prostar 325 (Varian, Darmstadt, Germany)
fraction collector	model 701 (Varian, Darmstadt, Germany)
stationary phase	Microsorb packed column (C-18 material, 200 × 50 mm i.d., 8 µm, Varian, Darmstadt, Germany)
packing	a load-and-lock packing station (Varian, Darmstadt, Germany)
flow	100 mL/min
detection UV	220 nm
eluent	eluent A: 0.1% aqueous formic acid eluent B: methanol
gradient	B; 0% → 0% (10 min) → 100% (13 min) → 100% (20 min)

3.7.2 Semipreparative high performance liquid chromatography (semipreparative HPLC)

System 1

pump	PU-2087 Plus (Jasco, Groß-Umstadt, Germany)
degasser	DG-2080-53 (Jasco, Groß-Umstadt, Germany)
gradient unit	LG-2080-02 (Jasco, Groß-Umstadt, Germany)
UV detector	MD-2010 Plus (Jasco, Groß-Umstadt, Germany)

System 1-1

stationary phase	Microsorb-MW 100-5 (C18, 250 × 21.2 mm i.d., 5 µm, Varian, Darmstadt, Germany)
flow	21.0 mL/min

detection UV	220 nm
eluent	eluent A: 0.1% aqueous formic acid eluent B: methanol
gradient 1	B; 0% → 0% (3 min) → 90% (33 min) → 100% (34 min) → 100% (39 min)
gradient 2	B; 20% → 30% (20 min) → 100% (23 min) → 100% (26 min)

System 1-2

stationary phase	Luna Phenyl-Hexyl (250 × 21.2 mm i.d., 5 µm, Phenomenex, Aschaffenburg, Germany)
flow	21.0 mL/min
detection UV	220 nm
eluent	eluent A: 0.1% aqueous formic acid eluent B: methanol
gradient 1	B; 10% → 20% (12 min) → 60% (32 min) → 100% (34 min) → 100% (39 min)
gradient 2	B; 0% → 0% (1 min) → 50% (15 min) → 100% (18 min) → 100% (21 min)
gradient 3	B; 0% → 0% (6 min) → 10% (16 min) → 100% (19 min) → 100% (22 min)
gradient 4	B; 20% → 60% (20 min) → 100% (23 min) → 100% (26 min)
gradient 5	B; 10% → 50% (20 min) → 100% (23 min) → 100% (26 min)
gradient 6	B; 0% → 30% (20 min) → 100% (23 min) → 100% (26 min)
gradient 7	B; 60% → 70% (20 min) → 100% (23 min) → 100% (26 min)
gradient 8	B; 45% → 45% (2 min) → 75% (22 min) → 100% (23 min) → 100% (26 min)

System 2

pump	PU-2087 Plus (Jasco, Groß-Umstadt, Germany)
degasser	DG-2080-53 (Jasco, Groß-Umstadt, Germany)
gradient unit	LG-2080-02 (Jasco, Groß-Umstadt, Germany)
UV detector	PU-2075 (Jasco, Groß-Umstadt, Germany)

System 2-1

stationary phase	Luna Phenyl-Hexyl (250 × 10.0 mm i.d., 5 µm, Phenomenex, Aschaffenburg, Germany)
flow	4.2 mL/min
detection UV	220 nm
eluent	eluent A: 0.1% aqueous formic acid eluent B: methanol
gradient	B; 50% → 75% (30 min) → 100% (35 min) → 100% (38 min)

System 2-2

stationary phase	Luna Phenyl-Hexyl (250 × 10.0 mm i.d., 5 µm, Phenomenex, Aschaffenburg, Germany)
flow	4.2 mL/min
detection UV	220 nm
eluent	eluent A: 0.1% aqueous formic acid eluent B: acetonitrile
gradient	B; 22% → 22% (35 min) → 100% (38 min) → 100% (42 min)

System 2-3

stationary phase	Luna Phenyl-Hexyl (250 × 10.0 mm i.d., 5 µm,

	Phenomenex, Aschaffenburg, Germany)
flow	4.2 mL/min
detection UV	300 nm
eluent	eluent A: 0.1% aqueous formic acid eluent B: methanol
gradient	B; 50% → 90% (16 min) → 100% (17 min) → 100% (22 min)

3.7.3 Medium pressure liquid chromatography (MPLC)

pump	Büchi Pump Module C-605 (Büchi Labortechnik AG, Flawil, Switzerland)
UV detector	Büchi UV-Photometer C-635 (Büchi Labortechnik AG, Flawil, Switzerland)
fraction collector	Büchi Fraction Collector C-660 (Büchi Labortechnik AG, Flawil, Switzerland)
stationary phase	Polypropylene cartridge filled with LiChroprep (RP18 material, 150 × 40 mm i.d., 25-40 µm, Merck KGaA, Darmstadt, Germany)
flow	40.0 mL/min
detection UV	220 nm
eluent	eluent A: 0.1% aqueous formic acid eluent B: methanol
gradient 1	B; 60% → 60% (1 min) → 100% (6 min) → 100% (9 min)
gradient 2	B; 30% → 30% (2 min) → 90% (22 min) → 100% (23 min) → 100% (26 min)

3.8 Spectroscopic methods

3.8.1 UV/vis spectroscopy

UV-spectra (200-650 nm) were measured during chromatographic analysis with a MD-2010 Plus detector (Jasco, Groß-Umstadt, Germany) in the corresponding eluents.

3.8.2 Mass spectroscopy (MS)

3.8.2.1 Ultra performance liquid chromatography - time of flight - mass spectroscopy (UPLC-TOF-MS)

LC-system	Acquity UPLC core sytem (Waters, Manchester, UK)
pump	binary solvent manager (Waters, Manchester, UK)
auto sampler	sample manager (Waters, Manchester, UK)
MS-spectrometer	Waters Synapt G2 HDMS (Waters, Manchester, UK)
calibration	sodium formate (5 mmol/L) in 2-propanol/water (9:1, v/v)
lock mass correction	leucine enkephaline ($[M+H]^+$ *m/z* 556.2771, $[M-H]^-$ *m/z* 554.2615)
capillary voltage	+2.5 kV or –3.0 kV
sampling cone	30
source temperature	150°C
desolvation temperature	450°C
cone gas	30 L/h
desolvation gas	850 L/h
software	MassLynx 4.1 (Waters, Manchester, UK)
stationary phase	BEH C-18 (150 × 2.0 mm i.d., 1.7 µm, Waters, Manchester, UK)
flow rate	300 µL/min
column temperature	40°C
eluent	eluent A: 0.1% aqueous formic acid eluent B: 0.1% formic acid in acetonitrile
gradient	B; 5% → 95% (3 min) → 95% (4 min)

3.8.2.2 Ultra performance liquid chromatography - mass spectroscopy (UPLC-MS/MS)

LC-system	Acquity UPLC i-class core sytem (Waters, Manchester, UK)
pump	binary solvent manager (Waters, Manchester, UK)
auto sampler	sample manager (Waters, Manchester, UK)
MS-spectrometer	Waters Xevo TQ-S (Waters, Manchester, UK)
calibration	phosphoric acid (0.1% in acetonitrile)
capillary voltage	–2.0 kV
sampling cone	50
source temperature	150°C
desolvation temperature	500°C
cone gas	150 L/h
desolvation gas	1000 L/h
software	MassLynx 4.1 (Waters, Manchester, UK)
stationary phase	BEH phenyl (150 × 2.0 mm i.d., 1.7 µm, Waters, Manchester, UK)
flow rate	400 µL/min
column temperature	45°C
eluent	eluent A: 0.1% aqueous formic acid eluent B: 0.1% aqueous acetonitrile
gradient	B; 12% → 40% (9 min) → 99% (9.1 min) → 99% (9.6 min)

3.8.2.3 Liquid chromatography - triple quadrupole-mass spectroscopy (LC-MS/MS)

LC-system	combination of the Agilent 1100 and 1200 series (Agilent, Waldbronn, Germany)
pump	1100-G1312A (Agilent, Waldbronn, Germany)
degasser	1100-G1379A (Agilent, Waldbronn, Germany)
auto sampler	1200-G1329A Autosampler with 1200-G1330B FC/ALS Therm (Agilent, Waldbronn, Germany)
MS-spectrometer	API 4000QTRAP triple quadrupole (Applied

	Biosystems, Darmstadt, Germany)
scan type	multiple reaction monitoring (MRM)
software	Analyst 1.5.1 (AB Sciex, Darmstadt, Germany)
ion spray voltage	+5500 V or -4500 V
gas temperature	450°C
nebulizer gas	nitrogen (45 psi)
turbo gas	nitrogen (55 psi)
curtain gas	nitrogen (20 psi)
collision gas	nitrogen (8.7 x 10^{-7} psi)
stationary phase	Luna Phenyl-Hexyl (150 × 2.1 mm i.d., 5.0 µm, Phenomenex, Aschaffenburg, Germany)
flow rate	250 µL/min
column temperature	40°C
eluent	eluent A: 0.1% aqueous formic acid eluent B: 0.1% aqueous acetonitrile
gradient	B; 5% → 5% (5 min) → 95% (25 min) → 95% (30 min)

3.8.3 Nuclear magnetic resonance spectroscopy (NMR)

All NMR spectroscopic measurements were conducted on an Avance-III-500 (500 MHz) spectrometer equipped with a triple res. Cryo probe (TCI) (Bruker, Rheinstetten, Germany) and a DRX or an Avance-III-400 (400 MHz) spectrometer equipped with a QNP or a Broadband Observe BBFOplus probe (Bruker, Rheinstetten, Germany). Samples transferred to NMR tubes (Schott Economics, 178 x 5 mm) were analyzed at 300 K (500/125 MHz) or 295 K (400/100 MHz). The chemical shift was referenced against TMS or the signal of the solvent. TOPSPIN (version 1.2 and 2.1, Bruker, Rheinstetten, Germany) was used for data acquision. ^{1}H-, ^{13}C-, 135DEPT-, COSY-, HSQC-, and HMBC-spectra were generated using standard pulse sequences of the Bruker software library. Interpretation of the obtained spectra was performed with MestReNova® 5.1.0-2940 (Mestrelab Research S.L., Santiago de Compostella, Spain).

3.8.4 Circular dichroism spectroscopy (CD)

All CD spectroscopic measurements were acquired by means of a Jasco J810 spectropolarimeter (Jasco, Tokyo, Japan) in the corresponding eluents.

4 Summary

All biological systems are exposed to ROS, either generated intentionally or as by-products. When ROS exceeds the inherent biological antioxidant system, it results in oxidative stress. Injury and lipid peroxidation induced by oxidative stress have been suggested as major causes of cardiovascular diseases and cancer. Dietary antioxidants may increase the total antioxidant capacity of cells, and may contribute to prevention or treatment of ROS-mediated diseases. Therefore, intake of antioxidant-rich foods, especially fruits and vegetables, is considered to be important for health.

Garlic has been recognized as one of the healthy food from historical eating experience for centuries as well as from the evidences in plenty of studies. The most unique and valuable constituents of garlic are sulfur-containing compounds such as, e.g. *S*-alk(en)yl-L-cysteine sulfoxides, γ-glutamyl *S*-alk(en)yl-L-cysteines, and thiosulfinates like allicin. Garlic has been shown its pharmacological usefulness in a diverse of studies, but its adverse effects have also been reported.

Aged garlic extract (AGE) is the most beneficial garlic preparation, which is manufactured by extraction and aging of garlic in aqueous ethanol for more than 10 months. During aging process, chemical and biological reactions lead to formation of water-soluble organosulfur compounds, which are not present in raw garlic. AGE has never been reported to show any toxic effects in the studies with the normal dose. A great number of studies including clinical trials concluded AGE to have various pharmacological effects on diseases, such as infection, cancer, and cardiovascular disease. Since some of these diseases are associated with ROS, antioxidants in AGE may play a vital role in the effects. Among the constituents known to be present in AGE, several sulfur-containing compounds and Maillard reaction products have been shown to display high antioxidant activity. However, the activity at their natural concentration in AGE can’t account for the overall activity of AGE, suggesting the existence of unidentified antioxidants in AGE.

In the present study, antioxidant activity-guided fractionation of AGE was performed, resulting in isolation of two dilignols: (–)-(*2R*,*3S*)-dihydrodehydrodiconiferyl alcohol (**1**) and (+)-(*2S*,*3R*)-dehydrodiconiferyl alcohol (**2**). Their structures were elucidated by means of LC-MS/MS, NMR, and CD spectroscopy. Existence of these dilignols suggested other coniferyl alcohol-derived compounds may be present in AGE as well. Oxidative dimerization of coniferyl alcohol revealed two β-O-4 linked dilignols, namely, *erythro*-guaiacylglycerol-β-O-4'-coniferyl ether (**3**) and *threo*-guaiacylglycerol-β-O-4'-coniferyl ether (**4**). UPLC-ESI-MS/MS screening, followed by cochromatography with the corresponding reference compounds, led to the unequivocal identification of these two dilignols in AGE.

By means of model reactions and synthetic experiments, some Amadori compounds, tetrahydro-β-carbolines, *N*-phenylpropenoic acid amides, and ethyl esters were obtained. MS screening of these compounds resulted in the identification of 18 compounds in AGE; *N*α-(1-deoxy-D-fructos-1-yl)-*S*-allyl-L-cysteine (**5**), *N*α-(1-deoxy-D-fructos-1-yl)-γ-glutamyl-*S*-allyl-L-cysteine (**6**), *trans*-*N*α-(1-deoxy-D-fructos-1-yl)-γ-glutamyl-*S*-1-propenyl-L-cysteine (**7**), *N*α-(1-deoxy-D-fructos-1-yl)-L-phenylalanine (**8**), *N*α-(1-deoxy-D-fructos-1-yl)-L-tyrosine (**9**), *N*α-(1-deoxy-D-fructos-1-yl)-L-tryptophan (**10**), *trans*-1-[(*1R*,*2R*,*3S*,*4S*)-1,2,3,4,5-pentahydroxypent-1-yl]-1,2,3,4-tetrahydro-β-carboline-3-carboxylic acid (**11**), *cis*-1-[(*1R*,*2R*,*3S*,*4S*)-1,2,3,4,5-pentahydroxypent-1-yl]-1,2,3,4-tetrahydro-β-carboline-3-carboxylic acid (**12**), 1-methyl-1,2,3,4-tetrahydro-β-carboline (**13**), *N*-*trans*-feruloyltyramine (**14**), *N*-*trans*-feruloylphenetylamine (**15**), *N*-*trans*-*p*-coumaroyltyramine (**16**), *N*-*trans*-*p*-coumaroylphenetyramine (**17**), and *N*-*trans*-cinnamoyltyramine (**18**), ethyl ferulate (**19**), ethyl coumarate (**20**), ethyl vanillate (**21**), and ethyl 4-hydroxybenzoate (**22**).

According to the results of quantitative study and antioxidant assay for all the identified compounds, the compounds **1**, **2**, **4**, **14**, and **16** showed great contribution to the whole antioxidant activity of AGE. Although this is just within *in vitro* activity, these compounds were considered to be one of the key antioxidants in AGE.

However, a total of the contribution of all the constituents identified in AGE is still less than 30% of the overall activity of AGE, indicating the presence of unidentified antioxidants. As described in chapter **2.1.1**, there are some fractions with strong antioxidant activity, from which unidentified antioxidants could be isolated. Moreover, since lignols were found in this study for the first time, more lignans should be present in AGE. The results of the present study revealed some individual key antioxidants, however, the majority of AGE's antioxidant activity seem to be due to a vast number of trace antioxidants showing additive and/or synergistic effects.

5 Cited literature

Adler, E. Lignin chemistry-past, present and future. *Wood Sci. Technol.* **1977**, *11*, 169-218.

Adrover, M.; Vilanova, B.; Frau, J.; Muñoz, F.; Donoso, J. The pyridoxamine action on Amadori compounds: A reexamination of its scavenging capacity and chelating effect. *Bioorg. Med. Chem.* **2008**, *16* (10), 5557-5569.

Allison, GL.; Lowe, GM.; Rahman, K. Aged garlic extract and its constituents inhibit platelet aggregation through multiple mechanisms. *J Nutr.* **2006**, *136* (3 Suppl), 782S-788S.

Al-Taweel, AM.; Perveen, S.; El-Shafae, AM.; Fawzy, GA.; Malik, A.; Afza, N.; Iqbal, L.; Latif, M. Bioactive phenolic amides from *Celtis africana*. *Molecules.* **2012**, *17* (13), 2675-2682.

Amagase, H.; Petesch, BL.; Matsuura, H.; Kasuga, S.; Itakura, Y. Intake of garlic and its bioactive components. *J Nutr.* **2001**, *131*, 955S-62S.

Ankri, S.; Mirelman, D. Antimicrobial properties of allicin from garlic. *Microbes Infect*. **1999**, *1* (2), 125-129.

Arivazhagan, S.; Velmurugan, B.; Bhuvaneswari, V.; Nagini, S. Effects of aqueous extracts of garlic (*Allium sativum*) and neem (*Azadirachta indica*) leaf on hepatic and blood oxidant-antioxidant status during experimental gastric carcinogenesis. *J. Med. Food* **2004**, *7* (3), 334-339.

Banerjee, SK.; Maulik, SK. Effect of garlic on cardiovascular disorders: a review. *Nutr J.* **2002**, *1* (4), 14 pages.

Barbosa-Filho, JM.; Lima, CS.; Amorim, EL.; de Sena, KX.; Almeida, JR.; da-Cunha EV.; Silva, M.; Agra, MF.; Braz-Filho, R. Botanical study, phytochemistry and antimicrobial activity of *Tabebuia aurea*. *Phyton (Buenos Aires)* **2004**, 221-228.

Bashan, N.; Kovsan, J.; Kachko, I.; Ovadia, H.; Rudich, A. Positive and negative regulation of insulin signaling by reactive oxygen and nitrogen species. *Physiol. Rev.* **2009**, *89* (1), 27-71.

Beato, VM.; Orgaz, F.; Mansilla, F.; Montaño, A. Changes in phenolic compounds in garlic (Allium sativum L.) owing to the cultivar and location of growth. *Plant Foods Hum Nutr.* **2011**, *66* (3), 218-23.

Bedard, K.; Krause, KH. The NOX family of ROS-generating NADPH oxidases: physiology and pathophysiology. *Physiol. Rev.* **2007**, *87*, 245-313.

Bellion, P.; Digles, J.; Will, F.; Dietrich, H.; Baum, M.; Eisenbrand, G.; Janzowski, C. Polyphenolic apple extracts: effects of raw material and production method on antioxidant effectiveness and reduction of DNA damage in Caco-2 cells. *J. Agric. Food Chem.* **2010**, *58* (11), 6636-6642.

Block, E.; Naganathan, S.; Putman, D.; Zhao, SH. Organosulfur chemistry of garlic and onion: Recent results. *Pure Appl. Chem.* **1993**, *65* (4), 625-632.

Boffetta, P.; Couto, E.; Wichmann, J.; Ferrari, P.; Trichopoulos, D.; Bueno-de-Mesquita, HB.; van Duijnhoven, FJ.; Büchner, FL.; Key, T.; Boeing, H.; Nöthlings, U.; Linseisen, J.; Gonzalez, CA.; Overvad, K.; Nielsen, MR.; Tjønneland, A.; Olsen, A.; Clavel-Chapelon, F.; Boutron-Ruault, MC.; Morois, S.; Lagiou, P.; Naska, A.; Benetou, V.; Kaaks, R.; Rohrmann, S.; Panico, S.; Sieri, S.; Vineis, P.; Palli, D.; van Gils, CH.; Peeters, PH.; Lund, E.; Brustad, M.; Engeset, D.; Huerta, JM.; Rodríguez, L.; Sánchez, MJ.; Dorronsoro, M.; Barricarte, A.; Hallmans, G.; Johansson, I.; Manjer, J.; Sonestedt, E.; Allen, NE.; Bingham, S.; Khaw, KT.; Slimani, N.; Jenab, M.; Mouw, T.; Norat, T.; Riboli, E.; Trichopoulou, A. Fruit and vegetable intake and overall cancer risk in the European Prospective Investigation into Cancer and Nutrition (EPIC). *J. Natl. Cancer Inst.* **2010**, *102* (8), 529-537.

Boonstra, J.; Post, JA. Molecular events associated with reactive oxygen species and cell cycle progression in mammalian cells. *Gene* **2004**, *337*, 1-13.

Cao, G.; Alessio, HM.; Cutler, RG. Oxygen-radical absorbance capacity assay for antioxidants. *Free Radical Biol. Med.* **1993**, *14* (3), 303-311.

Caragay, AB. Cancer-preventive foods and ingredients. *Food Technol.* **1992**, *4*, 65-68.

Colín-González, AL.; Santana, RA.; Silva-Islas, CA.; Chánez-Cárdenas, ME.; Santamaría, A.; Maldonado, PD. The antioxidant mechanisms underlying the aged garlic extract- and *S*-allylcysteine-induced protection. *Oxid. Med. Cell. Longevity* **2012**, *Article ID 907162,* 16 pages.

Davies, KJ.; Quintanilha, AT.; Brooks, GA.; Packer, L. Free radicals and tissue damage produced by exercise. *Biochem. Biophys. Res. Commun.* **1982**, *107* (4), 1198-1205.

Delgado-Andrade, C.; Rufián-Henares, JA.; Morales, FJ. Assessing the antioxidant activity of melanoidins from coffee brews by different antioxidant methods. *J. Agric. Food Chem.* **2005**, *53* (20), 7832-7836.

Devkota, HP.; Watanabe, M.; Watanabe, T.; Yahara, T. Phenolic compounds from the aerial parts of *Diplomorpha canescens*. *Chem. Pharm. Bull.* **2012**, *60* (4), 554-556.

Ellmore, GS.; Feldberg, RS. Alliin lyase localization in bundle sheaths of the garlic clove (*Allium sativum*). *Am. J. Bot.* **1994**, *81* (1), 89-94.

Esterbauer, H.; Dieber-Rotheneder, M.; Striegl, G.; Waeg, G. Role of vitamin E in preventing the oxidation of low-density lipoprotein. *Am. J. Clin. Nutr.* **1991**, *53* (1 Suppl), 314S-321S.

Etoh, T.; Watanabe, H.; Iwai, S. RAPD variation of garlic clones in the center of origin and the westernmost area of distribution. *Mem. Fac. Agr. Kagoshima Univ.* **2001**, *37*, 21-27.

Fiot, J.; Sanon, S.; Azas, N.; Mahiou, V.; Jansen, O.; Angenot, L.; Balansard, G.; Ollivier, E. Phytochemical and pharmacological study of roots and leaves of *Guiera senegalensis* J.F. Gmel (Combretaceae). *J. Ethnopharmacol.* **2006**, *106* (2), 173-178.

Food and Agricultural Organization of the United Nations, FAO Statistical Database (FAOSTAT), Food and Agricultural commodities production, **2012**, http://faostat.fao.org/.

Fossen, T.; Andersen, ØM. Malonated anthocyanins of garlic *Allium sativum* L. *Food Chem.* **1997**, *58* (3), 215-217.

Frei, B.; Stocker, R.; Ames, BN. Antioxidant defenses and lipid peroxidation in human blood plasma. *Proc. Natl. Acad. Sci. U. S. A.* **1988**, *85* (24), 9748-9752.

Fukuyama, Y.; Nakahara, M.; Minami, H.; Kodama, M. Two new benzofuran-type lignans from the wood of *Viburnum awabuki*. *Chem. Pharm. Bull.* **1996**, *44* (7), 1418-1420.

Gang, DR.; Kasahara, H.; Xia, ZQ.; Vander, Mijnsbrugge, K.; Bauw, G.; Boerjan, W.; Van, Montagu, M.; Davin, LB.; Lewis, NG. Evolution of plant defense mechanisms. *J. Biol. Chem.* **1999**, *274* (11), 7516-7527.

García-Muñoz, S.; Jiménez-González, L.; Álvarez-Corral, M.; Muñoz-Dorado, M.; Rodríguez-García, I. Benzo[*f*][1,2]oxasilepines in the synthesis of dihydro[*b*]benzofuran neolignans. *Synlett* **2005**, *19*, 3011-3013.

Gutsche, B.; Grun, C.; Scheutzow, D.; Herderich, M. Tryptophan glycoconjugates in food and human urine. *Biochem. J.* **1999**, *343*, 11-19.

Haigis, MC.; Yankner, BA. The aging stress response. *Mol. Cell* **2010**, 40, 333-344.

Han, HY.; Wang, XH.; Wang, NL.; Ling, MT.; Wong, YC.; Yao, XS. Lignans isolated from *Campylotropis hirtella* (Franch.) Schindl. decreased prostate specific antigen and androgen receptor expression in LNCaP cells. *J. Agric. Food Chem.* **2008**, *56* (16), 6928-6935.

Heber, D. Vegetables, fruits and phytoestrogens in the prevention of diseases. *J. Postgrad. Med.* **2004**, *50* (2), 145-149.

Herraiz, T.; Galisteo, J. Tetrahydro-beta-carboline alkaloids occur in fruits and fruit juices. Activity as antioxidants and radical scavengers. *J. Agric. Food Chem.* **2003**, *51* (24), 7156-7161.

Hirai, N.; Okamoto, M.; Udagawa, H.; Yamamuro, M.; Kato, M; Koshimizu, K. Absolute configuration of dehydrodiconiferyl acohol. *Biosci. Biotechnol. Biochem.* **1994**, *58* (9), 1679-1684.

Hsu, CC.; Huang, CN.; Hung, YC.; Yin, MC. Five cysteine-containing compounds have antioxidative activity in Balb/cA mice. *J. Nutr.* **2004**, *134* (1), 149-152.

Huo, C.; Wang, C.; Zhao, M.; Peng, S. Stereoselective synthesis of natural *N*-(1-Deoxy-D-β-fructos-1-yl)-L-amino acids and their effect on lead decorporation. *Chem. Res. Toxicol.* **2004**, *17* (8), 1112-1120.

Ichikawa, M.; Ryu, K.; Yoshida, J.; Ide, N.; Yoshida, S.; Sasaoka, T.; Sumi S. Antioxidant effects of tetrahydro-beta-carboline derivatives identified in aged garlic extract. *Biofactors*. **2002**, *16* (3-4), 57-72.

Ide, N.; Lau, BH. Aged garlic extract attenuates intracellular oxidative stress. *Phytomedicine* **1999a**, *6* (2), 125-131.

Ide, N.; Lau, BH. Garlic compounds protect vascular endothelial cells from oxidized low density lipoprotein-induced injury. *J. Pharm. Pharmacol.* **1997**, *49* (9), 908-911.

Ide, N.; Lau, BH.; Ryu, K.; Matsuura, H.; Itakura, Y. Antioxidant effects of fructosyl arginine, a Maillard reaction product in aged garlic extract. *J. Nutr. Biochem.* **1999b**, *10* (6), 372-376.

Imai, J.; Ide, N.; Nagae, S.; Moriguchi, T.; Matsuura, H.; Itakura, Y. Antioxidant and radical scavenging effects of aged garlic extract and its constituents. *Planta Med.* **1994**, *60* (5), 417-420.

Ishikawa, H.; Saeki, T.; Otani, T.; Suzuki, T.; Shimozuma, K.; Nishino, H.; Fukuda, S.; Morimoto, K. Aged garlic extract prevents a decline of NK cell number and activity in patients with advanced cancer. *J. Nutr.* **2006**, *136* (3 Suppl), 816S-820S.

Ito, T.; Hayase, R.; Kawai, S.; Ohashi, H.; Higuchi, T. Coniferyl aldehyde dimers in dehydrogenative polymerization: model of abnormal lignin formation in cinnamyl alcohol dehydrogenase-deficient plants. *J. Wood Sci.* **2002**, *48* (3), 216-221.

Jialal, I.; Vega, GL.; Grundy, SM. Physiologic levels of ascorbate inhibit the oxidative modification of low density lipoprotein. *Atherosclerosis* **1990**, *82* (3), 185-191.

Kadoma, Y.; Ishihara, M.; Fujisawa, S. A quantitative approach to the free radical interaction between alpha-tocopherol and the coantioxidants eugenol, resveratrol or ascorbate. *In Vivo* **2006**, *20* (1), 61-67.

Kikuzaki, H.; Hisamoto, M.; Hirose, K.; Akiyama, K.; Taniguchi, H. Antioxidant properties of ferulic acid and its related compounds. *J. Agric. Food Chem.* **2002**, *50* (7), 2161-2168.

Kim, Y.; Kim, H.; Bae, S.; Choi, J.; Lim, SY.; Lee, N.; Kong, JM.; Hwang, Y.; Kang, JS.; Lee, WJ. Vitamin C is an essential factor on the anti-viral immune responses through the production of interferon-α/β at the initial stage of influenza a virus (H3N2) infection. *Immune Netw.* **2013**, *13* (2), 70-74.

Koch, HP.; Lawson, LD. Garlic: The science and therapeutic application of *Allium Sativum* L. and related species. *Williams & Wilkins* **1996**, p.42.

Kowaltowski, AJ.; Souza-Pinto, NC.; Castilho, RF.; Vercesi, AE. Mitochondria and reactive oxygen species. *Free Radical Biol. Med.* **2009**, *47* (3), 333-343.

Kyo, E.; Uda, N.; Suzuki, A.; Kakimoto, M.; Ushijima, M.; Kasuga, S.; Itakura, Y. Immunomodulation and antitumor activities of Aged Garlic Extract. *Phytomedicine*. **1998**, *5* (4), 259-267.

Labuza, TP.; Reineccius, GA.; Monnier,VM.; O'Brien, J.; Baynes, JW. Maillard reactions in chemistry, food, and health. *The Royal Society of Chemistry* **1994**.

Lahaie-Collins, V.; Bournival, J.; Plouffe, M.; Carange, J.; Martinoli, MG. Sesamin modulates tyrosine hydroxylase, superoxide dismutase, catalase, inducible NO synthase and interleukin-6 expression in dopaminergic cells under MPP+-induced oxidative stress. *Oxid. Med. Cell. Longevity* **2008**, *1* (1), 54-62.

Lancaster, JE.; Shaw, ML. γ-Glutamyl peptides in the biosynthesis of *S*-alk(en)yl-l-cysteine sulphoxides (flavour precursors) in *Allium*. *Phytochemistry* **1989**, *28* (2), 455-460.

Lawson, KA.; Anderson, K.; Menchaca, M.; Atkinson, J.; Sun, L.; Knight, V.; Gilbert, BE.; Conti, C.; Sanders, BG.; Kline, K. Novel vitamin E analogue decreases syngeneic mouse mammary tumor burden and reduces lung metastasis. *Mol. Cancer Ther.* **2003**, *2* (5), 437-444.

Lawson, LD.; Wang, ZJ.; Hughes, BG. γ-Glutamyl-*S*-alkylcysteines in garlic and other *Allium* spp.: precursors of age-dependent *trans*-1-propenyl thiosulfinates. *J. Nat. Prod.* **1991**, *54* (2), 436-444.

Lee, HC.; Wei, YH. Oxidative stress, mitochondrial DNA mutation, and apoptosis in aging. *Exp. Biol. Med. (Maywood)* **2007**, *232* (5), 592-606.

Lee, J.; Seo, EK.; Jang, DS.; Ha, TJ.; Kim, JP.; Nam, JW.; Bae, G.; Lee, YM.; Yang, MS.; Kim, JS. Two new stereoisomers of neolignan and lignan from the flower buds of Magnolia fargesii. *Chem Pharm Bull (Tokyo).* **2009**, *57* (3), 298-301.

Li, S.; Lundquist, K.; Wallis, AFA. Revised structure for a neolignan from *Brucea javanica*. *Phytochemistry* **1998**, *49* (7), 2125-2128.

Li, X.; Cao, W.; Shen, Y.; Li, N.; Dong, XP.; Wang, KJ.; Cheng, YX. Antioxidant compounds from *Rosa laevigata* fruits. *Food Chem.* **2012**, *130*, 575-580.

Lourith, N.; Katayama, T.; Suzuki, T. Stereochemistry and biosynthesis of 8-*O*-4' neolignans in *Eucommia ulmoides*: diastereoselective formation of guaiacylglycerol-8-*O*-4'-(sinapyl alcohol) ether. *J. Wood Sci.* **2005**, *51* (4), 370-378.

Madamanchi, NR.; Vendrov, A.; Runge, MS. Oxidative stress and vascular disease. *Arterioscler., Thromb., Vasc. Biol.* **2005**, *25* (1), 29-38.

Malhotra, JD.; Kaufman, RJ. Endoplasmic reticulum stress and oxidative stress: a vicious cycle or a double-edged sword? *Antioxid. Redox Signaling.* **2007**, *9* (12), 2277-2293.

Manini, P.; d'Ischia, M.; Prota, G. An unusual decarboxylative Maillard reaction between L-DOPA and D-glucose under biomimetic conditions: factors governing competition with Pictet-Spengler condensation. *J. Org. Chem.* **2001**, *66* (15), 5048-5053.

Maritim, AC.; Sanders, RA.; Watkins, JB 3rd. Diabetes, oxidative stress, and antioxidants: a review. *J. Biochem. Mol. Toxicol.* **2003**, *17* (1), 24-38.

Martín, MA.; Ramos, S.; Mateos, R.; Rufián-Henares, JA.; Morales, FJ.; Bravo, L.; Goya, L. Biscuit melanoidins of different molecular masses protect human HepG2 cells against oxidative stress. *J. Agric. Food Chem.* **2009**, *57* (16), 7250-7258.

Matsuda, N.; Satao, H.; Yaoita, Y.; Kikuchi, M. Isolation and absolute structures of the neolignan glycosides with the enantimetric aglycones from the leaves of *Viburnum awabuki* K. KOCH. *Chem. Pharm. Bull.* **1996**, *44* (5), 1122-1123.

Milatovic, D.; Zaja-Milatovic, S.; Gupta, RC.; Yu, Y.; Aschner, M. Oxidative damage and neurodegeneration in manganese-induced neurotoxicity. *Toxicol. Appl. Pharmacol.* **2009**, *240* (2), 219-225.

Mizuno, M.; Tsuchida, H.; Kozukue, N.; Mizuno, S. Rapid quantitative analysis and distribution of free quercetin in vegetables and fruits. *Nippon Shokuhin Kogyo Gakkaishi* **1992**, *39* (1), 88-92.

Mizunuma, T.; Kajikawa, T.; Kishino, Y. Effect of exercise and vitamin E on lipid peroxide in skeletal muscle in respect to enzyme activity for antioxidant protection. *Tairyoku Kagaku* **1993**, *42* (1), 69-81.

Moree, SS.; Rajesha, J. Investigation of in vitro and in vivo antioxidant potential of secoisolariciresinol diglucoside. *Mol. Cell. Biochem.* **2013**, *373* (1-2), 179-187.

Morihara, N.; Hayama, M.; Fujii, H. Aged garlic extract scavenges superoxide radicals. *Plant Foods Hum. Nutr.* **2011**, *66* (1), 17-21.

Morihara, N.; Nishihama, T.; Ushijima, M.; Ide, N.; Takeda, H.; Hayama, M. Garlic as an anti-fatigue agent. *Mol. Nutr. Food Res.* **2007**, *51* (11), 1329-1334.

Morreel, K.; Kim, H.; Lu, F.; Dima, O.; Akiyama, T.; Vanholme, R.; Niculaes, C.; Goeminne, G.; Inzé, D.; Messens, E.; Ralph, J.; Boerjan, W. Mass spectrometry-based fragmentation as an identification tool in lignomics. *Anal. Chem.* **2010**, *82* (19), 8095-8105.

Mütsch-Eckner, M.; Meier, B.; Wright, AD.; Sticher, O. γ-Glutamyl peptides from *Allium sativum* bulbs. *Phytochemistry* **1992**, *31* (7), 2389-2391.

Nakagawa, S.; Kasuga, S.; Matsuura, H. Prevention of liver damage by aged garlic extract and its components in mice. *Phytother. Res.* **1989**, *3* (2), 50-53.

Nakagawa, S.; Masamoto, K.; Sumiyoshi, H.; Kunihiro, K.; Fuwa, T. Effect of raw and extracted-aged garlic juice on growth of young rats and their organs after peroral administration. *J. Toxicol. Sci.* **1980**, *5* (1), 91-112.

Neudörffer, A.; Bonnefont-Rousselot, D.; Legrand, A.; Fleury, MB.; Largeron, M. 4-Hydroxycinnamic ethyl ester derivatives and related dehydrodimers: Relationship between oxidation potential and protective effects against oxidation of low-density lipoproteins. *J. Agric. Food Chem.* **2004**, *52* (7), 2084-2091.

Niki, E. Assessment of antioxidant capacity *in vitro* and *in vivo*. *Free Radical Biol. Med.* **2010**, *49* (4), 503-515.

Noguchi, N.; Watanabe, A.; Shi, H. Diverse functions of antioxidants. *Free Radical Res.* **2000**, *33* (6), 809-817.

O'Gara, EA.; Hill, DJ.; Maslin, DJ. Activities of garlic oil, garlic powder, and their diallyl constituents against Helicobacter pylori. *Appl Environ Microbiol*. **2000**, *66* (5), 2269-2273.

Omar, SH.; Al-Wabel, NA. Organosulfur compounds and possible mechanism of garlic in cancer. *Saudi Pharm. J.* **2010**, *18* (1), 51-58.

Orfali, RS.; Ebada, SS.; El-Shafae, AM.; Al-Taweel, AM.; Lin, WH.; Wray, V.; Proksch, P. 3-*O*-*trans*-Caffeoylisomyricadiol: a new triterpenoid from *Tamarix nilotica* growing in Saudi Arabia. *Z. Naturforsch., C.* **2009**, *64* (9-10), 637-643.

Ou, B.; Hampsch-Woodill, M.; Prior, RL. Development and validation of an improved oxygen radical absorbance capacity assay using fluorescein as the fluorescent probe. *J. Agric. Food Chem.* **2001**, *49* (10), 4619-4626.

Oyebode, O.; Gordon-Dseagu, V.; Walker, A.; Mindell, JS. Fruit and vegetable consumption and all-cause, cancer and CVD mortality: analysis of Health Survey for England data. *J. Epidemiol. Community Health.* **2014**, *68* (9), 856-862.

Pan, JS.; Hong, MZ.; Ren, JL. Reactive oxygen species: a double-edged sword in oncogenesis. *World J. Gastroenterol.* **2009**, *15* (14), 1702-1707.

Papageorgiou, C.; Corbet, JP.; Menezes-Brandao, F.; Pecegueiro, M.; Benezra, C. Allergic contact dermatitis to garlic (*Allium sativum* L.). Identification of the allergens: the role of mono-, di-, and trisulfides present in garlic. A comparative study in man and animal (guinea-pig). *Arch. Dermatol. Res.* **1983**, *275* (4), 229-234.

Park, JB. Isolation and characterization of *N*-feruloyltyramine as the P-selectin expression suppressor from garlic (Allium sativum). *J. Agric. Food Chem.* **2009**, *57* (19), 8868-8872.

Park, JG.; Oh, GT. The role of peroxidases in the pathogenesis of atherosclerosis. *BMB Rep.* **2011**, *44* (8), 497-505.

Pasteur, L. Memoire sur la fermentation appelee lactique (Extrait par l'auteur)* *C. R. Seances Acad. Sci.* **1857**, *Tome 45*, 913-916.

Pedraza-Chaverrí, J.; Barrera, D.; Maldonado, PD.; Chirino, YI.; Macías-Ruvalcaba, NA.; Medina-Campos, ON.; Castro, L.; Salcedo, MI.; Hernández-Pando, R. *S*-Allylmercaptocysteine scavenges hydroxyl radical and singlet oxygen *in vitro* and attenuates gentamicin-induced oxidative and nitrosative stress and renal damage *in vivo*. *BMC Clin. Pharmacol.* **2004**, *4* (5), 13 pages.

Penttinen, P.; Jaehrling, J.; Damdimopoulos, AE.; Inzunza, J.; Lemmen, JG.; van der Saag, P.; Pettersson, K.; Gauglitz, G.; Mäkelä, S.; Pongratz, I. Diet-derived polyphenol metabolite enterolactone is a tissue-specific estrogen receptor activator. *Endocrinology* **2007**, *148* (10), 4875-4886.

Pool-Zobel, BL.; Bub, A.; Liegibel, UM.; Treptow-van Lishaut, S.; Rechkemmer, G. Mechanisms by which vegetable consumption reduces genetic damage in humans. *Cancer Epidemiol., Biomarkers Prev.* **1998**, *7* (10), 891-899.

Prasad, K. Regression of hypercholesterolemic atherosclerosis in rabbits by secoisolariciresinol diglucoside isolated from flaxseed. *Atherosclerosis* **2008**, *197* (1), 34-42.

Prior, RL.; Wu, X.; Schaich, K. Standardized methods for the determination of antioxidant capacity and phenolics in foods and dietary supplements. *J. Agric. Food Chem.* **2005**, *53* (10), 4290-4302.

Rahman, K. Historical perspective on garlic and cardiovascular disease. *J. Nutr.* **2001**, *131* (3s), 977S-979S.

Rahman, K.; Lowe, GM. Garlic and cardiovascular disease: a critical review. *J. Nutr.* **2006**, *136* (3), 736S-740S.

Ray, PD.; Huang, BW.; Tsuji, Y. Reactive oxygen species (ROS) homeostasis and redox regulation in cellular signaling. *Cell. Signalling.* **2012**, *24* (5), 981-990.

Reale, S.; Attanasio, F.; Spreti, N.; De Angelis, F. Lignin chemistry: biosynthetic study and structural characterisation of coniferyl alcohol oligomers formed in vitro in a micellar environment. *Chemistry.* **2010**, *16* (20), 6077-6087.

Rösler, J.; Krekel, F.; Amrhein, N.; Schmid, J. Maize phenylalanine ammonia-lyase has tyrosine ammonia-lyase activity. *Plant Physiol.* **1997**, *113* (1), 175-179.

Rurián-Henares, JA.; Morales, FJ. Antimicrobial activity of melanoidins against *Escherichia coli* is mediated by a membrane-damage mechanism. *J. Agric. Food Chem.* **2008**, *56* (7), 2357-2362.

Ryu, K.; Ide, N.; Matsuura, H.; Itakura, Y. *N*α-(1-Deoxy-D-fructos-1-yl)-L-arginine, an antioxidant compound identified in aged garlic extract. *J. Nutr.* **2001**, *131* (3), 972S-976S.

Seidel, V.; Bailleul, F.; Waterman, PG. Novel oligorhamnosides from the stem bark of *Cleistopholis glauca*. *J. Nat. Prod.* **2000**, *63* (1), 6-11.

Seiquer, I.; Ruiz-Roca, B.; Mesías, M.; Muñoz-Hoyos, A.; Galdó, G, Ochoa, JJ.; Navarro, MP. The antioxidant effect of a diet rich in Maillard reaction products is attenuated after consumption by healthy male adolescents. *In vitro* and *in vivo* comparative study. *J. Sci. Food Agric.* **2008**, *88* (7), 1245-1252.

Sharma, P.; Jha, AB.; Dubey, RS.; Pessarakli, M. Reactive oxygen species, oxidative damage, and antioxidative defense mechanism in plants under stressful conditions. *J. Bot.* **2012**, *Article ID 217037*, 26 pages.

Shukla, V.; Mishra, SK.; Pant, HC. Oxidative stress in neurodegeneration. *Adv. Pharmacol. Sci.* **2011**, *Article ID 572634*, 13 pages.

Song, CW.; Wang, SM.; Zhou, LL.; Hou, FF.; Wang, KJ.; Han, QB.; Li, N.; Cheng, YX. Isolation and identification of compounds responsible for antioxidant capacity of *Euryale ferox* seeds. *J. Agric. Food Chem.* **2011**, *59* (4), 1199-1204.

Sparnins, VL.; Barany, G.; Wattenberg, LW. Effects of organosulfur compounds from garlic and onions on benzo[*a*]pyrene-induced neoplasia and glutathione *S*-transferase activity in the mouse. *Carcinogenesis* **1988**, *9* (1), 131-134.

Steiner, M.; Kham, AH.; Holbert, D.; Lin, RIS. A double-blind crossover study in moderately hypercholesteremic men that compared the effect of aged garlic extract and placebo administration on blood lipids. *Am. J. Clin. Nutr.* **1996**, *64* (6), 866-870.

Stocker, R.; Keaney, JF, Jr. Role of oxidative modifications in atherosclerosis. *Physiol. Rev.* **2004**, *84* (4), 1381-1478.

Sugii, M.; Suzuki, T.; Nagasawa, S.; Kawashima, K. Isolation of gamma-1-glutamyl-*S*-allylmercapto-L-cysteine and *S*-allylmercapto-L-cysteine from garlic. *Chem. Pharm. Bull. (Tokyo)* **1964**, *12*, 1114-1115.

Sumiyoshi, H.; Kanezawa, A.; Masamoto, K.; Harada, H.; Nakagami, S.; Yokota, A.; Nishikawa, M.; Nakagawa, S. Chronic toxicity test of garlic extract in rats. *J. Toxicol. Sci.* **1984**, *9* (1), 61-75.

Sumiyoshi, H.; Wargovich, MJ. Chemoprevention of 1,2-dimethylhydrazine-induced colon cancer in mice by naturally occurring organosulfur compounds. *Cancer Res.* **1990**, *50* (16), 5084-5087.

Tahara, EB.; Navarete, FD.; Kowaltowski, AJ. Tissue-, substrate-, and site-specific characteristics of mitochondrial reactive oxygen species generation. *Free Radical Biol. Med.* **2009**, *46* (9), 1283-1297.

Tanaka, S.; Haruma, K.; Kunihiro, M.; Nagata, S.; Kitadai, Y.; Manabe, N.; Sumii, M.; Yoshihara, M.; Kajiyama, G.; Chayama, K. Effects of aged garlic extract (AGE) on colorectal adenomas: a double-blinded study. *Hiroshima J. Med. Sci.* **2004**, *53* (3-4), 39-45.

Trachootham, D.; Alexandre, J.; Huang, P. Targeting cancer cells by ROS-mediated mechanisms: a radical therapeutic approach? *Nat. Rev. Drug Discovery* **2009**, *8* (7), 579-591.

USDA National Nutrient database, Agricultural Research Service, National Nutrient Database for Standard Reference, Release 27, NDB No. 11215 (garlic, raw), **2014**, http://ndb.nal.usda.gov/ndb/.

Ushijima, M.; Sumioka, I.; Kakimoto, M.; Yokoyama, K.; Uda, N.; Matsuura, H.; Kyo, E.; Suzuki, A.; Kasuga, S.; Itakura, Y.; Petesch, BL.; Amagase, H. Effect of garlic and garlic preparations on physiological and psychological stress in mice. *Phytother. Res.* **1997**, *11* (3), 226-230.

Ushirotake, T.; Ushirotake, A.; Suzuki, M.; Shimizu, A.; Shiratori, T.; Uematsu, K.; Sato, H.; Watanabe, Y.; Kira, K.; Sumiyoshi, H.; Fuwa T. Epidemiological investigation for common cold preventive effect of Kyoleopin and Leopin Five. *Clinical Drug and Pharmacology* **2004**, *20* (7), 785-793.

Uttara, B.; Singh, AV.; Zamboni, P.; Mahajan, RT. Oxidative stress and neurodegenerative diseases: a review of upstream and downstream antioxidant therapeutic options. *Curr. Neuropharmacol.* **2009**, *7* (1), 65-74.

Volk, GM.; Henk, AD.; Richards, CM. Genetic diversity among US garlic clones as detected using AFLP method. *J. Am. Soc. Hortic. Sci.* **2004**, *129* (4), 559-569.

Weber, T.; Lu, M.; Andera, L.; Lahm, H.; Gellert, N.; Fariss, MW.; Korinek, V.; Sattler, W.; Ucker, DS.; Terman, A.; Schro¨der, A.; Erl, W.; Brunk, UT.; Coffey, RJ.; Weber, C.; Neuzil, J. Vitamin E succinate is a potent novel antineoplastic agent with high selectivity and cooperativity with tumor necrosis factorrelated apoptosis-inducing ligand (Apo2 ligand) *in vivo*. *Clin. Cancer Res.* **2002**, *8*, 863-869.

Wei, YH. Mitochondrial DNA alterations as ageing-associated molecular events. *Mutat. Res.* **1992**, *275* (3-6), 145-155.

Wei, Z.; Lau, BHS. Garlic inhibits free radical generation and augments antioxidant enzyme activity in vascular endothelial cells. *Nutr. Res.* **1998**, *18* (1), 61-70.

Weinberg, DS.; Manier, ML.; Richardson, MD.; Haibach, FG. Identification and quantification of organosulfur compliance markers in a garlic extract. *J. Agric. Food Chem.* **1993**, *41* (1), 37-41.

Wolfe, KL.; Liu, RH. Structure-activity relationships of flavonoids in the cellular antioxidant activity assay. *J. Agric. Food Chem.* **2008**, *56* (18), 8404-8411.

Wu, H.; Hu, X.; Zhang, X; Chen, S; Yang, J; Xu, X. Benzyl 2-β-glucopyranosyloxybenzoate, a new phenolic acid glycoside from *Sarcandra glabra*. *Molecules.* **2012a**, *17* (5), 5212-5218.

Wu, XQ.; Kong, X.; Zhou, Y.; Huang, K.; Yang, JR.; Li, XL. Sesamin exerts renoprotective effects by enhancing NO bioactivity in renovascular hypertensive rats fed with high-fat-sucrose diet. *Eur. J. Pharmacol.* **2012b**, *683* (1-3), 231-237.

Xiao, D.; Pinto, JT.; Soh, JW.; Deguchi, A.; Gundersen, GG.; Palazzo, AF.; Yoon, JT.; Shirin, H.; Weinstein, IB. Induction of apoptosis by the garlic-derived compound *S*-allylmercaptocysteine (SAMC) is associated with microtubule depolymerization and c-Jun NH_2-terminal kinase 1 activation. *Cancer Res.* **2003**, *63* (20), 6825-6837.

Yaguchi, S.; Tokoro, K.; Tada, M. Clinical evaluations of Aged garlic extract combined with ginseng, oriental bezoar, antler velet, cuscuta see, and epimedium herb (Leopin Royal; LER) on various unexplained complaints. *Shinyaku to Rinsho (New Drug Clin.)*, **2005**, *42*, 189-196.

Yamabe, N.; Kim, YJ.; Lee, S.; Cho, EJ.; Park, SH.; Ham, J.; Kim, HY.; Kang, KS. Increase in antioxidant and anticancer effects of ginsenoside Re-lysine mixture by Maillard reaction. *Food Chem.* **2013**, *138* (2-3), 876-883.

Yang, Y.; Song, ZG.; Liu, ZQ. Synthesis and antioxidant capacities of hydroxyl derivatives of cinnamoylphenethylamine in protecting DNA and scavenging radicals. *Free Radical Res.* **2011**, *45* (4), 445-453.

Yatkin, E.; Polari, L.; Laajala, TD.; Smeds, A.; Eckerman, C.; Holmbom, B.; Saarinen, NM.; Aittokallio, T.; Mäkelä, SI. Novel lignan and stilbenoid mixture shows anticarcinogenic efficacy in preclinical PC-3M-luc2 prostate cancer model. *PLoS One* **2014**, *9* (4), e93764.

Yeh, YY.; Liu, L. Cholesterol-lowering effect of garlic extracts and organosulfur compounds: human and animal studies. *J. Nutr.* **2001**, *131* (3), 989S-993S.

Yeo, H.; Chin, YW.; Park, SY.; Kim, J. Lignans of *Rosa multiflora* roots. *Arch. Pharmacal Res.* **2004**, *27* (3), 287-290.

You, WC.; Zhang, L.; Gail, MH.; Ma, JL.; Chang, YS.; Blot, WJ.; Li, JY.; Zhao, CL.; Liu, WD.; Li, HQ.; Hu, YR.; Bravo, JC.; Correa, P.; Xu, GW.; Fraumeni, JF Jr. Helicobacter pylori infection, garlic intake and precancerous lesions in a Chinese population at low risk of gastric cancer. *Int. J. Epidemiol.* **1998**, *27* (6), 941-944.

Zhang, N.; Huang, X.; Zeng, Y.; Wu, X.; Peng, X. Study on prebiotic effectiveness of neutral garlic fructan *in vitro*. *Food Science and Human Wellness.* **2013**, *2*, 119-123.